The Dissertation Committee for Julie Ann Rytlewski Certifies that this is the approved version of the following dissertation:

Understanding Mechanisms of Stem Cell Tubulogenesis in PEGylated Fibrin for Improving Neovascularization Therapies

Committee:

Laura J. Suggs, Supervisor

Aaron Baker

Patrick Kelly

Krishnendu Roy

Janet Zoldan

Understanding Mechanisms of Stem Cell Tubulogenesis in PEGylated Fibrin for Improving Neovascularization Therapies

by

Julie Ann Rytlewski, B.S.Biomed.E.

Dissertation

Presented to the Faculty of the Graduate School of

The University of Texas at Austin

in Partial Fulfillment

of the Requirements

for the Degree of

Doctor of Philosophy

The University of Texas at Austin

December 2013

Dedication

To my fiancé, Chris, whose steady shoulder has provided more comfort and support than he could ever know. To my friends and family, who have lent an empathetic ear and offered many words of encouragement. And to Nicholas and Stephanie—your memory continues to inspire; I hope you'd be proud.

Acknowledgements

Many individuals have contributed their time and expertise to my doctoral project, and I am sincerely grateful to each of them. Two people in particular have been instrumental in my growth as a researcher and scientist:

To Dr. Suggs—I'm unable to fully express how thankful I am to have been a part of your lab and to have had the pleasure of your mentorship. Your guidance has been unwavering, your criticism firm but never harsh, and your patience for discussion endless.

To Dr. Roy—You gave me my first opportunity to pick up a pipettor and begin my journey as a researcher. That opportunity meant the world to me then and still means as much, if not more, to this day. Your kindness and humor will always be cherished.

My labmates over the years have been an amazing support system, both personally and professionally. For all of the advice, collaboration, and cathartic coffee breaks, thank you Dr. Eunna Chung, Dr. Charlie Drinnan, Dr. Mary Nguyen, Dr. Ryan Nagao, Laura Geuss, Laura Ricles, Ryan Stowers, Kevin Eckes, Jeehyun Park, and Daniela Santiesteban. To my brilliant and dedicated undergraduate research assistants, thank you Evan Lewis and Alejandra Aldon for all of the hours you've contributed to this work.

I would also like to thank several UT staff for their time, assistance, and professionalism: Dr. Dwight Romanovicz, Angela Bardo, Julie Hayes, Bobby Knight, Jim Pollard, Chris Cooper, Stephanie Tomlinson, Krystal Peralez, Cindy Zimmerman, Jeff Hallock, Yma Revuelta, and Heidi Mallon.

Understanding Mechanisms of Stem Cell Tubulogenesis in PEGylated Fibrin for Improving Neovascularization Therapies

Julie Ann Rytlewski, Ph.D.

The University of Texas at Austin, 2013

Supervisor: Laura J. Suggs

Stem cell-based therapies are an important developing technology for treating cardiovascular ischemic disease, including subsequent co-morbidities such as ulcerative wounds. Mesenchymal stem cells (MSCs) have a proven ability to augment wound healing and neovascularization processes and have been more recently investigated for their endothelial-like behavior. This doctoral work aims to understand mechanisms underlying matrix-driven MSC tubulogenesis within PEGylated fibrin gels, specifically (1) why this behavior occurs and (2) if this behavior has clinical utility.

Briefly, a three-dimensional morphological quantification pipeline was first developed for analyzing the maturity of vascular networks (Chapter 2). This method was applied in later studies that examined the full spectrum of MSC behavior in PEGylated fibrin gels, linking biomaterial properties with network development (Chapter 3). Mechanisms underlying the cell-matrix relationship were more fully clarified through gain-of-function cell studies. These studies indicated that PEGylated fibrin promotes endothelial-like MSC behavior through a combination of hypoxic stress and bioactive fibrin cues (Chapter 4). Notably, this endothelial-like MSC behavior closely mirrored vasculogenic mimicry, a process whereby tumors establish non-endothelialized vasculature in response to hypoxic stress. The functionality of these tumor vessels

suggests that mature endothelial differentiation of MSCs may not be necessary to achieve therapeutically beneficial tissue perfusion. This hypothesis opens up new mechanisms for exploitation in vascular tissue engineering strategies.

Table of Contents

List of Tables

List of Figures

Chapter 1: Introduction

BACKGROUND AND MOTIVATION

Ischemic disease and cell-based revascularization

Ischemic cardiovascular diseases continue to be the leading source of death and disability in the Western World and a tremendous fiscal burden on the healthcare system.[1,2] Coronary heart disease (CHD) and peripheral arterial disease (PAD) are particularly widespread.[1,3,4] Patients with these conditions are at a heightened risk for further complications, including myocardial infarction, critical limb ischemia, and chronic wounds, which require increasingly costly medical intervention.[5,6] Since ischemic cardiovascular diseases are frequently symptomatic of a more systemic co-morbidity (e.g., metabolic syndrome, diabetes, or obesity), many of these patients have compromised healing abilities and make poor surgical candidates.[5] This trend leads to an increasing population of "no-option" patients who are either ineligible for current interventions or for whom interventions fail to alleviate disabling ischemia.[2] New strategies are needed to treat these "no-option" patients as well as improve long-term outcomes for the general populace, thereby reducing the rate of future revisional procedures and overall healthcare costs.

Regenerative medicine and tissue engineering are at the forefront of next-generation therapies to revascularize ischemic tissues. After suboptimal trials with angiogenic protein and gene delivery,[4,7] stem cell-based therapies rapidly gained popularity among medical and research communities. Specifically, bone marrow-derived and adipose-derived mesenchymal stem cells (MSCs) have emerged as viable candidate populations: these progenitors are easy to harvest through a simple biopsy, can be readily expanded *ex vivo*, and potentiate angiogenesis and tissue repair.[8-12] Autologous stem cell

transplants have yielded promising results in laboratory and early clinical studies. In post-myocardial infarction patients, an infusion of bone marrow MSCs led to a sustained 18% increase in left ventricular ejection fractions.[13] Similarly, intramuscular injection of MSC significantly reduced limb ischemia associated with PAD by increasing local angiogenesis. They found that MSC-generated neovascular networks provided an auxiliary blood flow to restore limb perfusion and reduce ischemia-associated limb pain.[5] In another clinical trial, MSCs topically delivered within a fibrin spray facilitated the closure of severely chronic wounds.[14] Results showed that the probability of wound closure correlated strongly with the number of MSCs delivered and that MSC-treated wounds had diminished scarring and improved tensile strength. These early trials showcased the feasibility of MSC therapies becoming a reality as well as the adaptability of application and flexibility of delivery these cells offer.

Challenges facing stem cell-based ischemic therapies

Despite the successes of early trials, MSC therapies have also experienced a number of setbacks. Diabetic patients, for example, suffer from hyperinsulinemia-induced oxidative stress that limits the regenerative and angiogenic potential of their stem cells.[15] In a type-II diabetes mouse model, MSCs favored adipocytic over endothelial differentiation and resulted in significantly fewer animals with resolved limb ischemia.[15] Other diseased states may be similarly contraindicative for stem cell-based therapies.[16] These patients would require an additional therapeutic step during *ex vivo* expansion that restores normal MSC function prior to transplantation.

On top of intrinsic patient health issues, MSC retention at the transplantation site has been and remains universally poor. *In vivo* studies have reported transplanted cell

death up to 70-100%.[17] A considerable percentage of dead cells are located in construct cores, which are diffusionally limited and prone to hypoxia-induced apoptosis. This phenomenon is a known challenge in engineering thick tissue constructs. However, cells located along the periphery of constructs surprisingly fail to thrive as well. Studies verified that MSCs are not migrating away from the implant site nor are they experiencing extreme hypoxia like the cells in the construct core.[17] Instead, evidence suggests an alternative (but unknown) mechanism is triggering the cascade of peripheral cell death. Attempts to salvage MSC retention have focused on activating survival mechanisms by heat or hypoxic stress preconditioning, specifically heat shock protein (HSP) and hypoxia inducible factor (HIF) pathways.[18-21] Although the nomenclature suggests that these pathways are two distinct survival mechanisms, studies have demonstrated a great deal of molecular overlap between HSP- and HIF-mediated cell behavior.[22,23] Both families of survival proteins have also been the focus of MSC gene therapies that mimic the beneficial effects of preconditioning without the physical presence of stress.[24] HIF pathways, though, have been specifically linked to an upregulation of angiogenic MSC behavior.[21,25] In gene activation studies, constitutive expression and stabilization of HIF-1α in MSCs enhanced paracrine production of angiogenic factors.[26] Given hypoxia's innate role in cuing wound revascularization, the relationship between hypoxic stress and angiogenic stem cell behavior follows as a natural extension of that paradigm.

MSC-to-endothelial differentiation: fact or false-positive?

The biggest setback to implementing MSC therapies—and perhaps the most controversial—is the ability (or inability) of these populations to fully differentiate into

endothelial cells.[27] While paracrine mechanisms are well characterized as the primary mode of MSC contribution to the ischemic wound environment,[28] this cell behavior undermines the central principle of tissue engineering: the physical replacement of dead or damaged tissue with a transplanted cell population.[29] This principle is especially crucial for patients with co-morbidities that limit their healing capacity; in such cases, paracrine signaling may not be enough to promote neovascularization.[30] The transplanted cells need to physically transition into the new desired tissue. In this case, the MSCs need to be directed into endothelialized vasculature.

As a mesenchyme or stromal progenitor, MSCs are generally defined by their ability to differentiate into adipocytes, chondrocytes, and osteoblasts.[8] Their ability to differentiate into other mesodermal lineages, such as myoblasts, has also been reported.[31,32] In the last ten years, MSCs have more recently been investigated for their endothelial potential as a new cell source for neovascularization.[33] Mature endothelial cells are characterized by a number of key phenotypic markers: von Willebrand Factor (vWF), vascular endothelial cadherin (VE-cadherin), platelet endothelial cell adhesion molecular (PECAM)-1, vascular endothelial growth receptor (VEGFR)-1 (i.e., Flt-1) and VEGFR-2 (i.e., KDR/Flk-1), CD34, and Tie-2.[34,35] Studies reporting successful differentiation of MSCs towards a putative endothelial cell type frequently cite positive gene and protein expression for a combination of these endothelial markers (Table 1.1). However, our group and others have experienced inconsistent reproducibility of these results. This inconsistency has raised questions regarding the purity of initial MSC cultures and the possibility of contaminating progenitors or rare endothelial cells leading to false-positive results.[27]

The purity and differentiation potential of MSC populations depends significantly on the tissue source and isolation method.[8,27,36] From bone marrow, MSCs are typically

harvested as the adherent cell fraction,[37] which is now known to be less homogenous than previously thought. Cell sorting for surface markers (CD29, CD90, CD105, CD73, CD44, and Stro-1)[38] can enrich the adherent fraction for MSCs but a margin of error up to 5-10% may remain. Additional sources of ambiguity arise in identifying contaminating cell populations. New studies indicate that endothelial cells can transdifferentiate towards a multipotent stromal lineage, adopting a spindle-like morphology and expressing surface markers CD90, CD44, and Stro-1 characteristic of MSCs.[39] Others have observed hybrid mesenchymal-endothelial phenotypes where subpopulations of progenitors simultaneously express MSC and endothelial surface markers.[36] Both scenarios highlight the present difficulty in distinguishing between true MSC-to-endothelial differentiation and false-positive results obtained from incidental subpopulations. Clear methods to untangle these overlapping cell populations are currently lacking.[40] The difficulty in verifying MSC purity confounds the results obtained from these populations and is a likely source of inter-study variability.

Our group's work is predicated on driving MSCs towards an endothelial-like phenotype to facilitate local revascularization. Throughout this endeavor, we have encountered phenotypic inconsistency with one endothelial marker in particular: PECAM-1.[41] PECAM-1 is highly specific to mature endothelium and is only second in specificity to Tie-2, since macrophages are also capable of PECAM-1 expression.[42,43] While our MSCs have consistently expressed vWF and VE-cadherin, the lack of PECAM-1 protein in recent studies has caused us to question the endothelial nature of our cell outcomes. The work presented here seeks to understand that very issue—is endothelial differentiation truly what MSCs are accomplishing and if not, do they still have therapeutic utility in cell-based ischemic therapies?

Matrix-directed MSC behavior for ischemic therapies

Biomaterials are often employed to enhance stem cell-based therapies. These engineered matrices can act as a delivery vehicle for improved cell retention *and* can coordinate and direct stem cell behavior to achieve specific outcomes.[44] For large dermal wounds, biomaterials also serve as a spatial filler to reduce the rate of purse-strong closure and minimize scar tissue formation.[11,45-47] The use of biomaterials to direct stem cell behavior through mechanotransduction and biochemical signaling has been well documented.[48,49] A landmark study by Engler *et al* importantly demonstrated that matrix stiffness alone could direct MSCs towards different lineages.[50] Synthetic polymers excel in facilitating highly tunable systems with specific biomechanical qualities and degradation profiles.[51] Similarly, the biomaterial itself is often a source of intrinsic biochemical cues, engineered to mimic the microenvironment of the target tissue. Natural polymers are inherently bioactive and elicit cellular responses based on normal physiologic programming; their bioactivity is highly advantageous over synthetic polymers where complex chemistries are usually required to decorate the matrix with growth factors and cell-binding peptides.[51]

PEGylated fibrin is a natural-synthetic polymer blend that merges the benefits of both polymer families. Fibrin, derived from thrombin's cleavage of fibrinogen, is a protein from the clotting cascade and initiates the natural wound-healing response and angiogenic cell behavior.[52] However, the body's natural anti-thrombotic mechanisms include fibrinolytic enzymes that lead to rapid degradation of naked fibrin *in vivo*.[53,54] Polyethylene glycol (PEG), on the other hand, is a biologically inert polymer frequently used in hydrogel applications and as a "stealth" coating that minimizes the immunogenicity of delivered biologics.[55] The merged PEGylated fibrin product

subsequently combines the bioactivity of fibrin with slowed enzymatic breakdown of the matrix imparted by PEG's "stealth" protection.[56-58]

The novelty of our work lies in *how* PEGylated fibrin directs MSC behavior. PEGylated fibrin is able to promote spontaneous MSC tubulogenesis *without* the addition of soluble factors in the culture media.[41] Tube network formation is complemented by the upregulation of several endothelial-like markers (vWF and VE-cadherin) and angiogenic paracrine factors (e.g., VEGF). Though biomaterials can provide significant cell-fate direction, growth factors are still frequently added to supplement these cues during the differentiation process.[50] Growth factors add expense and complexity, which are both barriers to clinical translatability. We believe that simplicity is key to successful translation of cell-based ischemic therapies to the clinic and PEGylated fibrin enables us to use one biomaterial and one cell source.

SPECIFIC AIMS

The doctoral work here aims to clarify how fibrin PEGylation contributes to the matrix dynamics facilitating MSC tubulogenesis and which cell mechanisms are active during this process. Elucidating mechanisms of MSC tubulogenesis will lay the groundwork for future re-engineering of our biomaterial matrix to achieve *in vivo* postnatal vasculogenesis of this progenitor population. By fully utilizing the regenerative capacity of progenitor populations, we can increase the clinical efficacy of cell-based vascular therapies.

Aim 1: Develop a morphological quantification method for analyzing vascular network development.

Rationale: Validating vascular tissue engineering strategies requires analysis of morphological outcomes. Current methods rely on two-dimensional techniques that eliminate valuable spatial information. A three-dimensional technique will provide more accurate analysis for future investigation of MSC tubulogenesis.

A. Optimize staining protocol for fluorescent microscopy of whole gel constructs.

B. Synthesize an image quantification pipeline for extracting three-dimensional data from microscopy images and outputting vascular-relevant metrics.

C. Validate new method using previous morphometry protocols and assays, including two-dimensional network tracing and aortic ring outgrowth.

Aim 2: Determine the impact of fibrin PEGylation on the morphologic and phenotypic changes of MSCs.

Rationale: Fibrin matrices are a common natural polymer in vascular tissue engineering but these networks are unable to induce tubulogenesis without additional soluble factors. Outcomes aim to characterize cell changes associated with biomaterial properties of PEGylated fibrin.

A. Characterize rheological and diffusional properties of fibrin-based gels.

B. Assess MSC tubular networks by quantitative morphometry (from Aim 1) and verify lumenal space development.

C. Determine cytoskeletal and integrin components responsible for cell motility

D. Measure biologic response of MSCs via cell proliferation, protein marker expression, and secreted factor production.

E. Implicate potential mechanisms that link results from 2A and 2B.

Aim 3: Investigate the mechanisms responsible for endothelial-like MSC behavior in PEGylated fibrin gels.

Rationale: MSCs in PEGylated fibrin exhibit a partial endothelial phenotype. The utility of endothelial-like cell behavior and why PEGylated fibrin elicits this cell response remains unknown. Understanding both questions is central to directing future applications of our cell-based ischemic therapy.

A. Compare phenotypic and morphologic outcomes of MSCs to endothelial cells.

B. From results of 2E, explore how implicated mechanisms modulate endothelial-like behavior of MSCs.

C. Validate findings of 3B with an *in vivo* model.

Study	*MSC source*	*Method of differentiation*	*Phenotypic outcomes*
Yan 2013[15]	mBM	Nox4 siRNA	↑CD31+ ↓adipocytic diff.
Wang 2013[59]	rBM hBM	VEGF (rBM) VEGF + bFGF (hBM) MRTF-A siRNA	↑Flt-1, Flk-1, vWF, VE-cadherin ↓Flt-1, Flk-1
Galas 2013[60]	hBM	EGM-2 (-VEGF)	vWF+/Flk-1+/VE-cadherin+ 1 week: ↑CD31 2 week: ↑vWF, DiI-ac-LDL uptake
Wang 2013[61]	hTB hBM	Matrigel + M200 EGM for 4h FOXC2 siRNA	hTB: ↑CD31, Flk-1, CD144, vWF hBM: (no expression observed) hTB: ↓CD31, CD144
Huang 2013[62]	mBM	miR-126 miRNA + VEGF + bFGF	↑PI3K p85, Akt, p38, ERK1 ↑CD31, E-selectin, vWF, Flk-1 ↓CD29, CD90, CD105 DiI-ac-LDL uptake day 9: cobblestone morphology
Janeczek 2012[63]	hBM	EGM-2 + shear flow for 10d + Matrigel	↑CD31, Flk-1, vWF DiI-ac-LDL uptake
Benavides 2012[64]	hAF	EGM + added VEGF	↑vWF, eNOS, CD31, VE-cadherin, Flk-1 ↓c-kit, SSEA4 DiI-ac-LDL uptake
Pankajakshan 2012[65]	pBM	EGM + added VEGF	↑vWF, VE-cadherin, CD31, Flt-1, Flk-1 DiI-ac-LDL uptake
Wingate 2012[49]	rBM	modulating stiffness of nanofiber grafts	3kPa graft: ↑Flk-1, ↓SMA >8kPa grafts: ↓Flk-1, ↑SMA
Zhang 2010[41]	hBM	PEGylated porcine fibrin matrices	CD31+/vWF+/VE-cadherin+/Flk-1+
Xu 2009[66]	rBM	simvastatin Notch1 siRNA, DAPT	↑vWF, CD31, VE-cadherin, Flk-1 ↑Notch1, Notch4, DLL4 ↓vWF, VE-cadherin, Flk-1
Hamou 2009[67]	mAT	hypoxia + VEGF	↑Flk-1+/CD31+ DiI-ac-LDL uptake
Jazayeri 2008[68]	hBM	VEGF + IGF-1	↑vWF, CD31, Flt-1, Flk-1, Tie-2, VCAM-1 formation of Weibel Palade bodies, caveolae, and pinocytic vesicle
Oswald 2004[33]	hBM	VEGF	↑KDR, Flt-1, vWF, VCAM-1, VE-cadherin

Table 1.1: Summary of recent studies analyzing MSC transdifferentiation towards an endothelial lineage. Abbreviations: bone marrow (BM), adipose tissue (AT), trabecular bone (TB), amniotic fluid (AF), endothelial growth media (EGM). Species of MSC source is denoted by human (h), rat (r), mouse (m), pig (p).

REFERENCES

1. Fukuda S, Yoshii S, Kaga S, Matsumoto M, Kugiyama K, Maulik N. Angiogenic strategy for human ischemic heart disease: Brief overview. Molecular and Cellular Biochemistry. 2005;264(1/2):143–149.

2. Copland IB. Mesenchymal stromal cells for cardiovascular disease. Journal of cardiovascular disease research. 2011 January;2(1):3–13.

3. Lawall H, Bramlage P, Amann B. Treatment of peripheral arterial disease using stem and progenitor cell therapy. Journal of vascular surgery : official publication, the Society for Vascular Surgery [and] International Society for Cardiovascular Surgery, North American Chapter. 2011 February;53(2):445–453.

4. Pons J, Huang Y, Takagawa J, Arakawa-Hoyt J, Ye J, Grossman W, Kan YW, Su H. Combining angiogenic gene and stem cell therapies for myocardial infarction. The Journal of Gene Medicine. 2009 September 1;11(9):743–753.

5. Varu VN, Hogg ME, Kibbe MR. Critical limb ischemia. Journal of vascular surgery : official publication, the Society for Vascular Surgery [and] International Society for Cardiovascular Surgery, North American Chapter. 2010 January;51(1):230–241.

6. Minar E. Critical limb ischaemia. Hämostaseologie. 2009.

7. Rissanen TT, Ylä-Herttuala S. Current status of cardiovascular gene therapy. Molecular therapy : the journal of the American Society of Gene Therapy. 2007 July;15(7):1233–1247.

8. Al-Nbaheen M, Vishnubalaji R, Ali D, Bouslimi A, Al-Jassir F, Megges M, Prigione A, Adjaye J, Kassem M, Aldahmash A. Human Stromal (Mesenchymal) Stem Cells from Bone Marrow, Adipose Tissue and Skin Exhibit Differences in Molecular Phenotype and Differentiation Potential. Stem Cell Reviews and Reports. 2012 April 14.

9. Hutton DL, Logsdon EA, Moore EM, Mac Gabhann F, Gimble JM, Grayson WL. Vascular morphogenesis of adipose-derived stem cells is mediated by heterotypic cell-cell interactions. Tissue Engineering Part A. 2012 August;18(15-16):1729–1740.

10. Rüger BM, Breuss J, Hollemann D, Yanagida G, Fischer MB, Mosberger I, Chott A, Lang I, Davis PF, Höcker P, et al. Vascular morphogenesis by adult bone marrow progenitor cells in three-dimensional fibrin matrices. Differentiation; research in biological diversity. 2008 September;76(7):772–783.

11. Sorrell JM, Caplan AI. Topical delivery of mesenchymal stem cells and their function in wounds. Stem cell research & therapy. 2010 September 24;1(4):30.

12. Menasché P. Stem cells for clinical use in cardiovascular medicine. Thromb Haemost. 2005.

13. Chen S-L, Fang W-W, Ye F, Liu Y-H, Qian J, Shan S-J, Zhang J-J, Chunhua RZ, Liao L-M, Lin S, et al. Effect on left ventricular function of intracoronary transplantation of autologous bone marrow mesenchymal stem cell in patients with acute myocardial infarction. The American journal of cardiology. 2004 July 1;94(1):92–95.

14. Falanga V, Iwamoto S, Chartier M, Yufit T, Butmarc J, Kouttab N, Shrayer D, Carson P. Autologous bone marrow-derived cultured mesenchymal stem cells delivered in a fibrin spray accelerate healing in murine and human cutaneous wounds. Tissue engineering. 2007 June 1;13(6):1299–1312.

15. Yan J, Tie G, Xu TY, Cecchini K, Messina LM. Mesenchymal stem cells as a treatment for peripheral arterial disease: current status and potential impact of type II diabetes on their therapeutic efficacy. Stem Cell Reviews and Reports. 2013 June;9(3):360–372.

16. Cipriani P, Guiducci S, Miniati I, Cinelli M, Urbani S, Marrelli A, Dolo V, Pavan A, Saccardi R, Tyndall A, et al. Impairment of endothelial cell differentiation from bone marrow-derived mesenchymal stem cells: new insight into the pathogenesis of systemic sclerosis. Arthritis and Rheumatism. 2007 June;56(6):1994–2004.

17. Becquart P, Cambon-Binder A, Monfoulet L-E, Bourguignon M, Vandamme K, Bensidhoum M, Petite H, Logeart-Avramoglou D. Ischemia is the prime but not the only cause of human multipotent stromal cell death in tissue-engineered constructs in vivo. Tissue Engineering Part A. 2012 October;18(19-20):2084–2094.

18. Moloney TC, Hoban DB, Barry FP, Howard L, Dowd E. Kinetics of thermally induced heat shock protein 27 and 70 expression by bone marrow-derived mesenchymal stem cells. Protein science : a publication of the Protein Society. 2012 June;21(6):904–909.

19. Lee EY, Xia Y, Kim W-S, Kim MH, Kim TH, Kim KJ, Park B-S, Sung J-H. Hypoxia-enhanced wound-healing function of adipose-derived stem cells: increase in stem cell proliferation and up-regulation of VEGF and bFGF. Wound repair and regeneration : official publication of the Wound Healing Society [and] the European Tissue Repair Society. 2009 July;17(4):540–547.

20. Borcar A, Menze MA, Toner M, Hand SC. Metabolic preconditioning of mammalian cells: mimetic agents for hypoxia lack fidelity in promoting phosphorylation of pyruvate dehydrogenase. Cell and tissue research. 2013 January;351(1):99–106.

21. Tsai C-C, Yew T-L, Yang D-C, Huang W-H, Hung S-C. Benefits of hypoxic culture on bone marrow multipotent stromal cells. American journal of blood research. 2012;2(3):148–159.

22. Shipp C, Derhovanessian E, Pawelec G. Effect of culture at low oxygen tension on the expression of heat shock proteins in a panel of melanoma cell lines. PloS one. 2012;7(6):e37475.

23. Wang X, Zhao T, Huang W, Wang T, Qian J, Xu M, Kranias EG, Wang Y, Fan G-C. Hsp20-engineered mesenchymal stem cells are resistant to oxidative stress via enhanced activation of Akt and increased secretion of growth factors. Stem cells (Dayton, Ohio). 2009 December;27(12):3021–3031.

24. Gao F, Hu X-Y, Xie X-J, Xu Q-Y, Wang Y-P, Liu X-B, Xiang M-X, Sun Y, Wang J-A. Heat shock protein 90 protects rat mesenchymal stem cells against hypoxia and serum deprivation-induced apoptosis via the PI3K/Akt and ERK1/2 pathways. Journal of Zhejiang University. Science. B. 2010 August;11(8):608–617.

25. Das R, Jahr H, van Osch GJVM, Farrell E. The role of hypoxia in bone marrow-derived mesenchymal stem cells: considerations for regenerative medicine approaches. Tissue engineering. Part B, Reviews. 2010 April;16(2):159–168.

26. Razban V, Lotfi AS, Soleimani M, Ahmadi H, Massumi M, Khajeh S, Ghaedi M, Arjmand S, Najavand S, Khoshdel A. HIF-1α Overexpression Induces Angiogenesis in Mesenchymal Stem Cells. BioResearch open access. 2012 August;1(4):174–183.

27. Crisan M. Transition of mesenchymal stem/stromal cells to endothelial cells. Stem cell research & therapy. 2013 August 14;4(4):95.

28. Hocking AM, Gibran NS. Mesenchymal stem cells: paracrine signaling and differentiation during cutaneous wound repair. Experimental Cell Research. 2010 August 15;316(14):2213–2219.

29. Soker S, Machado M, Atala A. Systems for therapeutic angiogenesis in tissue engineering. World journal of urology. 2000 February 1;18(1):10–18.

30. Yan J, Tie G, Wang S, Messina KE, DiDato S, Guo S, Messina LM. Type 2 Diabetes Restricts Multipotency of Mesenchymal Stem Cells and Impairs Their Capacity to Augment Postischemic Neovascularization in db/db Mice. Journal of the American Heart Association. 2012 October 30;1(6):e002238–e002238.

31. Weir C, Morel-Kopp M-C, Gill A, Tinworth K, Ladd L, Hunyor SN, Ward C. Mesenchymal stem cells: isolation, characterisation and in vivo fluorescent dye tracking. Heart, lung & circulation. 2008 October;17(5):395–403.

32. Akavia UD, Veinblat O, Benayahu D. Comparing the transcriptional profile of mesenchymal cells to cardiac and skeletal muscle cells. Journal of Cellular Physiology. 2008 September 1;216(3):663–672.

33. Oswald J, Boxberger S, Jørgensen B, Feldmann S, Ehninger G, Bornhäuser M, Werner C. Mesenchymal Stem Cells Can Be Differentiated Into Endothelial Cells In Vitro. Stem cells (Dayton, Ohio) [Internet]. 2004 May;22(3):377–384.

34. Pusztaszeri MP, Seelentag W, Bosman FT. Immunohistochemical expression of endothelial markers CD31, CD34, von Willebrand factor, and Fli-1 in normal human tissues. Journal of Histochemistry and Cytochemistry. 2006 April;54(4):385–395.

35. Urbich C, Dimmeler S. Endothelial progenitor cells: characterization and role in vascular biology. Circulation research. 2004 August 20;95(4):343–353.

36. Corotchi MC, Popa MA, Remes A, Sima LE, Gussi I, Lupu Plesu M. Isolation method and xeno-free culture conditions influence multipotent differentiation capacity of human Wharton's jelly-derived mesenchymal stem cells. Stem cell research & therapy. 2013 July 11;4(4):81.

37. Wolfe M, Pochampally R, Swaney W, Reger RL. Isolation and culture of bone marrow-derived human multipotent stromal cells (hMSCs). Methods in molecular biology (Clifton, N.J.). 2008;449:3–25.

38. Gaafar TM, Abdel Rahman HA, Attia W, Hamza HS, Brockmeier K, Hawary El RE. Comparative characteristics of endothelial-like cells derived from human adipose mesenchymal stem cells and umbilical cord blood-derived endothelial cells. Clinical and experimental medicine. 2013 May 7.

39. Medici D, Shore EM, Lounev VY, Kaplan FS, Kalluri R, Olsen BR. Conversion of vascular endothelial cells into multipotent stem-like cells. Nature medicine. 2010 December;16(12):1400–1406.

40. Mund J. The ontogeny of endothelial progenitor cells through flow cytometry. Current opinion in hematology. 2011.

41. Zhang G, Drinnan CT, Geuss LR, Suggs LJ. Vascular differentiation of bone marrow stem cells is directed by a tunable three-dimensional matrix. Acta Biomaterialia. 2010 September;6(9):3395–3403.

42. Starke RD, Ferraro F, Paschalaki KE, Dryden NH, McKinnon TAJ, Sutton RE, Payne EM, Haskard DO, Hughes AD, Cutler DF, et al. Endothelial von Willebrand factor regulates angiogenesis. Blood. 2011 January 20;117(3):1071–1080.

43. Moldovan NI, Goldschmidt-Clermont PJ, Parker-Thornburg J, Shapiro SD, Kolattukudy PE. Contribution of monocytes/macrophages to compensatory neovascularization: the drilling of metalloelastase-positive tunnels in ischemic myocardium. Circulation research. 2000;(87):378–384.

44. Lutolf MP, Gilbert PM, Blau HM. Designing materials to direct stem-cell fate. Nature. 2009 November 26;462(7272):433–441.

45. Coolen NA, Vlig M, van den Bogaerdt AJ, Middelkoop E, Ulrich MMW. Development of an in vitro burn wound model. Wound repair and regeneration : official publication of the Wound Healing Society [and] the European Tissue Repair Society. 2008 July;16(4):559–567.

46. Athanassopoulos A, Tsaknakis G, Newey SE, Harris AL, Kean J, Tyler MP, Watt SM. Microvessel networks in pre-formed in artificial clinical grade dermal substitutes in vitro using cells from haematopoietic tissues. Burns : journal of the International Society for Burn Injuries. 2012 August;38(5):691–701.

47. Leonardi D, Oberdoerfer D, Fernandes MC, Meurer RT, Pereira-Filho GA, Cruz P, Vargas M, Chem RC, Camassola M, Nardi NB. Mesenchymal stem cells combined with an artificial dermal substitute improve repair in full-thickness skin wounds. Burns : journal of the International Society for Burn Injuries. 2012 December;38(8):1143–1150.

48. Reilly GC, Engler AJ. Intrinsic extracellular matrix properties regulate stem cell differentiation. Journal of biomechanics. 2010 January 5;43(1):55–62.

49. Wingate K, Bonani W, Tan Y, Bryant SJ, Tan W. Compressive elasticity of three-dimensional nanofiber matrix directs mesenchymal stem cell differentiation to vascular cells with endothelial or smooth muscle cell markers. Acta Biomaterialia. 2012 April;8(4):1440–1449.

50. Engler AJ, Sen S, Sweeney HL, Discher DE. Matrix elasticity directs stem cell lineage specification. Cell. 2006 August 25;126(4):677–689.

51. Gonen-Wadmany M, Goldshmid R, Seliktar D. Biological and mechanical implications of PEGylating proteins into hydrogel biomaterials. Biomaterials. 2011 September;32(26):6025–6033.

52. Janmey PA, Winer JP, Weisel JW. Fibrin gels and their clinical and bioengineering applications. Journal of the Royal Society, Interface / the Royal Society. 2009 January 6;6(30):1–10.

53. Urech L, Bittermann AG, Hubbell JA, Hall H. Mechanical properties, proteolytic degradability and biological modifications affect angiogenic process extension into native and modified fibrin matrices in vitro. Biomaterials. 2005.

54. Ahmed TAE, Griffith M, Hincke M. Characterization and inhibition of fibrin hydrogel-degrading enzymes during development of tissue engineering scaffolds. Tissue engineering. 2007 July;13(7):1469–1477.

55. Veronese FM. Peptide and protein PEGylation: a review of problems and solutions. Biomaterials. 2001 March;22(5):405–417.

56. Gonen-Wadmany M, Oss-Ronen L, Seliktar D. Protein-polymer conjugates for forming photopolymerizable biomimetic hydrogels for tissue engineering. Biomaterials. 2007 September 1;28(26):3876–3886.

57. Almany L, Seliktar D. Biosynthetic hydrogel scaffolds made from fibrinogen and polyethylene glycol for 3D cell cultures. Biomaterials [Internet]. 2005 May 1;26(15):2467–2477.

58. Frisman I, Orbach R, Seliktar D, Bianco-Peled H. Structural investigation of PEG-fibrinogen conjugates. Journal of Materials Science: Materials in Medicine. 2010 January 1;21(1):73–80.

59. Wang N, Zhang R, Wang S-J, Zhang C-L, Mao L-B, Zhuang C-Y, Tang Y-Y, Luo X-G, Zhou H, Zhang T-C. Vascular endothelial growth factor stimulates endothelial differentiation from mesenchymal stem cells via Rho/myocardin-related transcription factor-A signaling pathway. International Journal of Biochemistry and Cell Biology. 2013 July 1;45(7):1447–1456.

60. Galas RJ, Liu JC. Vascular endothelial growth factor does not accelerate endothelial differentiation of human mesenchymal stem cells. Journal of Cellular Physiology. 2013 June 21.

61. Wang C-H, Wang T-M, Young T-H, Lai Y-K, Yen M-L. The critical role of ECM proteins within the human MSC niche in endothelial differentiation. Biomaterials. 2013 June;34(17):4223–4234.

62. Huang F, Fang Z-F, Hu X-Q, Tang L, Zhou S-H, Huang J-P. Overexpression of mir-126 promotes the differentiation of mesenchymal stem cells toward endothelial cells via activation of pi3k/akt and mapk/erk pathways and release of paracrine factors. Biological chemistry. 2013 May 28.

63. Janeczek Portalska K, Leferink A, Groen N, Fernandes H, Moroni L, van Blitterswijk C, de Boer J. Endothelial Differentiation of Mesenchymal Stromal Cells Kerkis I, editor. PloS one. 2012 October 4;7(10):e46842.

64. Benavides OM, Petsche JJ, Moise KJ, Johnson A, Jacot JG. Evaluation of endothelial cells differentiated from amniotic fluid-derived stem cells. Tissue Engineering Part A. 2012 June;18(11-12):1123–1131.

65. Pankajakshan D, Kansal V, Agrawal DK. In vitro differentiation of bone marrow derived porcine mesenchymal stem cells to endothelial cells. Journal of tissue engineering and regenerative medicine. 2012 May 18.

66. Xu J, Liu X, Chen J, Zacharek A, Cui X, Savant-Bhonsale S, Liu Z, Chopp M. Simvastatin enhances bone marrow stromal cell differentiation into endothelial cells via notch signaling pathway. American journal of physiology Cell physiology. 2009 March;296(3):C535–43.

67. Hamou C, Callaghan MJ, Thangarajah H, Chang E, Chang EI, Grogan RH, Paterno J, Vial IN, Jazayeri L, Gurtner GC. Mesenchymal stem cells can participate in ischemic neovascularization. Plastic and reconstructive surgery. 2009 February;123(2 Suppl):45S–55S.

68. Jazayeri M, Allameh A, Soleimani M, Jazayeri SH, Piryaei A, Kazemnejad S. Molecular and ultrastructural characterization of endothelial cells differentiated from human bone marrow mesenchymal stem cells. Cell biology international. 2008 October;32(10):1183–1192.

Chapter 2: 3D Image Quantification as a New Morphometry Method for Evaluating Vascular Network Development

OVERVIEW AND AIMS

Chapter 2 focuses on the development of a three-dimensional morphological quantification method as described in Aim 1, which is applied in Chapters 3 and 4 to validate MSC network development.*

Aim 1: Develop a morphological quantification method for analyzing vascular network development.

Rationale: Validating vascular tissue engineering strategies requires analysis of morphological outcomes. Current methods rely on two-dimensional techniques that eliminate valuable spatial information. A three-dimensional technique will provide more accurate analysis for future investigation of MSC tubulogenesis.

A. Optimize staining protocol for fluorescent microscopy of whole gel constructs.

B. Synthesize an image quantification pipeline for extracting three-dimensional data from microscopy images and outputting vascular-relevant metrics.

C. Validate new method using previous morphometry protocols and assays, including two-dimensional network tracing and aortic ring outgrowth.

*Significant portions of this chapter have been published in Rytlewski JA, Geuss LR, Anyaeji CI, Lewis EW, Suggs LJ. Three-dimensional image quantification as a new morphometry method for tissue engineering. Tissue Engineering Part C: Methods. 2012 July;18(7):507–516. Portions have been used with copyright permission from Mary Ann Liebert, Inc.

INTRODUCTION

Since the concept of tissue engineering was first introduced, in vitro cell culture has progressed from two-dimensional (2D) monolayers to three-dimensional (3D) extracellular matrix (ECM)-mimicking materials.[1] Now, encapsulating cells in 3D matrices is a common approach towards recapitulating the physiological niches of the human body. While numerous 3D substrates are available for in vitro tissue engineering models and applications, most methods of validation and quantification are still limited to 2D space (e.g., histological sectioning or single-plane microscopy). For engineered tissues, determining the success or failure of an approach relies heavily on morphological characterization to ascertain whether or not the desired cell types have been achieved. Morphometry can be further confounded in tissues originating from stem cell or progenitor lines where cell morphologies have the potential for even greater variation. Thus, an objective quantification pipeline is ideal, if not essential, to generate morphologic results with reliable significance and clear biological relevance.

Over the last decade, computational methods have facilitated the transition from observer-based histology to more quantitative measures.[2,3] Researchers can now choose from powerful commercial suites (e.g., Imaris, Lucis, Metamorph) capable of 3D and 4D image analysis and data processing.[4,5] Unfortunately, commercial software is often cost-prohibitive; hence, many computational techniques utilize and modify open-source packages such as NIH's ImageJ (Bethesda, MD). For example, microscope images can be manually traced by the user to quantify branch-like cellular morphologies.[6,7] More semi-automated methods rely on image segmentation to quickly derive surface area, perimeter length, and lacunarity measurements of tissue structures or cell growths.[8-13] However, these methods are based on 2D image analysis, which approximates 3D cellular

architecture with 2D planar projections. This approach is even less accurate when tissues exhibit anisometric growth patterns that fall outside the plane of imaging.

A number of challenges exist in morphological quantification of engineered microvasculature. This subset of cardiovascular tissue engineering aims to repair ischemic tissues by enhancing the natural processes of angiogenesis and vasculogenesis.[14] On the gross morphological scale, native microvasculature exhibits an arborealized hierarchical organization; however, on the microscale, these tubular structures have highly irregular geometries, making morphological analysis a complex and difficult process.[15] Prior to computational methods, histological sections were either subjectively scored according to the degree of network extensiveness (e.g., graded 1-5) or vessel numbers could be manually determined with Chalkley counts.[16,17] Since the advent of computational methods, studies report 2D metrics like vascular outgrowth lengths, network surface area-to-perimeter ratios, and microvascular densities (MVD).[16,18] While such techniques provide relative measures for comparison, the indirectness of 2D quantification creates two fundamental flaws: these morphological metrics fail to capture all possible spatial information and can lead to misleading conclusions when taken out of context. Varying degrees of observer (or user)-based subjectivity may further diminish the data's credibility. Hence a need exists to improve the current approach of morphological quantification in vascular tissue engineering and in tissue engineering as a whole.

To overcome some of the pitfalls of 2D methods, we assembled a quantitative pipeline for 3D morphological analysis based on 3D Slicer (www.slicer.org), an open-source MRI/CT software package.[19-21] We chose an open-source package as the backbone

for this method to encourage method adoption and collaboration. Specifically, this pipeline consists of three distinct protocols: (1) fluorescent staining of cells concomitant with confocal imaging; (2) enhancement and segmentation of confocal images with 3D model generation in 3D Slicer's Vascular Modeling Toolkit (VMTK, www.vmtk.org)[22,23]; and (3) computational analysis of 3D data into quantitative metrics using MATLAB® (MathWorks, Natick, MA). In the work presented here, we used two well-established angiogenesis assays as bases for demonstrating the validity and utility of 3D morphological quantification. The Nehls-Drenckhahn microcarrier bead assay[24] was used to demonstrate progenitor-derived tubulogenesis within variations of our previously reported PEGylated fibrin gels. PEGylated fibrin is uniquely able to direct progenitor cells towards an endothelial phenotype without the addition of soluble factors.[25-27] Briefly, this assay encapsulated bone marrow-derived human mesenchymal stem cells (MSCs) seeded on collagen-coated microcarrier beads (MCBs) in fibrin-based gels. The MCBs served a dual purpose, to support tubulogenic sprouting and to provide an artificial origin for quantitative analysis. The rat aortic ring assay served as an alternative in vitro model to better understand implications of the MCB studies.[28,29] With these experiments, we aim to show that a) our quantification pipeline allows us to successfully generate tailored 3D metrics for engineered vascular networks and that b) 3D metrics are significantly more accurate and insightful than their 2D analogues.

MATERIALS AND METHODS

Experimental Design

To illustrate the utility of this 3D quantification method, we explored two variables of fibrin-based gel composition: PEGylation and fibrin concentration. In

PEGylated fibrin gels, the molar ratio of fibrin-to-PEG remained constant across fibrin concentrations. From these two variables, we devised three experimental groups: 10mg/mL fibrin + 1mg/mL PEG, 7.5mg/mL fibrin + 0.75mg/mL PEG, and 5mg/mL fibrin + 0.5mg/mL PEG. Each fibrin concentration had a corresponding fibrin (only) control: 10mg/mL fibrin, 7.5mg/mL fibrin, and 5mg/mL fibrin. Matrigel, as a well-characterized commercial material for angiogenesis, served as a reference-type control.[30]

Materials

Dulbecco's phosphate buffered saline (PBS), phenol red-free low-glucose Dulbecco's modified Eagle's medium (DMEM), fetal bovine serum (FBS), GlutaMAX™-I (100x), and Calcein AM were obtained from Invitrogen (Carlsbad, CA). Endothelial growth media-2 (EGM-2) was purchased as a bullet kit from Lonza (Basel, Switzerland). Fibrinogen from human plasma (50-70% protein, ≥80% clottable), thrombin from human plasma (≥1,000NIH units/mg protein), collagen-coated Sigma-Solohill microcarrier beads, and 37% formaldehyde were obtained from Sigma-Aldrich (St. Louis, MO). Penicillin-streptomycin and trypsin/EDTA were obtained from ATCC (Manassas, VA). Phenol red-free growth factor-reduced Matrigel was obtained from BD Biosciences (San Jose, CA). Homo-difunctional succinimidylglutarate polyethylene glycol (PEG-$(GS)_2$, 3400 Da) was obtained from NOF America (White Plains, NY).

Cell maintenance

Bone marrow-derived MSCs (Lonza, Basel, Switzerland) were cultured and expanded in tissue culture-treated plastic flasks (Corning, Corning, NY) with DMEM containing 10% FBS, 1% penicillin-streptomycin, and 2nM GlutaMAX™-I. As stated by

the manufacturer, MSCs were derived from normal bone marrow culture; this subpopulation tests positive for CD105, CD166, CD29, and CD44 and tests negative for CD14, CD34 and CD45. All cell cultures were incubated at 37°C with 5% CO_2.

Cell seeding of microcarrier beads

Collagen-coated microcarrier beads (MCBs) were autoclaved in PBS according to the manufacturer's instructions. MCBs were primed in serum-supplemented DMEM for 1 hour at 37°C. MSCs (passage 3-5) were then trypsinized, centrifuged into a pellet, and re-suspended with collagen-coated microcarrier beads (MCBs) at a concentration of 1.4x106 cells/20mg MCBs. The culture was gently agitated every 30 minutes over a 4-hour incubation period to minimize MCB aggregation. After seeding, the MCB culture was passed through a 70μm cell strainer and rinsed with PBS to remove unattached cells. The MCB culture was finally resuspended in media at a concentration of 20mg MCBs/mL.

Preparation of gel components

Human fibrinogen (Fgn) was prepared at concentrations of 80mg/mL, 60mg/mL, and 40mg/mL in PBS, pH 7.8, and solubilized for 2-3 hours in a 37°C water bath. PEG-$(GS)_2$ was solubilized immediately before use at 8mg/mL, 6mg/mL, and 4mg/mL in PBS, pH 7.8. Human thrombin was reconstituted in sterile ddH_2O at 100U/mL per the manufacturer's instructions and frozen at -80°C. Frozen thrombin aliquots were thawed and diluted to a final concentration of 25U/mL in 30mM CaCl2. All three solutions were sterile-filtered (0.22μm pore size).

PEGylation of fibrinogen and gelation

Fgn was combined with an equal volume of PEG-$(GS)_2$ (1:10 molar ratio) for 3 minutes at room temperature to allow for PEGylation. In control gels, PBS was substituted for PEG-$(GS)_2$. The MCB suspension was diluted 1:5 with media and combined with an equal volume of PEGylated Fgn (or PBS + Fgn) in two-chambered coverglass (Nuncbrand Lab-Tek II; Thermo Scientific, Rochester, NY). The solution was briefly mixed to evenly suspend MCBs. Gels were enzymatically crosslinked with an equal volume of thrombin, yielding a final concentration of 10mg/mL Fgn and 1mg/mL PEG-(GS)2. For the 1mL gels made here, exact volumes of each component were 125μL Fgn, 125μL PEG-$(GS)_2$ (or PBS), 250μL of 1:5 diluted MCBs, and 500μL thrombin. Unreacted PEG-$(GS)_2$ was removed by rinsing the gels with 3-4 volumes of media. Finally, serum-supplemented media was added to the gels and changed daily for 7 days.

Rat aortic ring culture

Rat aortas were a gift from the lab of Dr. Christine E Schmidt. Briefly, Fischer rats were given an intraperitoneal injection of 1000U/kg heparin 15min prior to perfusion with PBS. Proximal aortas were harvested and rinsed in PBS. Under a dissection scope, fibroadipose tissue was removed and aortas sliced into 1mm thick rings. Rings were rinsed three times in an anti-contamination cocktail (EMG-2 with Gentamicin) before a final rinse with EMG-2. 10mg/mL PEGylated fibrin gels were prepared as described above. To encapsulate aortic rings, 125μL of gel was first polymerized in each well of an eight-chambered coverglass (Nuncbrand Lab-Tek II). Aortic rings were vertically placed in the center of each well, and then another 125μL of gel was polymerized on top. As

before, gels were rinsed to remove unreacted PEG-$(GS)_2$. Aortic rings were cultured for 7 days with EGM-2.

Fluorescent staining

On Day 7, gels were rinsed with fresh PBS (with Ca^{+2}, Mg^{+2}) every 15 minutes for a total of 90 minutes. PBS was removed and 10μM Calcein AM was added for 1 hour. Gels were subsequently rinsed with PBS every 5 minutes for a total of 20 minutes, fixed with 4% neutral-buffered formalin for 30 minutes, and then rinsed again 2-3 times with PBS.

Confocal microscopy

A confocal scanning microscope (SP2 AOBS; Leica Microsystems, Bensheim Germany) was used to collect fluorescent image stacks. Under a 10x objective with 512x512 image resolution, Calcein AM was excited with an Argon laser at 496nm and emission was detected from 510-520nm. The z-slice thickness was adjusted to maintain isometric voxel dimensions (approximately 3μm in each plane). Three z-stacks were collected per experimental group. For the MCB assay, each stack focused on one MCB and its cellular outgrowth. For the aortic ring assay, we limited each field of view to approximately 50% of the specimen due to size constraints.

Image processing and 3D data generation

All image processing was done in a 64-bit Linux (Ubuntu, Natty Narwhal distribution) environment with 8GB of memory. Each confocal stack (Figure 2.1A) was

first converted into a Visualization Toolkit (.vtk) file using the VTK Writer in ImageJ's 3D IO plug-in (Release 1.2.4; ImageJ Plugin Project). The resulting binary .vtk was loaded into 3D Slicer (Release 3.6, 64-bit Linux) as a volume and processed as follows (default values were used unless otherwise stated):

1. An additive arithmetic filter was twice applied to quadruple original pixel values. This enhanced dimly fluorescent regions and improved the detectability of valuable pixels.

2. Prepared image volumes were preprocessed in VMTK's Vessel Enhancement module (downloaded June 2010), based on Frangi's vesselness function. Settings were changed to a minimum diameter of 0.1, maximum diameter of 5.0, plate-like and line-like structure of 0.2, blob-like structure of 200, and a contrast threshold of 10. This algorithm predicts which image regions contain tubular structures via eigenvalue analysis of the local Hessian matrix at multiple length scales.[31,32] Therefore, continuous paths of fluorescence were intensified while background noise was suppressed (Figure 2.1B).

3. Prior to segmentation, source seeds were manually placed at all network origins directly connected to the MCB and the threshold slider set to 0.05. Cell origins not directly attached to the MCB were ignored. These user-placed seeds initialized the Fast Marching Upwind Gradient (FMUG) used by VMTK's Easy Level Set Segmentation module.[23,33-35] By omitting target seeds at this step, the algorithm was allowed to determine terminal points for each network instead of the user. The 3D polydata model produced by FMUG (Figure 2.1C) was then

smoothed by Geodesic Active Contours evolution (Figure 2.1D and 2.1E). Evolution settings were changed to an inflation of 60, curvature of 60, and attraction to ridges of 40. Adequate model inflation was essential since the next step is extremely sensitive to surface noise.

4. In VMTK's Centerlines, target seeds were manually placed at all network ends as they appeared in the evolved 3D model (Figure 2.1F). Source and target fiducial lists were used by VMTK to calculate an imbedded Voronoi diagram (Figure 2.1G). Geometrically, the connected vertices of the Voronoi diagram correspond to the circumcenters of internal tetrahedra (based on Delaunay's tessellation).[23,33,35] Thus, these vertices represent a path equidistant to local surfaces at each plotted point, i.e., the model's centerline. Centerlines data were extracted (Figure 2.1H) and exported to a text (.txt) file as xyz-coordinates with associated radii.

Image data analysis and quantification

A brief MATLAB (Release 2008a for Macintosh) program was coded to process the centerlines.txt file into descriptive metrics. Table 2.1 lists and defines key terms and metrics used to define this data; a corresponding schematic of these definitions is provided in Figure 2.2. Non-unique coordinates were removed before parsing the remaining coordinates into their respective discrete paths (i.e., microvascular network segments) such that no regions were retraced. A user-input threshold determined the start of a new segment such that a distance greater than the threshold indicated a nonconsecutive coordinate; in all cases, a value of 5-10 voxels was sufficient. Voxel

space was converted back to original physical dimensions (microns) using the scalar information recorded during image capture. Five metrics were directly calculated from this coordinate data: (1) segment volume[36], (2) 3D segment length, (3) 2D xy-plane segment length, (4) 2D xz-plane segment length, and (5) 2D yz-plane segment length. Two additional metrics, (6) number of segments per network and (7) degree of branching per network were directly taken from the number of segments parsed and source/target fiducial lists, respectively. Segment metrics (1-5) were summed to obtain whole network metrics.

Statistical analysis

The assumption of normality was first confirmed with a Shapiro-Wilk w-test. A two-way analysis of variance was applied to each quantitative metric to determine significance between fibrin concentrations and PEGylation. Where significance was found, post-hoc tests were performed to further determine specific relationships of statistical significance. Bonferroni was applied where appropriate. Linear regression was used to determine the strength of correlation between types of length measurements (e.g., 3D versus 2D xy-plane) with a supplementary ANOVA to ascertain whether the slope was zero. All statistical tests were completed in JMP (Release 9.0.2; SAS Institute Inc., Cary, NC).

RESULTS AND DISCUSSION

Samples were stained, fixed, and imaged on day 7 of culture. Representative confocal images with overlaid models are given for each MCB group in Figure 2.3. From these images, we observed that PEGylated fibrin encouraged more extensive vascular

networks than fibrin. MSCs in fibrin possessed a more proliferative and migratory phenotype instead, with more cells present but fewer incorporated into networks. Marginal, if any, differences were evident between the fibrin concentrations examined within both the PEGylated fibrin and fibrin groups. These qualitative observations collectively suggest that fibrin PEGylation is the greater contributing factor in MSC tubulogenesis than fibrin concentration within our in vitro system.

Validity of 3D Slicer and computational artifacts

We noticed a consistent computational artifact during the generation of 3D models: in networks with extensive branching (primarily the PEGylated fibrin groups), some branches appeared to be prematurely cropped before their natural termini. We suspect inhomogeneous intracellular dye distribution created regions of weak fluorescent signal that the marching front segmentation algorithm was unable to bridge. To verify that this computational error did not adversely affect our results, we benchmarked our method against an existing 2D approach based on manual tracing of network outgrowths (ImageJ Simple Neurite Tracer). Lengths from each method were appropriately matched in the 2D xy-plane. Figure 2.4 shows 2D network lengths generated in 3D Slicer alongside those generated in ImageJ for 10mg/mL PEGylated fibrin and its corresponding (unmodified) fibrin control group. Network lengths calculated from 3D Slicer and ImageJ were not statistically different, indicating that the computational artifact did not skew the value of our calculations. Similarly, both methods were able to demonstrate that PEGylated fibrin networks were significantly longer than fibrin controls. This study led us to conclude that our method is reasonably calibrated to

previously reported techniques, producing similar values and maintaining statistical discrimination power.

Comparison of 2D versus 3D morphological quantification of vascular networks

Four different measures of vascular network length were calculated for all seven experimental groups (Figure 2.5): 3D length, 2D length in the xy-plane, 2D length in the xz-plane, and 2D length in the yz-plane. All measures were derived from 3D Slicer data. When comparing the four different length measures within each experimental group, we found that 2D lengths repeatably failed to agree with their 3D counterpart. This trend appears to directly correlate with the extent of network outgrowth, with PEGylated fibrin groups having the greatest variability. Despite overall inconsistencies, linear regression models indicated strong similarities between 2D xy-plane and 3D network lengths ($R2 > 0.99$). ANOVA confirmed this correlation for the 7.5mg/mL and 5mg/mL PEGylated fibrin groups ($p < 0.05$). These results suggest that 2D projections in the imaging (xy) plane are a reasonable estimate of true network length. However, this similarity is likely an incidental product of our vascular networks exhibiting significant growth bias "in-plane" with imaging; confocal volume aspect ratios ranged from 3:1 to 5:1 (xy-plane:z-axis). Such anisometric growth bias maximized spatial information in the xy-plane and facilitated a near-accurate 2D approximation of network length.

In culture systems with isometric growth or with anisometric growth that occurs "out-of-plane" with imaging, reliable correlation of 2D and 3D measures cannot be presumed. To substantiate this claim, we applied our 3D morphological quantification method to measure aortic ring outgrowth in 10mg/mL PEGylated fibrin gels. Outgrowth lengths plotted in Figure 2.6 show significant disagreement between (all three) 2D

estimates and the actual 3D value. We observed no statistically significant difference in 2D lengths between each of the three planes (xy, xz, yz), suggesting the aortic ring approximates an isometric growth pattern. Typically, this ring outgrowth would be quantified via manual tracing of a 2D image, similar to the protocol typically entailed by the MCB assay. The results of this study suggest that previously reported network lengths in fact significantly underestimated the true length of aortic ring outgrowth.

3D morphometry provides more biologically relevant metrics

As previously mentioned, 2D morphological analysis of vasculature is limited to reporting basic metrics such as surface area, perimeter length, and network length. While important, these 2D metrics fail to provide a complete picture. For example, studying the lumenal architecture of vascular networks necessitates accurate estimates of network volume. Volume estimates from current 2D analytical methods require simplifying assumptions that could distort or misrepresent the true spatial structure of the vascular network. Direct estimates obtained from 3D analysis would overcome such issues and provide clearer, more accurate measures. 3D morphological analysis easily provides a measure of volume (Figure 2.7A) in addition to network length (Figure 2.5) and other basic metrics such as the number of network segments and degree of network branching (Figure 2.7B and 2.7C, respectively). Through further studies, a predictive model may even be developed to correlate volume with lumen formation. More broadly, quantitative morphological outcomes may form the basis of predicting vascular function.

Translating qualitative observation into the quantitative domain

The premise of morphological quantification is to convert qualitative observations into numerical values that enable meaningful statistical analysis. In this sense, any one metric, especially one derived from 2D analysis, is unable to fully and accurately represent the complex morphologies of vascular networks. For example, two networks may exist with similar lengths but possess very different morphologies (e.g., short with many branches versus long with few branches). Here, we illustrate how a set of biologically relevant 3D metrics is able to fully capture the nuances of vascular network morphology, thus providing more robust quantitative support for our conclusions previously drawn using only qualitative observations.

From confocal images, we observed that (a) PEGylated fibrin produced more extensive vascular networks than fibrin only gels, and (b) fibrin PEGylation was more influential to vascular network development than fibrin concentration. Network length (3D and 2D), volume, and number of segments all trended in agreement with this qualitative assessment. ANOVA revealed fibrin PEGylation to be highly significant in MSC-derived vascular network formation (volume, $p < 0.001$; length and segment number, $p < 0.0001$). Post hoc tests confirmed PEGylated fibrin networks had significantly longer lengths (Figure 2.8), larger volumes (Figure 2.7A), and more segments per network (Figure 2.7B) than fibrin controls. Matched for PEGylation, no statistical significant differences were observed among samples with varying fibrin concentrations, including the degree of network branching (Figure 2.7C).

Interestingly, volume and number of network segments (Figures 2.7A and 2.7B, respectively) indicated Matrigel networks were similar to those of PEGylated fibrin. Network length, on the other hand, suggested a significant difference between the two

materials. As previously discussed, the use of a single metric produces misleading conclusions, and only the additional context from multiple metrics can provide a full picture of the network morphology. Here, the collective metrics suggest Matrigel networks are much shorter and broader than PEGylated fibrin networks despite having a similar number of branches.

CONCLUSIONS

Our 3D morphological quantification method was able to numerically capture the qualitative observations regarding vascular network development in fibrin-based gels. Final numerical outcomes paralleled the original observations: significant experimental differences (PEGylation) were highlighted while negligible differences failed to be recognized (fibrin concentration). Quantifying complex tissue properties such as morphology helps limit the error associated with subjective versus objective measures. Minimizing user-based decisions and relying more heavily on semi-automated computational approaches further improves objectivity. Additionally, matching the 3D nature of complex tissues with an appropriately 3D analytical technique can sharpen the accuracy of morphological assessment. As the field of tissue engineering continues to progress and produce increasingly complex constructs, methods of construct assessment must progress in tandem to ensure our results remain robust and relevant. The method described here will hopefully serve as a basic platform to grow more detailed 3D quantification approaches.

Metric	*Definition*
Network	The tubulogenic outgrowth of one microcarrier bead limited to cell growth directly attached to the microcarrier bead
Segment	A unique path within the tubulogenic outgrowth of one network; each segment has one origin and one terminus
Volume	Calculated via cylindrical approximation between adjacent coordinates of a segment[34]; cylindrical volume is assumed to have two radii of unequal length
Degree of Branching	Ratio of target:seed fiducials for a given network
3D Length	Segment length as calculated with 3D distance formula using (x,y,x) coordinates of centerlines; distances between adjacent coordinates of a segment were summed to achieve one segment length; segment lengths for a network were summed to achieve one network length
2D Length	Segment length as calculated with 2D distance formula using either (x,y), (x,z), or (y,z) coordinate pairs

Table 2.1: List of quantitative metrics and their corresponding conceptual and/or mathematical definition.

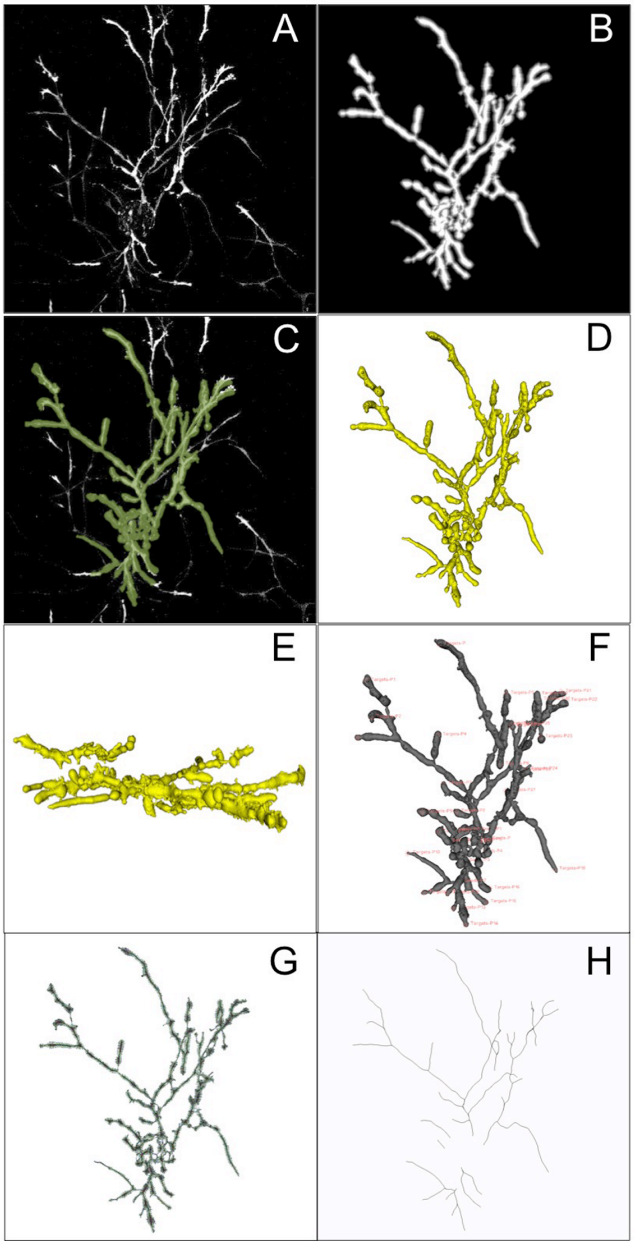

Figure 2.1: Image processing steps in 3D Slicer's VMTK. Sample shown is from the 10mg/mL PEGylated fibrin group. (A) Z-projection of the original confocal volume using standard deviation of pixel values; (B) Z-projection of the enhanced confocal volume after applying Frangi's vesselness; (C) image from (A) with overlay of segmented 3D model in green; (D&E) evolved model from (C) shown in the XY- and YZ-planes, respectively; (F) evolved model with source and target fiducial placement; (G) Voronoi diagram of evolved model; (H) centerlines skeleton extracted from (G).

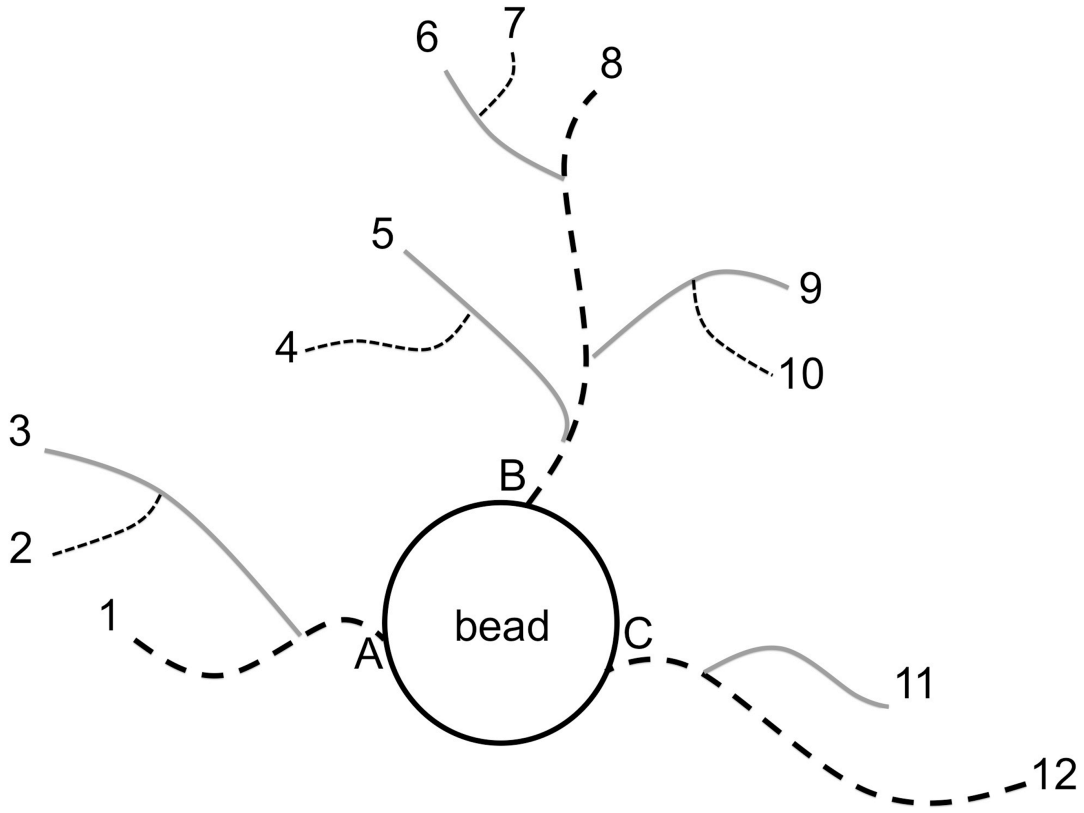

Figure 2.2: Centerline traces of an MCB with tubular outgrowths. Each numbered line represents a segment defined by a unique, non-overlapping path; all segments together (12 total) represent one network. Similarly, numbers correspond with target fiducials while letters correspond with source fiducials.

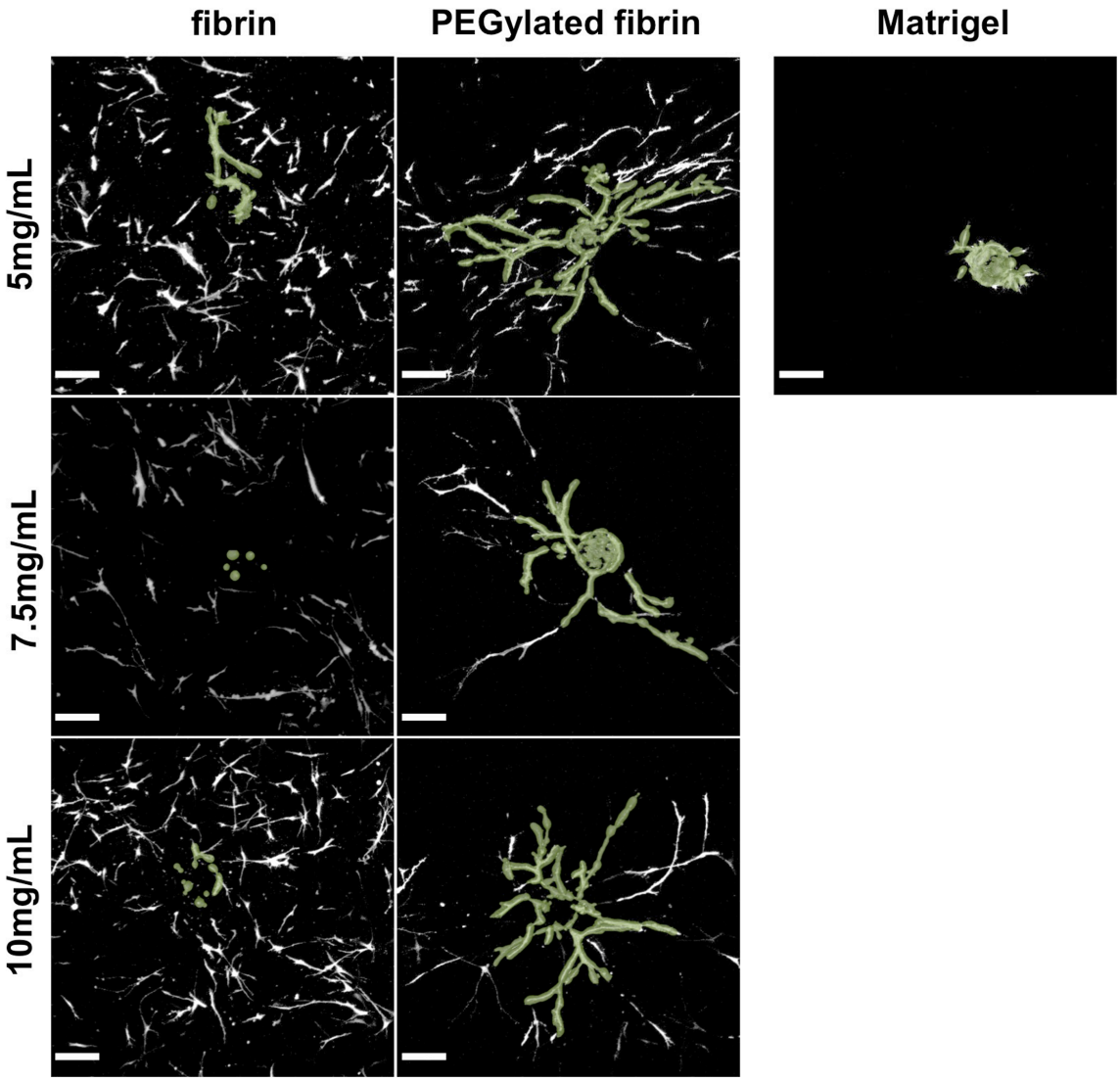

Figure 2.3: Confocal z-stack projections. Image stacks for each experimental group were captured under 10x objective; shown is a z-projection using the standard deviation of pixel values. Segmented 3D models are overlaid in green. Scale bar = 200μm.

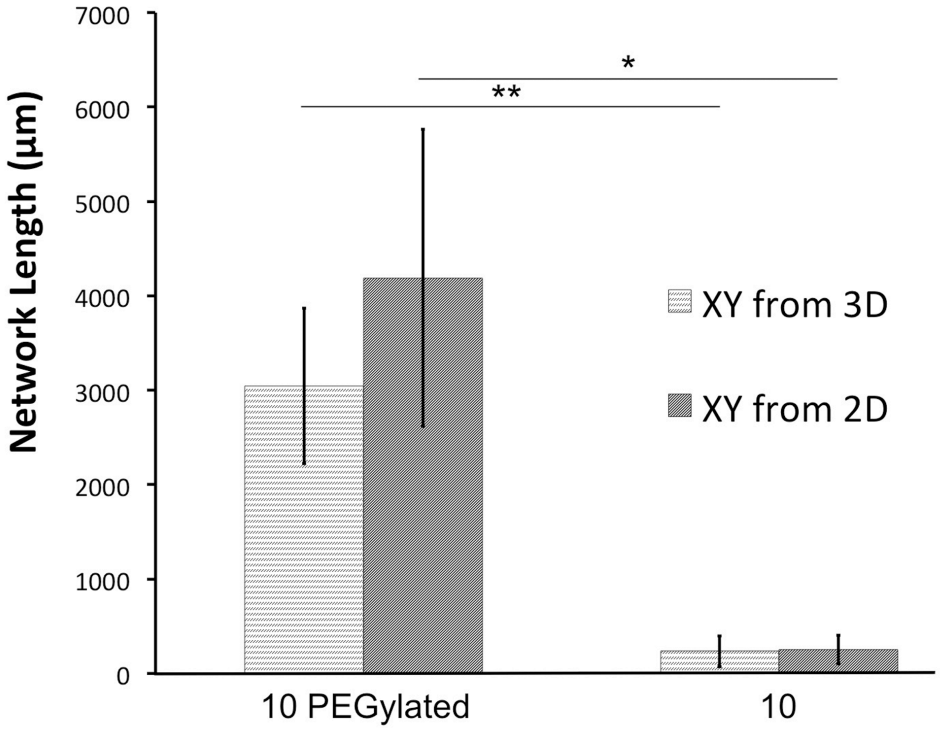

Figure 2.4: Validation of systematic error. X-axis indicates concentration of fibrin in mg/mL. Network branches were traced on z-projections of confocal stacks using ImageJ's Simple Neurite Tracer plug-in. Calculated network lengths based on our computational method were not significantly different than lengths manually traced. However, both methods were able to discern significance between vascular networks formed in PEGylated fibrin and fibrin controls; bars indicate standard error, * $p < 0.05$, ** $p < 0.01$.

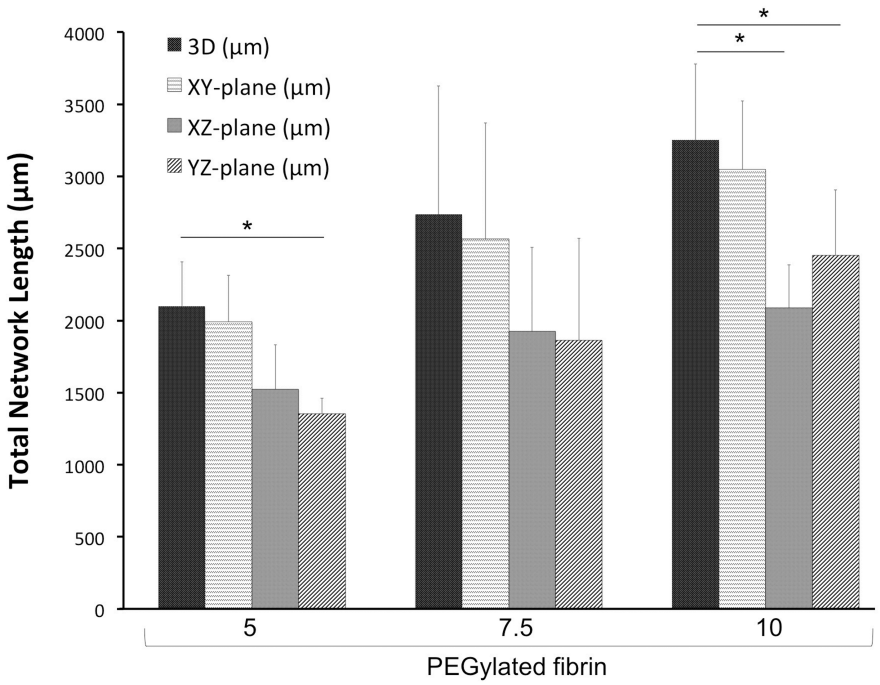

Figure 2.5: Comparison of 3D and 2D measurement of network length. X-axis indicates concentration of fibrin in mg/mL. 2D measures did not reliably agree with corresponding 3D values and underestimated network length by as much as 40%; bars indicate standard error, *$p < 0.05$.

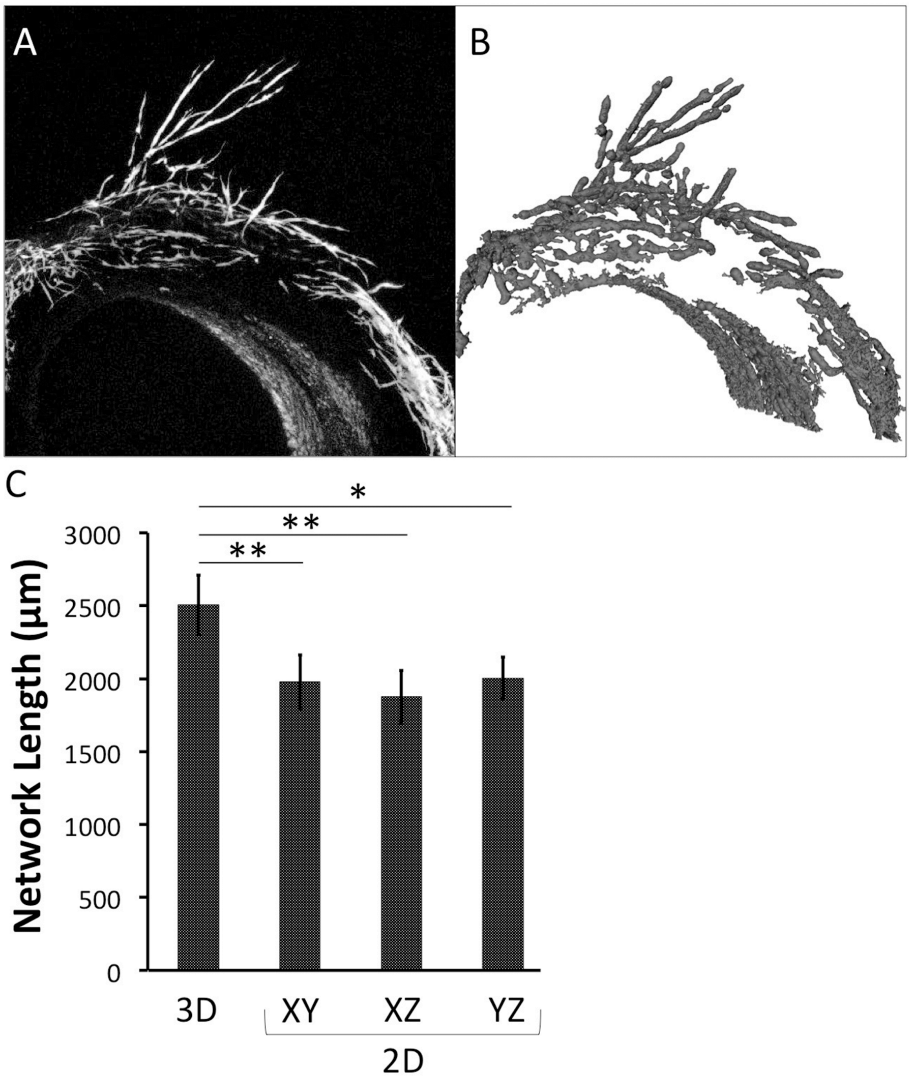

Figure 2.6: Comparison of 3D and 2D measurement of aortic ring outgrowth. (A) Confocal z-stack projection of a rat aortic ring with outgrowth in PEGylated fibrin. (B) 3D model generated from the image stack represented in (A). (C) 2D measures significantly underestimated actual 3D values in all three planes; bars indicate standard error, *$p < 0.05$, **$p < 0.01$.

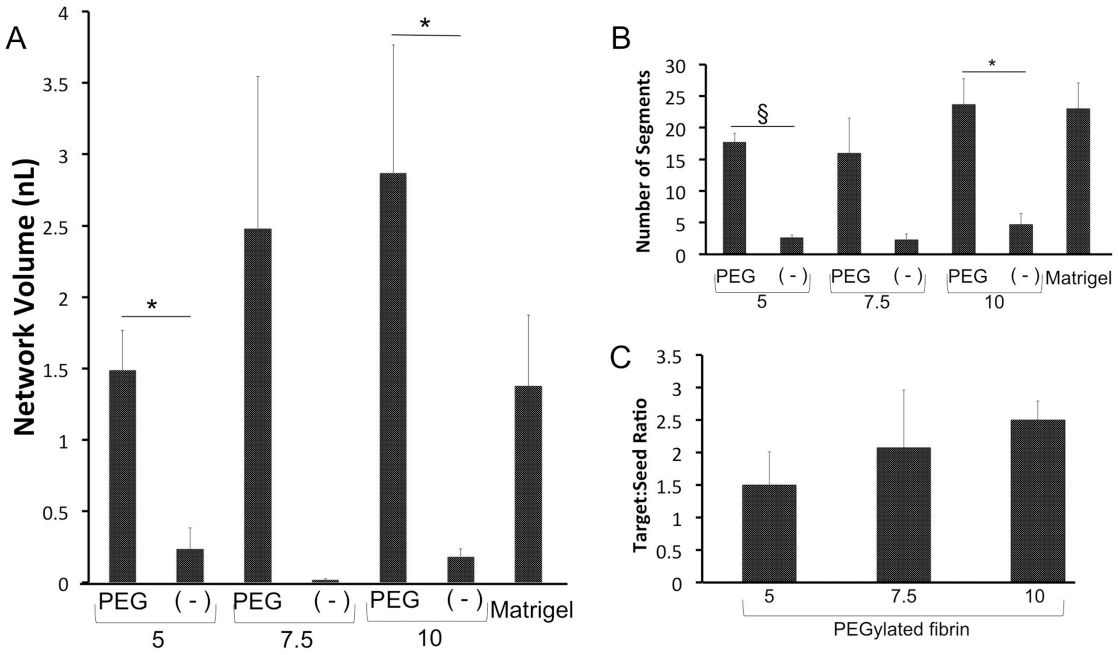

Figure 2.7: Quantification of angiogenesis-related metrics as processed in MATLAB. . X-axis indicates concentration of fibrin in mg/mL; "PEG" indicates PEGylated fibrin and "(-)" indicates fibrin control, (A) Average network volume from cylindrical approximation. (B) Average number of segments per network. (C) Degree of branching for PEGylated fibrin groups. Due to the lack of clear branching, this metric was unable to be calculated for fibrin controls or Matrigel groups. In (A) and (B), PEGylated fibrin had significantly higher group means than fibrin controls; bars indicate standard error, *$p < 0.05$, § $p < 0.001$.

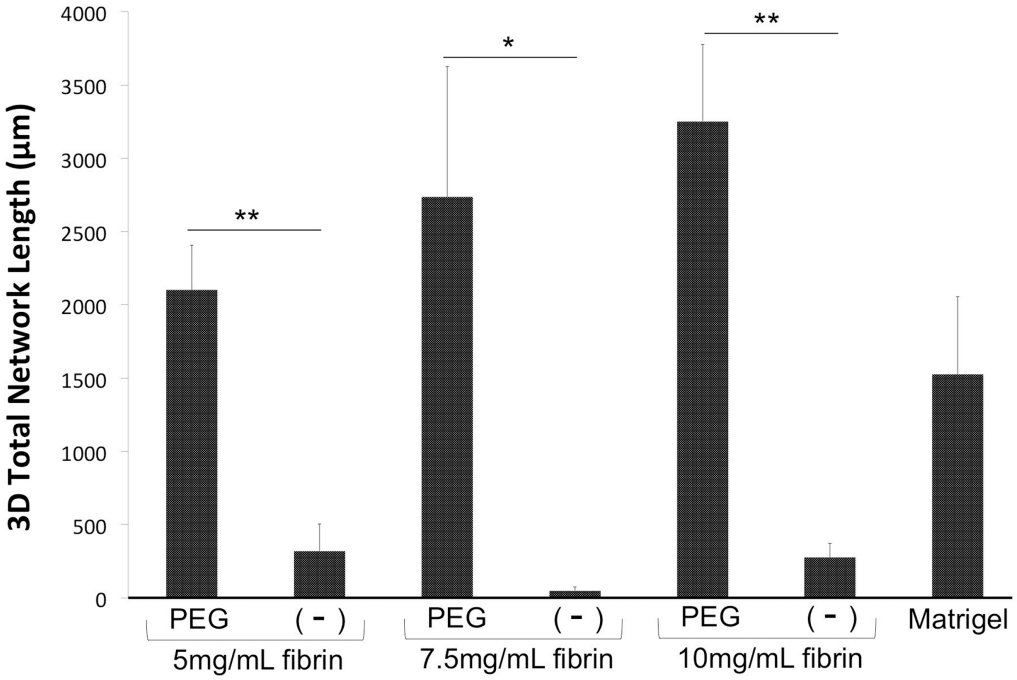

Figure 2.8: Comparison of PEGylated fibrin and fibrin network lengths as measured in 3D and 2D. "PEG" indicates PEGylated fibrin and "(-)" indicates fibrin control. PEGylated fibrin gels stimulated more extensive MSC network formation with significantly longer outgrowth than fibrin controls; bars indicate standard error, *$p < 0.05$, **$p < 0.01$.

REFERENCES

1. van Winterswijk P, Nout E, Matrix E. Tissue engineering and wound healing: an overview of the past, present, and future. Wounds. 2007.

2. Kirbas C, Quek F. A review of vessel extraction techniques and algorithms. ACM Computing Surveys. 2004;36(2):81–121.

3. Smith TG, Marks WB, Lange GD, Sheriff WH, Neale EA. A fractal analysis of cell images. Journal of neuroscience methods. 1989 March;27(2):173–180.

4. Ghajar CM, Kachgal S, Kniazeva E, Mori H, Costes SV, George SC, Putnam AJ. Mesenchymal cells stimulate capillary morphogenesis via distinct proteolytic mechanisms. Experimental Cell Research. 2010 March 10;316(5):813–825.

5. Walter T, Shattuck D, Baldock R, Bastin M. Visualization of image data from cells to organisms. Nat Methods. 2010.

6. Cregg JM, Wiseman SL, Pietrzak-Goetze NM, Smith MR, Jaroch DB, Clupper DC, Gilbert RJ. A rapid, quantitative method for assessing axonal extension on biomaterial platforms. Tissue Engineering Part C: Methods. 2010 April;16(2):167–172.

7. Martineau L, Doillon CJ. Angiogenic response of endothelial cells seeded dispersed versus on beads in fibrin gels. Angiogenesis. 2007 January 1;10(4):269–277.

8. Al-Kofahi KA, Lasek S, Szarowski DH, Pace CJ, Nagy G, Turner JN, Roysam B. Rapid automated three-dimensional tracing of neurons from confocal image stacks. IEEE transactions on information technology in biomedicine : a publication of the IEEE Engineering in Medicine and Biology Society. 2002 June 1;6(2):171–187.

9. Doukas CN, Maglogiannis I, Chatziioannou A, Papapetropoulos A. Automated angiogenesis quantification through advanced image processing techniques. Conference proceedings : ... Annual International Conference of the IEEE Engineering in Medicine and Biology Society. IEEE Engineering in Medicine and Biology Society. Conference. 2006;1:2345–2348.

10. Abdul-Karim M-A, Al-Kofahi K, Brown EB, Jain RK, Roysam B. Automated tracing and change analysis of angiogenic vasculature from in vivo multiphoton confocal image time series. Microvascular research. 2003 September;66(2):113–125.

11. Gould DJ, VADAKKAN TJ, POCHÉ RA, Dickinson ME. Multifractal and lacunarity analysis of microvascular morphology and remodeling. Microcirculation (New York, N.Y. : 1994). 2011 February;18(2):136–151.

12. Wild R, Ramakrishnan S, Sedgewick J, Griffioen AW. Quantitative assessment of angiogenesis and tumor vessel architecture by computer-assisted digital image analysis: effects of VEGF-toxin conjugate on tumor microvessel density. Microvascular research. 2000 May;59(3):368–376.

13. Bock F, Onderka J, Hos D, Horn F, Martus P, Cursiefen C. Improved semiautomatic method for morphometry of angiogenesis and lymphangiogenesis in corneal flatmounts. Experimental eye research. 2008 November;87(5):462–470.

14. Patan S. Vasculogenesis and angiogenesis as mechanisms of vascular network formation, growth and remodeling. Journal of neuro-oncology. 2000 January 1;50(1-2):1–15.

15. Grizzi F, Colombo P, Taverna G, Chiriva-Internati M, Cobos E, Graziotti P, Muzzio PC, Dioguardi N. Geometry of human vascular system: is it an obstacle for quantifying antiangiogenic therapies? Applied immunohistochemistry & molecular morphology : AIMM / official publication of the Society for Applied Immunohistochemistry. 2007 June;15(2):134–139.

16. Staton CA, Reed MWR, Brown NJ. A critical analysis of current in vitro and in vivo angiogenesis assays. International Journal of Experimental Pathology. 2009 June 1;90(3):195–221.

17. Fox SB, Leek RD, Weekes MP, Whitehouse RM, Gatter KC, Harris AL. Quantitation and prognostic value of breast cancer angiogenesis: comparison of microvessel density, Chalkley count, and computer image analysis. The Journal of pathology. 1995 November;177(3):275–283.

18. Fox SB, Harris AL. Histological quantitation of tumour angiogenesis. APMIS : acta pathologica, microbiologica, et immunologica Scandinavica. 2004 June;112(7-8):413–430.

19. Pieper S, Halle M, Kikinis R. 2004 2nd IEEE International Symposium on Biomedical Imaging: Macro to Nano (IEEE Cat No. 04EX821). In: Vol. 2. IEEE; 2004. pp. 632–635.

20. Pieper S, Lorensen B, Schroeder W, Kikinis R. The NA-MIC Kit: ITK, VTK, pipelines, grids and 3D slicer as an open platform for the medical image computing community. 2006:698–701.

21. Gering D, Nabavi A, Kikinis R, Grimson W, Hata N, Everett P, Jolesz F, Wells WM. An integrated visualization system for surgical planning and guidance using image fusion and interventional imaging. … Image Computing and …. 1999.

22. Lindig TM, Kumar V, Kikinis R, Pieper S, Schrödl F, Neuhuber WL, Brehmer A. Spiny versus stubby: 3D reconstruction of human myenteric (type I) neurons. Histochemistry and cell biology. 2009 January;131(1):1–12.

23. Antiga L, Piccinelli M, Botti L, Ene-Iordache B, Remuzzi A, Steinman DA. An image-based modeling framework for patient-specific computational hemodynamics. Medical & biological engineering & computing. 2008 November;46(11):1097–1112.

24. Nehls V, Drenckhahn D. A novel, microcarrier-based in vitro assay for rapid and reliable quantification of three-dimensional cell migration and angiogenesis. Microvascular research. 1995 November;50(3):311–322.

25. Zhang G, Drinnan CT, Geuss LR, Suggs LJ. Vascular differentiation of bone marrow stem cells is directed by a tunable three-dimensional matrix. Acta Biomaterialia. 2010 September;6(9):3395–3403.

26. Zhang G, Wang X, Wang Z, Zhang J, Suggs L. A PEGylated fibrin patch for mesenchymal stem cell delivery. Tissue engineering. 2006 January;12(1):9–19.

27. Liu H, Collins SF, Suggs LJ. Three-dimensional culture for expansion and differentiation of mouse embryonic stem cells. Biomaterials. 2006 December 1;27(36):6004–6014.

28. Go RS, Owen WG. The rat aortic ring assay for in vitro study of angiogenesis. Methods in molecular medicine. 2003;85:59–64.

29. Ueda EK, Walker AM. Rat aorta ring ex-vivo angiogenesis assay. 2010 June 29:1–9.

30. Crabtree B, Subramanian V. Behavior of endothelial cells on Matrigel and development of a method for a rapid and reproducible in vitro angiogenesis assay. In vitro cellular & developmental biology Animal. 2007 February 1;43(2):87–94.

31. Frangi AF, Niessen WJ, Vincken KL, Viergever MA. Lecture Notes in Computer Science. (Wells WM, Colchester A, Delp S, editors.). Berlin/Heidelberg: Springer-Verlag; 1998 pp. 130–137.

32. Enquobahrie A, Ibanez L, Bullitt E. Vessel enhancing diffusion filter. The Insight Journal. 2007.

33. Piccinelli M, Veneziani A, Steinman DA, Remuzzi A, Antiga L. A framework for geometric analysis of vascular structures: application to cerebral aneurysms. IEEE Transactions on Medical Imaging. 2009 August;28(8):1141–1155.

34. Cohen LD, Deschamps T. Segmentation of 3D tubular objects with adaptive front propagation and minimal tree extraction for 3D medical imaging. Computer methods in biomechanics and biomedical engineering. 2007 August;10(4):289–305.

35. Antiga L, Ene-Iordache B, Remuzzi A. Computational geometry for patient-specific reconstruction and meshing of blood vessels from MR and CT angiography. IEEE Transactions on Medical Imaging. 2003 May;22(5):674–684.

36. Vilanova A, Gröller E. Cylindrical approximation of tubular organs for virtual endoscopy. Proc of Comput Graphics and Imaging. 2000;283.

Chapter 3: Characterization of biomaterial and cellular changes induced by fibrin PEGylation

OVERVIEW AND AIMS

Chapter 3 focuses on characterization of both biomaterial properties and cellular behaviors as outlined in Aim 2. The morphological pipeline described in Chapter 2 is applied in this endeavor.

Aim 2: Determine the impact of fibrin PEGylation on the morphologic and phenotypic changes of MSCs.

Rationale: Fibrin matrices are a common natural polymer in vascular tissue engineering but these networks are unable to induce tubulogenesis without additional soluble factors. Outcomes aim to characterize cell changes associated with biomaterial properties of PEGylated fibrin.

A. Characterize rheological and diffusional properties of fibrin-based gels.
B. Assess MSC tubular networks by quantitative morphometry (from Aim 1) and verify lumenal space development.
C. Determine cytoskeletal and integrin components responsible for cell motility
D. Measure biologic response of MSCs via cell proliferation, protein marker expression, and secreted factor production.
E. Implicate potential mechanisms that link results from 2A and 2B.

INTRODUCTION

Autologous cell-based therapies are a developing strategy to address ischemic morbidities and promote revascularization of oxygen- and nutrient-deprived tissue. Currently, common targets include sites of acute injury, large or chronic wound beds, and critical limb ischemia.[1-6] For these applications, the end-goal is to achieve revascularization, which is often the rate-limiting step in wound healing.[7-10] Establishing a robust blood supply better sustains the high metabolic demands of inflammation and tissue remodeling and promotes more rapid resolution of the damaged tissue.[7] Healing outcomes have been further improved when biomaterial gels, foams, or scaffolds are co-delivered with the grafted stem cells.[11,12] These biomaterials serve a threefold purpose: (1) to act as a cell delivery vehicle, (2) to enhance and direct stem cell behavior, and (3) to serve as bioactive filler that physically and biochemically integrates with local tissues.

Biomaterials for vascular tissue engineering and wound healing applications typically utilize extracellular matrix (ECM) proteins, such as collagen, elastin, fibronectin, and laminin.[13-17] Fibrin, a clotting protein derived from thrombin proteolysis of fibrinogen, is another commonly used natural polymer.[12,18] Although ECM components are more physiologically abundant, fibrin has a superior ability to stimulate neovascularization.[19,20] Studies on soft matrix composition have showed that vascular network development is directly related to fibrin content and inversely correlated to matrix stiffness.[17,21-23] Fibrin matrices also stimulate stromal cell production of angiogenic paracrine factors, encouraging innate neovascularization mechanisms of the host vasculature. In stem cell populations, fibrin content has been associated with upregulation of endothelial-like genes.[24] Despite the bioactive advantages of fibrin matrices, pure fibrin is rapidly degraded *in vivo* via natural fibrinolytic cascades, which limits its

therapeutic window. Hence, fibrin-composites have gained popularity as a means of mitigating fibrin degradation and fine-tuning biomaterial properties.[21,25]

Our group has previously reported on PEGylated fibrin as a natural-synthetic polymer composite that promotes spontaneous network formation of encapsulated bone marrow-derived mesenchymal stem cells (MSCs), without added soluble factors. [26,27] Here, PEGylation slows fibrinolysis and extends the therapeutic window of MSCs localized within the matrix. Additionally, bone marrow-derived MSCs serve as an readily available autologous progenitor population that are responsive to substrate cues[28] and have a proven history of enhancing angiogenic activity and wound closure.[3,6,11,29] While we have previously observed a dramatic increase in vascular morphogenesis of MSCs in PEGylated fibrin gels (compared to pure fibrin gels),[30] the full breadth of differences in cellular behavior has not yet been characterized and nor have the underlying mechanisms. Understanding how PEGylation changes biomaterial properties is critical to understanding why MSC network development is significantly improved. Furthermore, gaining a clearer understanding of this cell-gel system will facilitate a more targeted clinical context for its implementation.

The studies presented here aim to characterize the biophysical properties of PEGylated fibrin gels and subsequent cell mechanisms of motility and relevant biological behavior, including production of secreted factors and markers of an endothelial phenotype. Experiments were designed to highlight differences between PEGylated fibrin and fibrin matrices as well as implicate potential mechanisms that motivate MSC vascular morphogenesis.

MATERIALS AND METHODS

Materials

Low-glucose Dulbecco's modified Eagle's medium (DMEM), phosphate buffered saline (PBS), fetal bovine serum (FBS), and Gluta-MAX™ -I (100x) were purchased from Invitrogen (Carlsbad, CA). Penicillin-streptomycin and trypsin/ethylenediaminetetraacetic acid were purchased from ATCC (Manassas, VA). Sigma-Solohill microcarrier beads (MCBs) coated in porcine collagen were obtained from Sigma-Aldrich (St. Louis, MO) as well as fibrinogen and thrombin from human plasma. Linear homo-difunctional succinimidylglutarate polyethylene glycol (PEG-$(SG)_2$, 3400 Da) was purchased from NOF America (White Plains, NY).

Cell culture of mesenchymal stem cells

Human bone marrow-derived mesenchymal stem cells (hMSCs) from Lonza (Basel, Switzerland) were cultured according to manufacturer specifications with growth medium in tissue culture-treated plastic flasks (Corning, Corning, NY) at 5000 cells/cm^2. Growth medium consisted of DMEM supplemented with 10% FBS, 1% penicillin-streptomycin, and 2mM GlutaMAX™ -I. Cells were tested by the manufacturer for trilineage differentiation potential and for positive expression of CD105, CD166, CD29, and CD44; cells were negative for CD14, CD34, and CD45. Population purity was greater than 95%. All cell cultures were maintained at 37°C and 5% CO_2.

Cell seeding of microcarrier-beads

hMSCs were seeded on MCBs according to our previously described protocol,[30] based on the modified bead-outgrowth assay developed by Nakatsu and Hughes.[31,32]

Briefly, MCBs were suspended at 2 mg/mL in PBS, autoclaved, and stored at 4°C before use. Prior to seeding, MCBs were distributed as 4mg aliquots into FACS tubes and briefly centrifuged into a pellet to remove the PBS. Growth media was added for 1h to prime MCBs for cell seeding, which was then removed immediately before adding cells. hMSCs at passages 4-6 were trypsinized, centrifuged into a pellet, and re-suspended at a minimum concentration of 1.4×10^5 cells/mL growth media. Cells were added to FACS tubes of MCBs for a final concentration of 7.0×10^4 cells/mg MCB and a total of 2mL growth media per FACS tube. Cells and MCBs were gently resuspended every 30min for the first 4h to evenly coat MCBs with cells. Seeded MCBs were strained through a 70μm mesh and rinsed with PBS to remove any unattached cells. Finally, MBCs were resuspended in 300μL growth media/mg MCB.

Three-dimensional gel culture *in vitro*

Gel fabrication followed our previously described protocol for enzymatically crosslinked PEGylated fibrin and fibrin gels.[26] Human fibrinogen was solubilized in PBS (without calcium or magnesium, pH 7.8) at three different concentrations: 80, 60, and 40 mg/mL. PEG-SG_2 was similarly dissolved in PBS at three different concentrations: 8, 6 and 4 mg/mL. The PEG-SG_2 concentrations correspond with a 10:1 molar ratio of reactive groups to each fibrinogen solution. Human thrombin was reconstituted in nanopure ddH_2O to 100U/mL, which was further diluted to 25U/mL with 40mM $CaCl_2$. Gel components were passed through 0.22μm filters for sterility before use. Gels with 1mL total volumes were fabricated in 12-well plates and those with 0.5mL total volumes in 24-well plates. Gel components were mixed in the following order using the same volumetric ratio: 1 fibrinogen: 1 PEG-SG_2: 2 seeded MCBs: 4 thrombin. Gelation was

finalized at 37°C for 15min before rinsing with PBS (with calcium and magnesium), followed by growth media rinses at 5min, 10min, 30min, and 1h to remove cytotoxic unreacted PEG-SG_2. Gel culture was carried out to Day 7 with growth media unless otherwise specified.

Small molecules for functional assays

For some experimental groups, small molecules, proteins, or peptides were added to culture media. Table 3.1 lists each molecule, the concentration used, the experimental study in which it was applied, and the manufacturer's information.

Hypoxic culture

In addition to normoxic culture conditions, MSCs in PEGylated fibrin were also cultured under 1% O_2 and 2% O_2 using a hypoxia chamber (Stemcell Technologies; Tukwila, WA), generously loaned to us from Dr. Aaron Baker. Hypoxic gas mixes were composed of 5% CO_2, 1% or 2% O_2, and N_2 balance (Praxair; Danbury, CT). Cell cultures were sealed inside the hypoxia chamber with a petri dish of water for humidity. The chamber was purged with a hypoxic gas mix for 5min and then purged again 90min later to evacuate any residual oxygen content from the culture media. Thereafter, the chamber was purged every 48h to maintain hypoxic cultures unless opened for assay endpoints.

Rheology

Gels were prepared without cells by substituting PBS for the MCB volume during gel preparation. Gels were formed in 40mm diameter nonstick molds for a parallel plate

rheometer configuration and were kept hydrated with PBS prior to and during testing. Strain sweeps were measured from 0.1-2.5% at 15 rad/s at a plate temperature of 37°C. Storage and loss moduli were reported for statistical comparison at 1% strain.

Cryogenic scanning electron microscopy

Cell-free gels were prepared in small-volume molds and kept hydrated in PBS (with calcium and magnesium). Gels were briefly rinsed in ddH_2O before mounting on a cryogenic SEM stage with carbon tape. Mounted gels were then snap-frozen in liquid nitrogen and fractured with a scalpel to expose cross-sectional structures. Gels were transferred to the cryo prep unit within a vacuum cryo transfer shuttle (Leica EM VCT100) to minimize crystal formation from air exposure. In the prep unit (Leica EM MED020), the stage temperature was raised from -140°C to -110°C to sublimate water crystals from the gels. Samples were then sputter coated with palladium and shuttle-transferred to the SEM for imaging. The SEM stage was kept at -120°C to -123°C for the duration of imaging.

Diffusional characterization

Syringes (without the plunger) were used as molds for containing fibrin or PEGylated fibrin gels and the test solute. Cell-free gels (500μL volume) were formed at the 0cc demarcation of the syringe barrel, gelled to completion at 37°C, and rinsed with an equal volume of PBS. After the PBS was aspirated, the slip-tips of the syringes were carefully removed to expose the gel bottoms. Removal of the slip-tips ensured that diffusivity of the test solute was limited by the gel and not by capillary resistance of the solvent through the syringe. Syringes were vertically fixed in place and 500μL of

2.5mg/mL 10kDa dextran-Texas Red conjugate (Molecular Probes; Eugene, OR) was added directly on top of the gels. While fluorescence was not utilized, the purple appearance of Texas Red dye provided clear visualization of the dextran. Time-lapse photos of dye diffusion were taken every 15min for 7h.

Fluorescent cell staining for morphological quantification

On day 7 of gel culture, samples were rinsed six times with PBS (with calcium and magnesium) for 15min each. Calcein AM (Invitrogen; Carlsbad, CA), a live-cell cytoplasm stain, was added at 10μM for 1h. Samples were rinsed four times with PBS every 5min and then fixed with 4% neutral-buffered formalin for 30min. Finally, gels were briefly rinsed with 3 volumes of PBS to remove residual fixative and stored at 4°C overnight for imaging the next day.

Fluorescent cell staining for visualizing vacuolization

Texas Red-conjugated dextran (10kDa; Molecular Probes; Eugene, OR) was added to the media of gel culture as a cell-impermeable dye that could only be intracellularly localized through pinocytic uptake. For one-week endpoint cultures, 1.25mg/mL of dextran was added on Day 4; for two-week endpoint cultures, dextran was added on Day 7 and Day 11. After cultures were terminated, MSCs were fixed and additionally stained with FITC-phalloidin (F-actin) and DAPI (nuclei).

Two-photon microscopy

Fluorescent z-stacks were collected of MSC outgrowth from individual microcarrier beads with an Ultima Multiphoton Microscopy System (Prairie

Technologies; Middleton, WI). Two-photon excitation was achieved with a tunable Ti:sapphire laser (Spectra-Physics Mai Tai HP; Newport; Irvine, CA) set to 720nm under a 10x water-immersion objective. Z-slice thicknesses were adjusted to maintain isometric voxel dimensions. A thickness of 500-700μm was imaged along the z-axis for each image stack.

Three-dimensional morphological quantification

Image processing and three-dimensional morphological quantification followed our recently described method.[30] As before, z-stacks were preprocessed in ImageJ (Release 1.2.4; ImageJ Plugin Project) and exported as Visualization Toolkit (.vtk) files and loaded into 3D Slicer (Release 3.6, 64-bit Linux), an open-source program for MRI/CT analysis. The Vascular Modeling Toolkit in 3D Slicer was used for image segmentation and 3D model generation. Centerline tracings of 3D models were exported as large data clouds of x,y,z coordinates with corresponding radii; the measured radius represented the model's maximum cross-sectional diameter at each coordinate point. The data cloud was processed in MATLAB (Release 2008a for Macintosh) into quantitative metrics that describe relevant attributes of network development: total network length, volume, and number of branches (per MCB).

Cell proliferation

The CellTiter 96® Aqueous One Solution Cell Proliferation Assay (Promega; Madison, WI) was used to quantify the cell content of gels. On days 1, 3, 5, and 7 of gel culture, the culture supernatant was removed and saved for future protein analysis. Fresh growth media + 20% (v/v) CellTiter 96® solution was then added for 4h. Supernatants

were thoroughly homogenized before transferring 200μL samples in triplicate to a 96-well plate. Absorbance was measured at 490nm with a microplate reader (BioTek Synergy HT Multi-Mode Microplate Reader; Winooski, VT).

Secreted protein detection with ELISA

Quantikine ELISA kits (R&D Systems; Minneapolis, MN) were procured for VEGF, matrix metalloproteinase-2 (MMP-2), and MMP-9 proteins. Supernatant collected from cell proliferation samples were assayed according to the manufacturer's instructions. Optical density was measured at 490nm. Secreted protein quantities were normalized to cell number using the results of the matched-sample MTS assay.

Cellular protein detection with western blot analysis

Cells in gel matrices were lysed with RIPA buffer (Santa Cruz Biotechnology; Dallas, TX) and homogenized for 30s with a soft tissue grinder. Cell-gel lysates were passed through a 21-gauge needle 20× for further homogenization and solid gel remnants were removed through sample centrifugation at 14000×*g* for 10min at 4°C. The supernatants were denatured in a reducing buffer of Laemmli sample buffer with 5% β-mercaptoethanol at 95C for 5min. Denatured samples were separated with 10% mini-Protean® TGX™ precast gels (Biorad; Hercules, CA) at 20μg protein per gel lane and blotted onto PVDF membranes. Membranes were blocked for 1h at room temperature with 5% (w/v) nonfat milk in TBST and then incubated overnight with a primary antibody at 4C. Membranes were then rinsed with TBST 3× for 5min each and incubated with an HRP-conjugated secondary antibody for 1h at room temperature. After a second set of TBST rinses, 3mL of SuperSignal West Dura Chemiluminescent Substrate (Pierce

Thermo Fisher Scientific; Rockford, IL) was added per blot for 5min prior to image capture with a FluorChem CCD system (ProteinSimple; Santa Clara, CA). Chemiluminescent signal was quantified with AlphaView software for statistical analysis. For a list of antibodies and their dilutions, refer to Table 3.2.

Statistical analysis

A one- or two-way analysis of variance was used to determine significance between fibrin concentrations and PEGylation. Where significance was found, post-hoc tests were performed to further determine specific relationships of statistical significance. Tukey's correction for multiple comparisons was applied where appropriate. P-values less than 0.05 were considered statistically significant. All statistical tests were completed in Prism (Version 6.0 for Mac OS X; GraphPad, La Jolla, CA).

RESULTS AND DISCUSSION

Fibrin PEGylation changes biophysical gel properties

Rheological properties of fibrin and PEGylated fibrin were compared across three increasing concentrations (5-10mg/mL fibrin), using a parallel plate rheometer (Figure 3.1A). At 1% strain, the storage modulus indicated a significant increase in gel elasticity as fibrin concentration increased. This trend suggests that gel elasticity of both fibrin and PEGylated fibrin is governed by fibrin crosslinking, which is reflective of total fibrin content. Significant differences between the storage moduli of fibrin and PEGylated fibrin gels were only observed at 10mg/mL fibrin.

The loss modulus indicated no significant changes in viscous properties between fibrin and PEGylated fibrin, nor between fibrin concentrations within each gel type.

However, general trends showed the loss modulus only increased with fibrin concentration in unmodified fibrin gels, remaining unchanged across PEGylated fibrin gels. In fact, the loss moduli for all PEGylated fibrin gels were comparable to the loss modulus of the 5mg/mL unmodified fibrin group. This loss modulus behavior can be attributed to the bound versus free water content of each gel system. Bound water contributes to bulk elastic properties of biopolymers whereas free water will flow and contribute to the energy dissipation imparted by the viscous component.[33] This information suggests that PEG buffers the increasing free water content of fibrin as the total water absorption capacity rises with concentration. In unmodified fibrin, the ratio of unbound:free water remains the same since no such buffer exists; thus, we see an increase in loss modulus in tandem with the storage modulus.

Morphological analysis of gel cross-sections highlighted more dramatic changes between the two materials. Under cryo-SEM, fibrin gels had a characteristic fibrosity that resembled a heterogeneous sponge-like structure (Figure 3.1B and 3.1D). This fibrosity yields the overall whitish, opaque appearance of fibrin gels. PEGylated fibrin, however, had more solid amorphous regions (Figure 3.1C and 3.1E, "a") interspersed with fibrous layers (Figure 3.1E, "f"), giving these gels a more optically clear appearance.

The functional impact of these morphological differences between fibrin and PEGylated fibrin was illustrated with a simple diffusional study. Here we used time-lapse photography to track liquid filtration and diffusion of a 10kDa dextran-Texas Red conjugate in both fibrin and PEGylated fibrin gels (Figure 3.1F). After only 2.5h, the dextran completely diffused through the fibrin gel and can be clearly seen in the filtrate. Along with the fast-moving dye front, we also observed a significant drop in the liquid level above the fibrin gel, such that >80% of the liquid had completely filtered through the gel by 7h. PEGylated fibrin, however, showed approximately 20-25% dextran

penetration at 2.5h and approximately 50% after 7 hours, with the liquid level unchanged from 0h.

Based on these material characterizations, we find that fibrin PEGylation is uniquely responsible for a number of biologically-relevant material changes. While PEGylation can result in a lower elastic modulus at higher fibrin concentrations, initial work from our group showed that this trend can vary depending on the molecular weight and reactivity of the PEG used.[26] Additionally, the amorphous regions in PEGylated fibrin (that were lacking in fibrin) can be attributed to a shift in molecular aggregation kinetics. Literature on PEG-fibrin conjugates suggest that PEGylated fibrin products maintain a cylindrical fibrin core with a hydrodynamic radius dictated by linear PEG tails.[34] The PEG-induced hydrodynamics disrupt tertiary and quaternary protein folding without damaging the bioactivity of fibrin's secondary structure. Furthermore, PEG-fibrin conjugates have intensified light scattering upon gelation, indicating an increase in inhomogeneities from the aggregate solution to gel transition. These features of amorphous gel packing are the most pronounced physical change introduced by fibrin PEGylation; the slowed dextran diffusion can be subsequently linked to the physical transformation from a highly porous, fibrous matrix to an amorphous, pseudo-fibrous gel.

Slowed diffusivity in PEGylated fibrin gels will have a direct impact on nutrient and oxygen diffusion for encapsulated cells. While cell encapsulation will impart some degree of hypoxic stress by virtue of transport dynamics,[35] the diffusional properties of PEGylated fibrin are likely to induce a higher degree of hypoxic stress than fibrin alone. Studies on oxygen transport in fibrin-based matrices at 30mg/mL fibrin had 10× slower oxygen diffusion than water, which generated a hypoxic scaffold core.[36] Extrapolating this data to our system, 10mg/mL fibrin gels may have diffusion kinetics up to 3× slower than that of water. Since PEGylated fibrin is empirically more diffusion-limited than

fibrin, we can infer that PEGylated fibrin matrices diffuse oxygen at a rate *at least* 3× slower or more than water, though likely more.

MSCs in PEGylated fibrin develop networks with lumenal space

A defining step in endothelial network development is the coalescence of large vacuoles into an intercellular lumenal space.[37-40] In vascular development, lumens are known to form through two distinct mechanisms: cell hollowing and cord hollowing.[41,42] Cell hollowing is characterized by a chain of individual cells forming large intracellular vacuoles through pinocytic uptake of interstitial fluid. These large vacuoles form intercellular fusions, creating a seamless continuous tube. Cord hollowing is a newer paradigm for vascular development where multicellular columns (i.e., cords) are polarized by VE-cadherin-dependent mechanisms into apposing cellular walls. During polarization, pinocytosed vesicles are trafficked towards the apical axis and fuse.[43] Cell boundaries along the apical axis repel and separate, further creating a central extracellular lumen. Tubes formed by cell hollowing generally have narrower diameters than those formed by cord hollowing due to fewer cells contributing to the overall structure. Both mechanisms require subsequent lumenal expansion to accommodate blood flow.[41,42]

Confirmation of lumenal development with standard two-dimensional light microscopy is unreliable; these images are unable to unequivocally differentiate between flat, tube-like networks and true voluminous tubes. Therefore, we opted for z-stack image collection and 3D model generation with 3D Slicer to fully capture evidence of 3D lumenal space formation. Based on a study by George Davis's group on endothelial network development,[44] we added 10kDa dextran-Texas Red conjugate to the gel culture media to label pinocytosed vesicles and developing lumenal spaces. Networks were co-

stained with FITC-phalloidin (F-actin) and DAPI (nuclei) and imaged with fluorescent microscopy. Localization of large, intracellular compartments containing dextran-Texas Red indicated pinocytic dye uptake (Figure 3.2). Dextran-containing vesicles spanning multiple cell lengths further suggest intercellular vacuole fusion. Given the distribution of non-overlapping nuclei and narrow tube diameter, this pattern of dye uptake is highly reflective of cell-hollowing lumen assembly. This finding substantiates our claims that MSC networks are in fact tubular and not merely flat projections of cell bodies.

Vascular morphogenesis of MSCs is mediated by tubulin assembly and integrin binding

In endothelial vascular morphogenesis, network assembly and lumen formation rely on generating intracellular tension via cytoskeletal assembly and traction via integrin-mediated adhesions.[45] Specifically, endothelial networks are most dependent on tubulin polymerization, concomitant with matrix-appropriate integrin expression.[46] In fibrin matrices, $\alpha v\beta 3$ and $\alpha 5\beta 1$ are preferentially expressed and have a known affinity for RGD binding motifs.[47,48] For MSCs in PEGylated fibrin, network formation was moderately disrupted by cytochalasin B inhibition of actin assembly and significantly blocked by colchicine inhibition of tubulin dynamics (Figure 3.3A, C, and D). Similarly, when cyclic G<u>RGD</u>SP was added, MSCs were also unable to migrate off of the microcarrier bead (Figure 3.3E); MSCs cultured with the cyclic G<u>RGE</u>SP control continued to form normal networks that were statistically similar to non-doped PEGylated fibrin controls (Figure 3.3F and B). The ability of cyclic G<u>RGD</u>SP to out-compete matrix binding motifs indicates that a) MSCs are binding RGD-based matrix sites and b) that MSC have no alternative means of generating traction forces within PEGylated fibrin aside from integrin-mediated events.

These results, though unsurprising, were necessary to verify that MSCs both parallel the cellular mechanics of endothelial vascular morphogenesis and also exhibit normative, non-malignant behavior. Integrin-*independent* motility is typical of immune cell populations.[49,50] However, in mesenchymal populations, deviation from integrin-dependent migration can signal a mesenchymal-amoeboid transition, which is linked to aggressive cancer metastases.[51] We can assume, then, that the ability of MSCs to coalesce networks in PEGylated fibrin (and not fibrin) is the result of normative cell mechanisms guided by matrix cues and not the emergence of a malignant phenotype.

PEGylated fibrin increases production of angiogenic factors and expression of endothelial markers

We have previously reported on morphological differences between MSCs cultured in fibrin and PEGylated fibrin, particularly that cells in fibrin appear highly proliferative and migratory while those in PEGylated fibrin form continuous tubular networks.[30] With a tetrazolium-based metabolic assay, we quantified the growth kinetics of MSCs in both gels. Figure 3.4A clearly illustrates the rapid exponential growth of MSCs in fibrin and slower (more linear) growth of MSCs in PEGylated fibrin. The divergence in growth kinetics was significantly evident by Day 3. Interestingly, we observed the opposite matrix-proliferation relationship in previous work: MSCs were more proliferative in PEGylated fibrin than in fibrin matrices.[26] However, a number of variables in our gel materials and protocol have changed since that first report. We now use human instead of porcine fibrinogen, PEG succinimidyl glutarate instead of PEG benzoyltriazole carbonate, and PEGylate fibrinogen in PBS instead of TBS (pH 7.8). Additionally, porcine fibrin matrices rapidly collapsed during culture, limiting MSC growth to the gel surface. The premature collapse of fibrin matrices may have

underrepresented the true proliferation capacity of these gels, skewing the data. Present fibrin matrices from human fibrinogen do degrade more rapidly than PEGylated fibrin matrices but do not experience catastrophic collapse. Thus, present data is more likely to accurately reflect MSC proliferation in fibrin, but past and present data on PEGylated fibrin is believed to be consistent.

Stem cell proliferation also has a well-known bimodal correlation with stem cell differentiation. The slower rate of proliferation in PEGylated fibrin may allow for an increase in differentiation behavior. In support of this possibility, MSC secretion of angiogenic factors and expression of endothelial markers were significantly elevated in PEGylated fibrin gels over fibrin controls. ELISA analysis of secreted factors showed an increase in early production of VEGF and later production of MMP-2 (Figures 3.4D and 3.4E, respectively) in PEGylated fibrin MSCs. Additional analyses of cellular markers indicated that MSCs in PEGylated fibrin also express higher levels of vWF and VE-cadherin proteins (Figures 3.4B and 3.4C, respectively), which are characteristic of an endothelial lineage. The vascular morphology driven by PEGylated fibrin matrices clearly extends to complementary MSC development of endothelial functions and phenotypic features.

Other groups have reported similar combinations of MSC endothelial-like behavior as well. In early studies, VEGF was initially used as a morphogen to drive MSC differentiation towards an endothelial lineage. By adding 50ng/mL VEGF to the culture media, MSCs began expressing a number of endothelial markers after seven days in culture, including vWF, VE-cadherin, VEGF receptors 1 and 2, and VCAM-1.[52] Fibrin-based substrates, with angiogenic growth factors, were also able to induce MSC endothelial marker expression *in vitro*. However, when these substrates were tested in *in vivo* models of ischemia and wound healing, the therapeutic value of MSCs was primarily

derived from their paracrine production of VEGF, hepatocyte growth factor (HGF), transforming growth factor (TGF)-β1, and a milieu of other cytokines.[6,53,54] These factors encourage local proliferation and survival of endothelial cells and curb excessive inflammation.[29,55,56] In our work here, VEGF production is likely acting as both an endothelial morphogen and an indicator of angiogenic paracrine activity; fibrin may cue initial VEGF production, but once produced, endogenous VEGF enables a positive feedback mechanism that perpetuates further endothelial development of MSCs.[56]

Matrix metalloproteinases are another critical component of vascular network development. *In vitro* models of angiogenesis and vasculogenesis have implicated MMPs as necessary for precursor development of vascular guidance tunnels and later lumenal space formation.[40,57,58] However, work by Davis *et al* suggests that overly aggressive matrix degradation prevents stabilization of neovascular sprouts,[59] and this MMP-laden environment can culminate in a chronic wound.[60] MMP-2, which is cleaved and activated by MT1-MMP (i.e., MMP-14), is a contributing factor to fibrinolytic mechanisms of cell motility.[61,62] Furthermore, MMP-2 has a co-dependent regulatory relationship with VEGF: VEGF can stimulate an increase in MMP-2 production;[63] similarly, knockdown of MMP-2 can abrogate VEGF secretion via αvβ3-mediated phosphatidylinositol 3-kinase (PI3K)/HIF-1α signaling pathways.[64] In PEGylated fibrin, MSCs secreted elevated levels of VEGF at early time points, followed by elevated levels of MMP-2. Others have also observed maximum MMP-2 expression on day 7.[62] The literature on these two molecules suggests that later elevation of MMP-2 may be a direct response to elevated VEGF. Thus, increased VEGF expression further perpetuates the development of MSC vascular morphogenesis.

The biological impact of fibrin PEGylation on MSC behavior was made further evident by the significant upregulation of endothelial phenotypic markers, vWF and VE-

cadherin, over fibrin controls. In endothelialized vasculature, vWF mediates hemostasis via platelet adhesion as well as angiogenesis through regulation of angiopoietin (Ang)-2 levels.[65,66] Strong expression of vWF and presence of Weibel-Palade bodies are therefore considered an important phenotypic factor in evaluating endothelial functionality. Similarly, VE-cadherin provides intercellular junctions that regulate vascular permeability and establish apical/basal cell polarity.[67,68] MSCs have previously been observed to express both in vascular tissue engineering models. Interestingly, VE-cadherin expression is known to fluctuate indirectly with MMP-2 and MMP-9 activity.[69] This evidence suggests that maximum VE-cadherin expression in PEGylated fibrin MSCs is likely to occur sometime after day 7, given MMP-2 activity is at its peak. Future studies that evaluate later time points would help inform this association.

Perturbing the VEGF-hypoxia axes modulates MSC tubulogenesis in PEGylated fibrin

Physiologically, tissues greater than 2mm thick are prone to hypoxic necrosis unless a vascular supply is able to intervene, and capillary diffusion is typically limited to distances of 200μm or less.[70,71] *In vitro*, studies have demonstrated that encapsulated cells will experience some degree of hypoxia even when cultured under normoxic conditions.[35,36] More recently, studies have focused on hypoxic culture of MSCs as a means of prolonging their undifferentiated state and encouraging more normative physiological programs;[72] this work has been especially relevant to bone marrow-derived MSCs since the bone marrow niche is considered a mildly hypoxic environment.[73-77] However, under ischemic-related hypoxic stress (approximately 1-2% O_2),[78] the angiogenic programming of MSCs can be activated as part of the natural wound healing response.[79,80]

From our material characterization studies, the significant diffusional limitations found in PEGylated fibrin prompted further investigation of hypoxia as a previously overlooked matrix cue in MSC vascular morphogenesis. Incidentally, hypoxia-mediated pathways can also regulate VEGF and MMP-2 production as well as VE-cadherin expression.[81,82] Here we stimulated both VEGF and hypoxia pathways and evaluated MSCs in PEGylated fibrin for a heightened vascular morphogenic response.

We found that soluble VEGF had no mitogenic effects on MSCs in PEGylated fibrin, nor did it elicit an increase in MMP-2 production (Figures 3.5A and 3.5E, respectively). In fact, by Day 7, the VEGF group had significantly fewer MSCs than the control group. Endogenous VEGF production could not be accurately quantified in this case due to the magnitude of added soluble VEGF overshadowing any measurable changes. VEGF-stimulated MSC networks were morphologically shorter than the PEGylated fibrin control (Figure 3.5C, F, and E), likely associated with the decrease in cell number. Despite VEGF being a potent vascular morphogen, a recent paper demonstrated a similarly lack of VEGF sensitivity in MSC monolayers. In monolayer, addition of VEGF did not result in further upregulation of endothelial gene expression over high-density cell culture conditions.[83] However, concentrations of 50ng/mL or higher did induce stronger MSC expression of Ephrin-B1, suggesting high doses of VEGF can play a role in determining arterial cell fate.[83] They postulated that their results—which may apply to our results as well—culminated from oversaturation of VEGF receptors; endogenous levels of VEGF in PEGylated fibrin may be sufficient for maintaining activation of MSC vascular pathways and adding further VEGF is merely unproductive. This insensitivity further suggests that MSCs are producing VEGF as a paracrine factor for auxiliary cell recruitment, rather than autocrine self-promoting differentiation.

Cobalt chloride, a chemical stabilizer of hypoxia inducible factor 1-alpha (HIF-1α),[84,85] also failed to increase MSC proliferation (Figure 3.5A), VEGF and MMP-2 production (Figures 3.5D and 3.5E, respectively), and network formation (Figure 3.5C, G). While we could have chosen a higher concentration of cobalt chloride, we were limited by dose-dependent cytotoxicity. Increasing HIF-1α stabilization with more cobalt chloride may have resulted in a stronger HIF-mediated improvement in MSC vascular outcomes, but long-term cultures (> 48h) would have experienced dramatic cytotoxicity.[86] Hence, we opted for a mild-to-moderate concentration of 75μM cobalt chloride, which is commonly found in commercial lysates marketed as HIF-1α positive controls. Furthermore, hypoxia mimetics such as cobalt chloride and desferrioxamine have been shown to incompletely activate relevant downstream effectors of HIF-1α.[87-89] These inactive effectors may be vital to HIF-mediated vascular morphogenesis, underlying the moot result observed in this MSC group.

True hypoxia, however, with 1% oxygen had a significant impact on both cell proliferation and protein production;[75,77] minimal impact was observed in vascular network formation (Figure 3.5C, H). MSCs cultured under hypoxic stress in PEGylated fibrin exhibited markedly slower cell proliferation (Figure 3.5A). Conversely, their production of VEGF and MMP-2 proteins was elevated for all seven days of culture (Figures 3.5D and 3.5E, respectively), which is a well-documented effect of hypoxic stress.[73,76] Constitutively induced HIF-1α expression, without hypoxia, is also known to activate the paracrine secretion of angiogenic factors, supporting the idea of HIF-mediated induction of angiogenesis. Though hypoxic networks were statistically similar in length to controls, the data trends suggest these networks may be at the brink of downsizing. Given the significantly slowed MSC proliferation under 1% O_2, we find it unsurprising that hypoxic networks would tend towards the shorter end of the normal

developmental spectrum. Fewer cells in the gel mean fewer cells contributing to network size. The limited cell growth also suggests that MSCs may be at their "stress limit" and the low oxygen tension is metabolically hindering cell growth. This theory was confirmed by measuring MSC proliferation under 2% O_2, where cell numbers returned to levels comparable to controls (Figure 3.5B). Other studies have indicated that hypoxic stress has a biphasic impact on cell survival: mild hypoxia (1-2% oxygen) induces an advantageous rescue response whereas more severe hypoxia maximizes HIF-1α expression but results in slowed proliferation or even significant cell death.[75,90] Slowed MSC proliferation may alternatively be the result of a normal lag phase experienced at early time points of hypoxic exposure. Overall, enhanced angiogenic behavior under 1% O_2 coupled with the previously discussed diffusional limitations of PEGylated fibrin strongly implicate hypoxic stress as a relevant mediator of MSC vascular morphogenesis.

CONCLUSIONS

PEGylated fibrin has a unique ability to promote MSC vascular morphogenesis without the typical use of soluble factors. By relying solely on matrix cues, we have the potential to simplify the clinical translation of MSC-based ischemic therapies and improve their utility. The barrier to this implementation has been our lack of thorough understanding regarding mechanisms of PEGylated fibrin-induced MSC vascular morphogenesis. Here we were able to highlight changes in both physical material properties and biological cell outcomes that arise from fibrin PEGylation. We found that PEGylated fibrin is significantly diffusion-limited compared to pure fibrin matrices. The subsequent increase in MSC production of paracrine and proteolytic factors along with endothelial marker expression can therefore be linked directly to this hallmark

characteristic. However, MSCs in fibrin were also capable of these behaviors, just to a lesser extent. Most interesting, though, was the lack of MSC sensitivity to an added VEGF stimulus. In contrast, when PEGylated fibrin matrices were cultured under hypoxic conditions, we observed a further increase in secreted factors, despite minimal change in morphology. MSC sensitivity to hypoxic stress suggests that this pathway may be active during vascular morphogenesis. While we cannot rule out the importance of fibrin-related bioactivity and influence, these results give us cause to further investigate HIF-mediated mechanisms as a potential underlying source of PEGylated fibrin's increased activity.

Molecule	*Concentration*	*Study*	*Manufacturer*
Cyclo-GRGDSP	500 μg/mL	MIC-axis	AnaSpec
Cyclo-GRGESP	500 μg/mL	MIC-axis	AnaSpec
Cytochalasin B	0.1 μM	MIC-axis	Sigma-Aldrich
Colchicine	0.1 μM	MIC-axis	Sigma-Aldrich
Human VEGF-165	50 ng/mL	HIF-axis	BioLegend
Cobalt chloride	75μM	HIF-axis	Fisher Scientific

Table 3.1: List of small molecules for functional inhibition assays. MIC-axis: matrix integrin cytoskeleton axis, Figure 3.3. HIF-axis: hypoxia inducible factor axis, Figure 3.5.

Antibody target	*1°/2°*	*Dilution*	*Manufacturer*
von Willebrand factor	primary	1:1000	Abcam (ab6994)
VE-cadherin	primary	1:700	Abcam (ab33168)
β-actin	primary	1:1000	Abcam (ab75186)
Rabbit IgG	secondary	1:5000	Santa Cruz Bio (sc-2004)

Table 3.2: List of polyclonal (rabbit) primary and (goat) secondary antibodies used for western blot detection of cellular proteins. Antibodies were diluted in blocking buffer (5% nonfat milk in TBST).

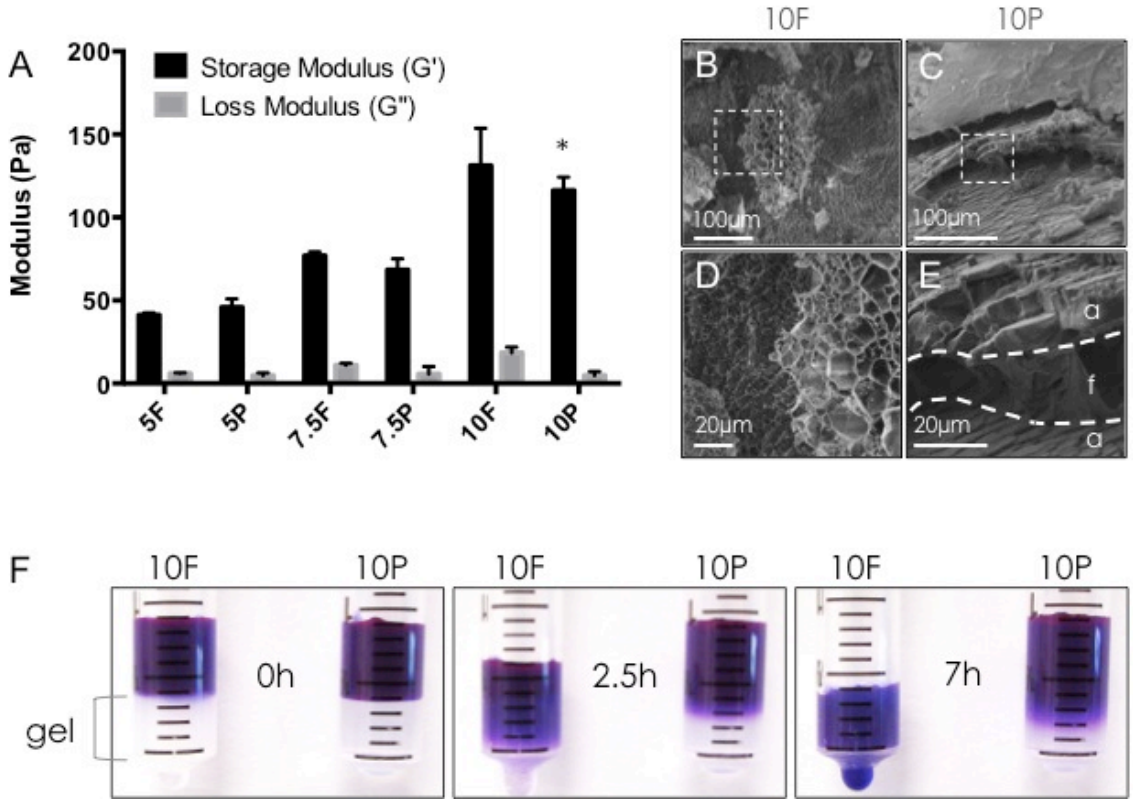

Figure 3.1: Characterization of fibrin and PEGylated fibrin gel properties. Abbreviations: 10F, pure fibrin at 10mg/mL fibrin; 10P, PEGylated fibrin at 10mg/mL fibrin. (A) Rheological analysis showed comparable elastic properties, except for at the highest fibrin concentration of 10mg/mL. No measurable differences were observed between loss moduli. (B-E) CryoSEM of fractured gel cross-sections showed that fibrin PEGylation introduces amorphous regions into the gel. Images (D) and (E) are magnified views of the insets from (B) and (C), respectively. (F) Time-lapse photography: diffusion of 10kDa dextran-Texas Red conjugate in PBS was significantly slower in PEGylated fibrin than fibrin. *$p < 0.05$, versus fibrin control.

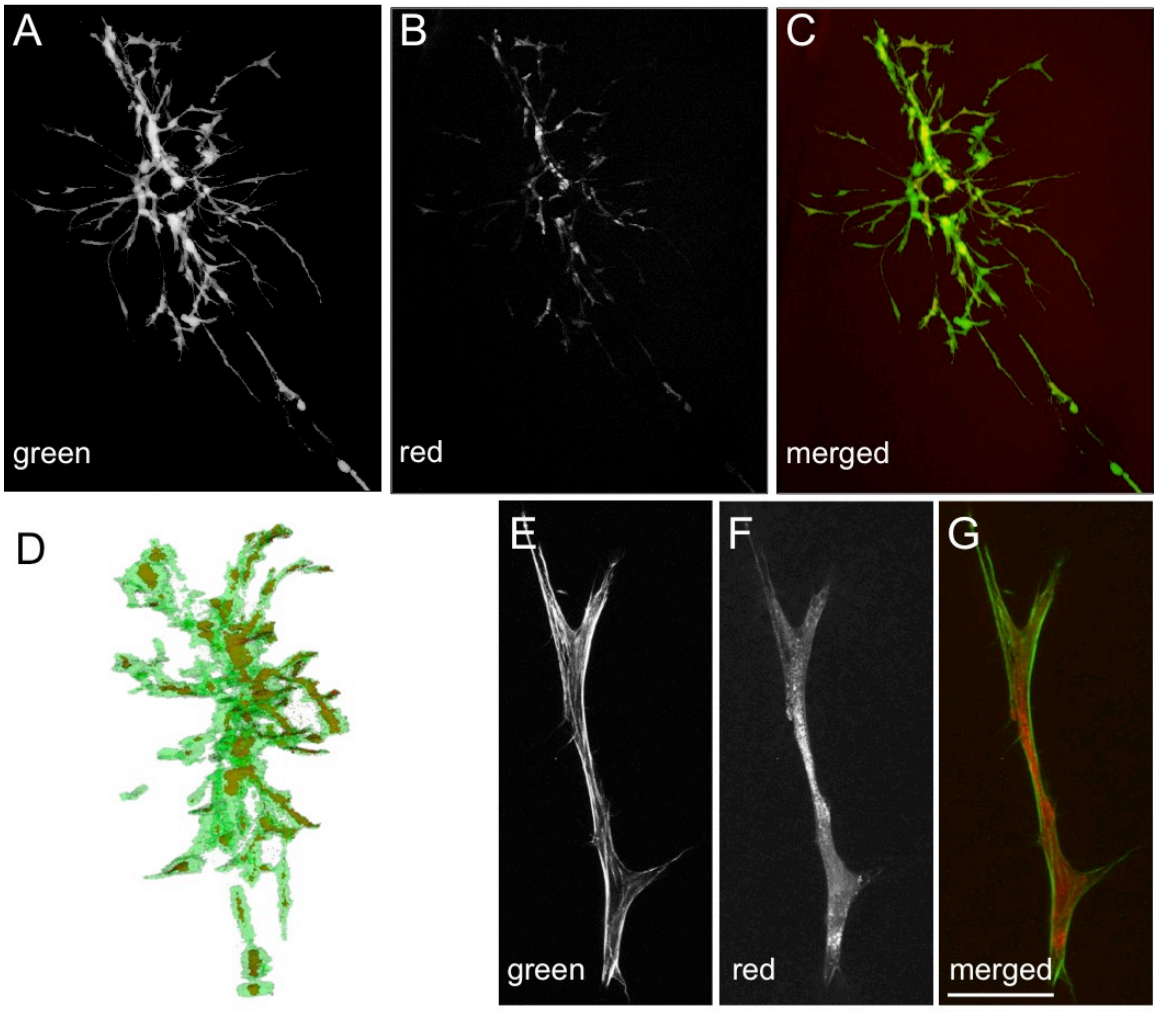

Figure 3.2: Lumen development of MSC networks in PEGylated fibrin. (A) Calcein AM signal of cell bodies and (B) dextran-Texas Red signal of vesicles; (C) merged fluorescent signals from (A) and (B) show co-localization (orange) of red vesicles within the green cell bodies. (D) Three-dimensional model rendered in 3D Slicer of network from (A-C). (E) FITC-phalloidin labeling of f-actin filaments and (F) dextran-Texas Red signal of vesicles; (G) merged fluorescent signals from (E) and (F), scale bar = 50μm.

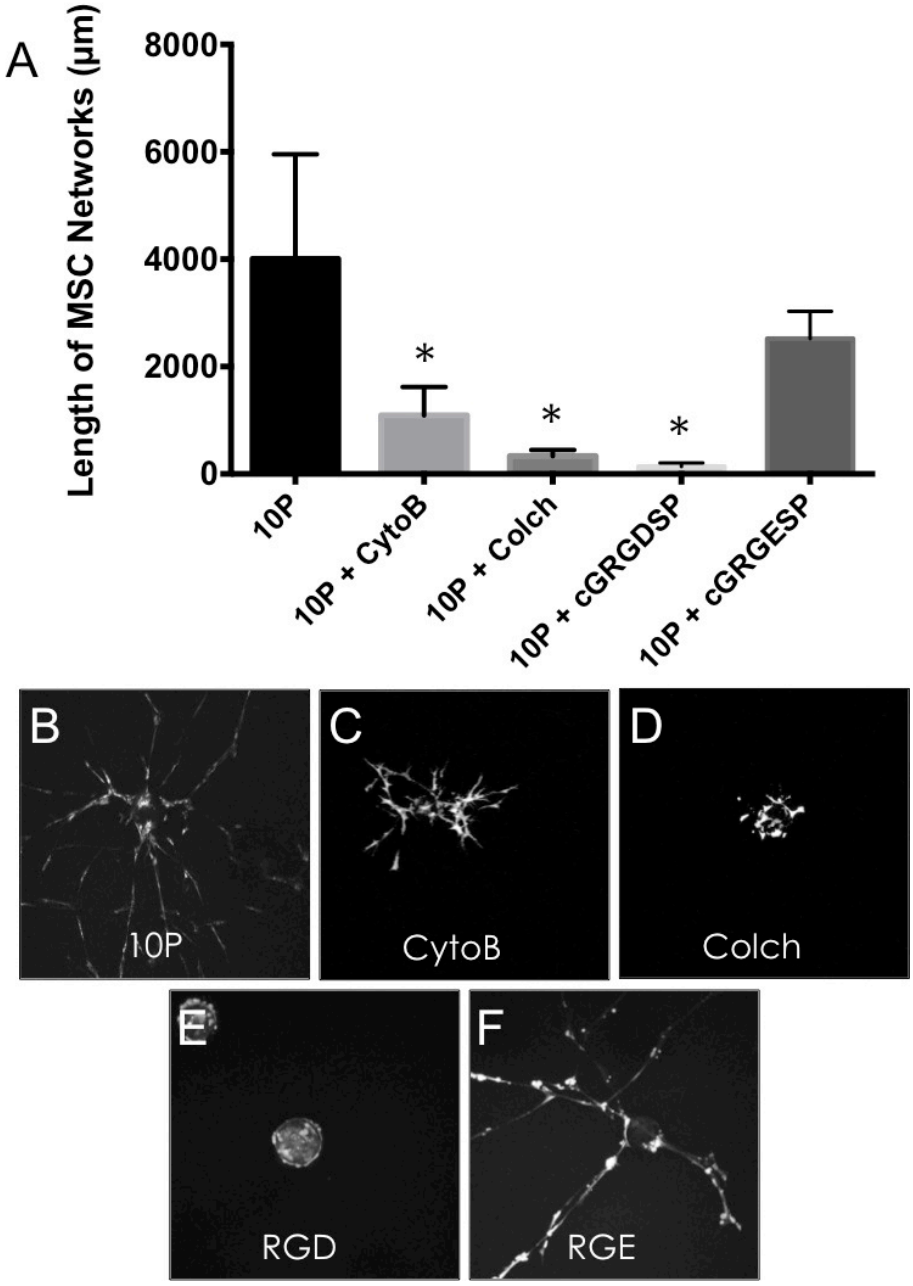

Figure 3.3: Matrix-integrin-cytoskeletal axis study. Abbreviations: CytoB, cytochalasin B; Colch, colchicine; RGD, cyclic GRGDSP; RGE, cyclic GRGESP. (A) Average network length per microcarrier bead as measured by our 3D quantification method. (B-F) Z-stack projections representative of morphological outcomes reported in (A). *$p < 0.05$, versus 10P control.

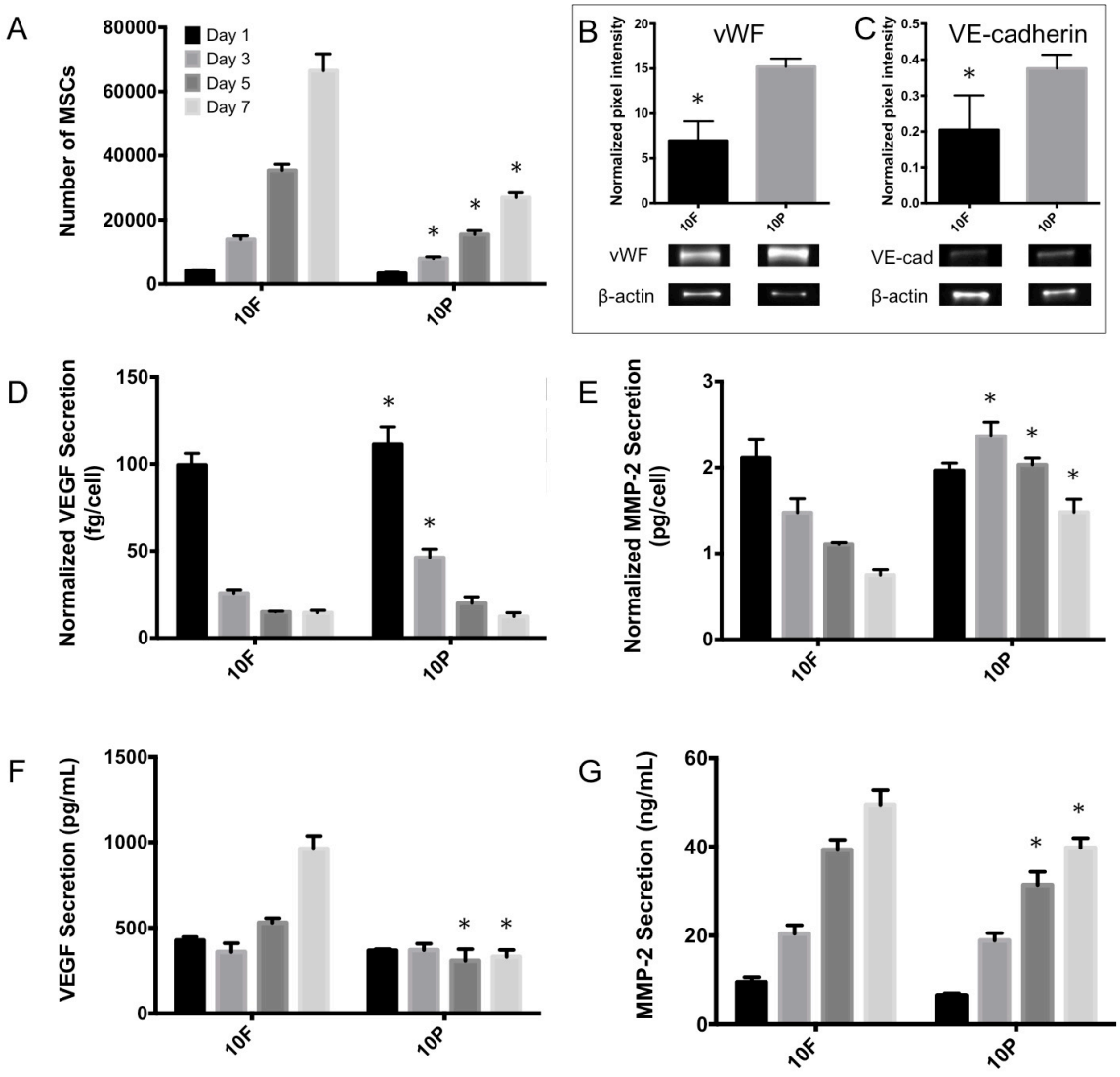

Figure 3.4: MSC proliferation (A), endothelial marker expression (B and C), and protein secretion (D-G). (A) Results of the CellTiter 96 assay indicate slower MSC proliferation in PEGylated fibrin gels. (B and C) MSCs in PEGylated fibrin expressed significantly higher levels of endothelial markers vWF and VE-cadherin, respectively. Images below graphs are representative of western blot chemiluminescent bands. (D) VEGF secretion and (E) MMP-2 secretion normalized to cell number from (A). (F) and (G) are raw values for protein secretion reported in (D) and (E), respectively. (A, D-G) *$p < 0.05$, versus 10F control at same time point. (B,C) *$p < 0.05$, versus 10P.

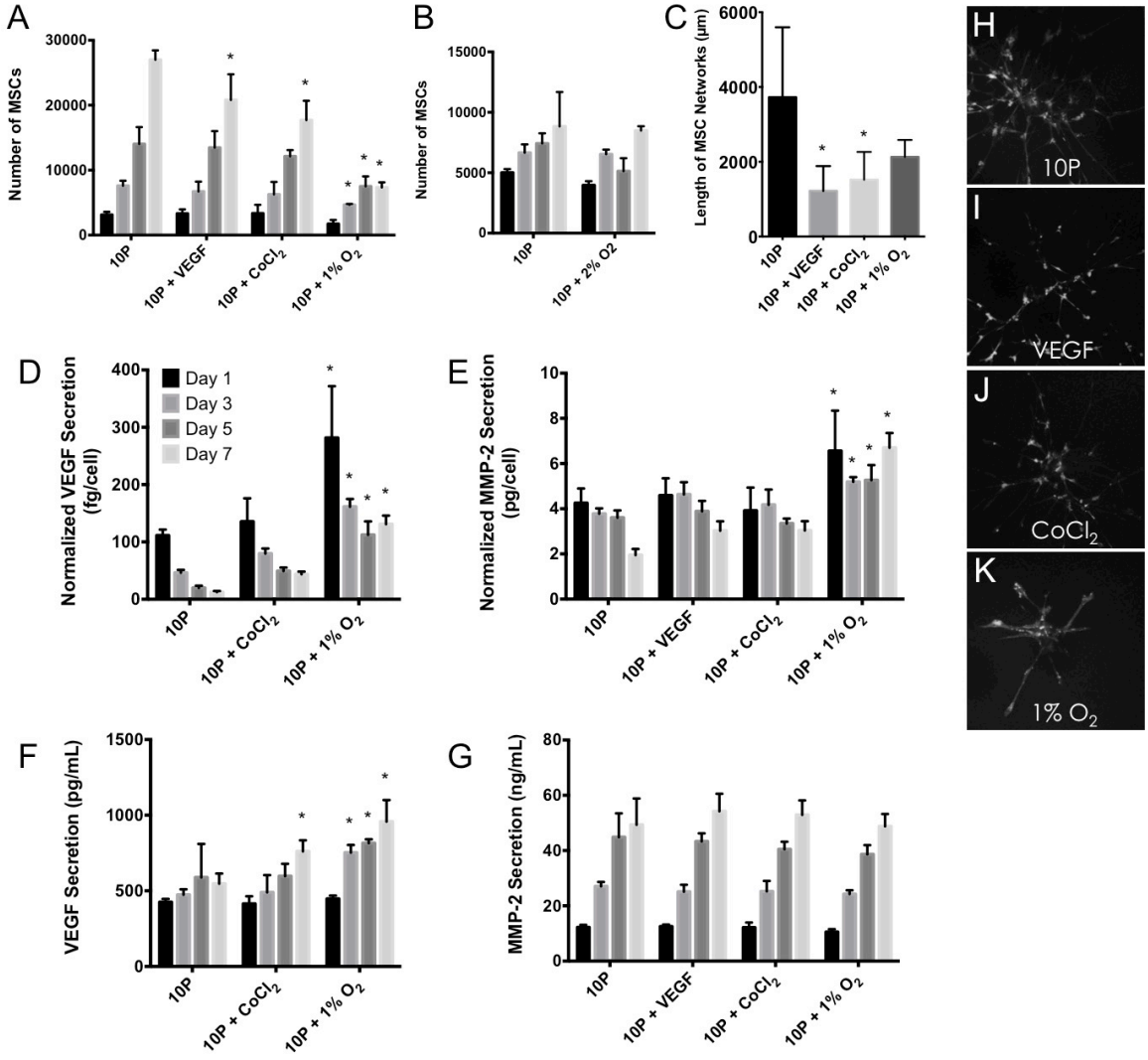

Figure 3.5: Hypoxia inducible factor axis study. (A) Results of CellTiter 96 assay indicated no mitogenic response to VEGF or CoCl2 but a significant decline in MSC proliferation under 1% O_2. (B) Increasing to 2% O_2 reduced hypoxia-associated lag in MSC proliferation. (C) Average network lengths per microcarrier bead as measured by our 3D quantification method. Hypoxic stress increased VEGF secretion (D) and MMP-2 production (E) of MSCs in PEGylated fibrin; values are normalized to cell numbers reported in (A). (F) and (G) are raw values for protein secretion reported in (D) and (E), respectively. (H-K) Z-stack projections representative of morphological outcomes in (C). *$p < 0.05$, versus 10P control at same time point.

REFERENCES

1. Fadini GP, Agostini C, Avogaro A. Autologous stem cell therapy for peripheral arterial disease meta-analysis and systematic review of the literature. Atherosclerosis. 2010 March;209(1):10–17.

2. Liu J, Hu Q, Wang Z, Xu C, Wang X, Gong G, Mansoor A, Lee J, Hou M, Zeng L, et al. Autologous stem cell transplantation for myocardial repair. American Journal of Physiology- Heart and Circulatory Physiology. 2004 August 1;287(2):H501–11.

3. Falanga V, Iwamoto S, Chartier M, Yufit T, Butmarc J, Kouttab N, Shrayer D, Carson P. Autologous bone marrow-derived cultured mesenchymal stem cells delivered in a fibrin spray accelerate healing in murine and human cutaneous wounds. Tissue engineering. 2007 June 1;13(6):1299–1312.

4. Chang EI, Bonillas RG, El-Ftesi S, Chang EI, Ceradini DJ, Vial IN, Chan DA, Michaels J, Gurtner GC. Tissue engineering using autologous microcirculatory beds as vascularized bioscaffolds. The FASEB journal : official publication of the Federation of American Societies for Experimental Biology. 2009 March 1;23(3):906–915.

5. Yang D, Guo T, Nie C, Morris SF. Tissue-engineered blood vessel graft produced by self-derived cells and allogenic acellular matrix: a functional performance and histologic study. Annals of plastic surgery. 2009 March 1;62(3):297–303.

6. Sorrell JM, Caplan AI. Topical delivery of mesenchymal stem cells and their function in wounds. Stem cell research & therapy. 2010 September 24;1(4):30.

7. Gibot L, Galbraith T, Huot J, Auger FA. A preexisting microvascular network benefits in vivo revascularization of a microvascularized tissue-engineered skin substitute. Tissue Engineering Part A. 2010 October;16(10):3199–3206.

8. Black AF, Berthod F, L'heureux N, Germain L, Auger FA. In vitro reconstruction of a human capillary-like network in a tissue-engineered skin equivalent. The FASEB journal : official publication of the Federation of American Societies for Experimental Biology. 1998 October;12(13):1331–1340.

9. Cassell OCS, Hofer SOP, Morrison WA, Knight KR. Vascularisation of tissue-engineered grafts: the regulation of angiogenesis in reconstructive surgery and in disease states. British journal of plastic surgery. 2002 December;55(8):603–610.

10. Chen X, Aledia AS, Ghajar CM, Griffith CK, Putnam AJ, Hughes CCW, George SC. Prevascularization of a fibrin-based tissue construct accelerates the formation of functional anastomosis with host vasculature. Tissue Engineering Part A. 2009 June;15(6):1363–1371.

11. Kim CH, Lee JH, Won JH, Cho MK. Mesenchymal stem cells improve wound healing in vivo via early activation of matrix metalloproteinase-9 and vascular

endothelial growth factor. Journal of Korean medical science. 2011 June;26(6):726–733.

12. Wu X, Ren J, Li J. Fibrin glue as the cell-delivery vehicle for mesenchymal stromal cells in regenerative medicine. Cytotherapy. 2011 December 16.

13. Hong H, Stegemann JP. 2D and 3D collagen and fibrin biopolymers promote specific ECM and integrin gene expression by vascular smooth muscle cells. Journal of biomaterials science. Polymer edition. 2008;19(10):1279–1293.

14. Whittington CF, Yoder MC, Voytik-Harbin SL. Collagen-Polymer Guidance of Vessel Network Formation and Stabilization by Endothelial Colony Forming Cells In Vitro. Macromolecular bioscience. 2013 July 5.

15. Bruggeman LA, Doan RP, Loftis J, Darr A, Calabro A. A cell culture system for the structure and hydrogel properties of basement membranes; Application to capillary walls. Cellular and molecular bioengineering. 2012 June 1;5(2):194–204.

16. Wang C-H, Wang T-M, Young T-H, Lai Y-K, Yen M-L. The critical role of ECM proteins within the human MSC niche in endothelial differentiation. Biomaterials. 2013 June;34(17):4223–4234.

17. Pankajakshan D, Krishnan LK. Design of fibrin matrix composition to enhance endothelial cell growth and extracellular matrix deposition for in vitro tissue engineering. Artificial Organs. 2009 January 1;33(1):16–25.

18. Janmey PA, Winer JP, Weisel JW. Fibrin gels and their clinical and bioengineering applications. Journal of the Royal Society, Interface / the Royal Society. 2009 January 6;6(30):1–10.

19. Jockenhoevel S, Zund G, Hoerstrup SP, Chalabi K, Sachweh JS, Demircan L, Messmer BJ, Turina M. Fibrin gel -- advantages of a new scaffold in cardiovascular tissue engineering. European journal of cardio-thoracic surgery: official journal of the European Association for Cardio-thoracic Surgery. 2001 April;19(4):424–430.

20. van Hinsbergh VWM, Collen A, Koolwijk P. Role of fibrin matrix in angiogenesis. Annals of the New York Academy of Sciences. 2001 January 1;936:426–437.

21. Rao RR, Peterson AW, Ceccarelli J, Putnam AJ, Stegemann JP. Matrix composition regulates three-dimensional network formation by endothelial cells and mesenchymal stem cells in collagen/fibrin materials. Angiogenesis. 2012 June;15(2):253–264.

22. Allen P, Melero-Martin J, Bischoff J. Type I collagen, fibrin and PuraMatrix matrices provide permissive environments for human endothelial and mesenchymal progenitor cells to form neovascular networks. Journal of tissue engineering and regenerative medicine. 2011 April;5(4):e74–86.

23. Kniazeva E, Kachgal S, Putnam AJ. Effects of extracellular matrix density and mesenchymal stem cells on neovascularization in vivo. Tissue Engineering Part A. 2011 April;17(7-8):905–914.

24. Huang NF, Chu J, Lee RJ, Li S. Biophysical and chemical effects of fibrin on mesenchymal stromal cell gene expression. Acta Biomaterialia. 2010 October;6(10):3947–3956.

25. Tschoeke B, Flanagan TC, Koch S, Harwoko MS, Deichmann T, Ellå V, Sachweh JS, Kellomåki M, Gries T, Schmitz-Rode T, et al. Tissue-engineered small-caliber vascular graft based on a novel biodegradable composite fibrin-polylactide scaffold. Tissue Engineering Part A. 2009 August 1;15(8):1909–1918.

26. Zhang G, Drinnan CT, Geuss LR, Suggs LJ. Vascular differentiation of bone marrow stem cells is directed by a tunable three-dimensional matrix. Acta Biomaterialia. 2010 September;6(9):3395–3403.

27. Zhang G, Wang X, Wang Z, Zhang J, Suggs L. A PEGylated fibrin patch for mesenchymal stem cell delivery. Tissue engineering. 2006 January;12(1):9–19.

28. Lutolf MP, Gilbert PM, Blau HM. Designing materials to direct stem-cell fate. Nature. 2009 November 26;462(7272):433–441.

29. Hocking AM, Gibran NS. Mesenchymal stem cells: paracrine signaling and differentiation during cutaneous wound repair. Experimental Cell Research. 2010 August 15;316(14):2213–2219.

30. Rytlewski JA, Geuss LR, Anyaeji CI, Lewis EW, Suggs LJ. Three-dimensional image quantification as a new morphometry method for tissue engineering. Tissue Engineering Part C: Methods. 2012 July;18(7):507–516.

31. Nehls V, Drenckhahn D. A novel, microcarrier-based in vitro assay for rapid and reliable quantification of three-dimensional cell migration and angiogenesis. Microvascular research. 1995 November;50(3):311–322.

32. Nakatsu MN, Hughes CCW. An optimized three-dimensional in vitro model for the analysis of angiogenesis. Methods in enzymology. 2008;443:65–82.

33. Yakimets I, Paes SS, Wellner N, Smith AC, Wilson RH, Mitchell JR. Effect of water content on the structural reorganization and elastic properties of biopolymer films: a comparative study. Biomacromolecules. 2007 May;8(5):1710–1722.

34. Frisman I, Orbach R, Seliktar D, Bianco-Peled H. Structural investigation of PEG-fibrinogen conjugates. Journal of Materials Science: Materials in Medicine. 2010 January 1;21(1):73–80.

35. Sahai S, McFarland R, Skiles ML, Sullivan D, Williams A, Blanchette JO. Tracking hypoxic signaling in encapsulated stem cells. Tissue Engineering Part C: Methods. 2012 July;18(7):557–565.

36. Demol J, Lambrechts D, Geris L, Schrooten J, Van Oosterwyck H. Towards a quantitative understanding of oxygen tension and cell density evolution in fibrin hydrogels. Biomaterials. 2011 January;32(1):107–118.

37. Iruela-Arispe ML, Davis GE. Cellular and molecular mechanisms of vascular lumen formation. Developmental Cell. 2009 February;16(2):222–231.

38. Koh W, Mahan RD, Davis GE. Cdc42-and rac1-mediated endothelial lumen formation requires Pak2, Pak4 and Par3, and PKC-dependent signaling. Journal of cell science. 2008;121(7):989–1001.

39. Davis GE, Camarillo CW. An alpha 2 beta 1 integrin-dependent pinocytic mechanism involving intracellular vacuole formation and coalescence regulates capillary lumen and tube formation in three-dimensional collagen matrix. Experimental Cell Research. 1996 April 10;224(1):39–51.

40. Sacharidou A, Stratman AN, Davis GE. Molecular mechanisms controlling vascular lumen formation in three-dimensional extracellular matrices. Cells, tissues, organs. 2012;195(1-2):122–143.

41. Lammert E, Axnick J. Vascular lumen formation. Cold Spring Harbor perspectives in medicine. 2012 April;2(4):a006619.

42. Nelson KS, Beitel GJ. More than a pipe dream: uncovering mechanisms of vascular lumen formation. Developmental Cell. 2009 October;17(4):435–437.

43. Tips, stalks, tubes: notch-mediated cell fate determination and mechanisms of tubulogenesis during angiogenesis. 2012 February;2(2):a006601–a006601.

44. Bayless K, Davis G. The Cdc42 and Rac1 GTPases are required for capillary lumen formation in three-dimensional extracellular matrices. Journal of cell science. 2002;115(6):1123–1136.

45. Davis GE, Stratman AN, Sacharidou A, Koh W. Molecular basis for endothelial lumen formation and tubulogenesis during vasculogenesis and angiogenic sprouting. International review of cell and molecular biology. 2011;288:101–165.

46. Davis GE, Bayless KJ, Mavila A. Molecular basis of endothelial cell morphogenesis in three-dimensional extracellular matrices. The Anatomical record. 2002 November 1;268(3):252–275.

47. Bayless KJ, Salazar R, Davis GE. RGD-dependent vacuolation and lumen formation observed during endothelial cell morphogenesis in three-dimensional fibrin matrices involves the alpha(v)beta(3) and alpha(5)beta(1) integrins. The American journal of pathology. 2000 May;156(5):1673–1683.

48. Davis GE, Bayless KJ. An integrin and Rho GTPase-dependent pinocytic vacuole mechanism controls capillary lumen formation in collagen and fibrin matrices. Microcirculation (New York, N.Y. : 1994). 2003 January;10(1):27–44.

49. Pinner SE, Sahai E. Integrin-independent movement of immune cells. F1000 biology reports. 2009;1:67.

50. Lämmermann T, Bader BL, Monkley SJ, Worbs T, Wedlich-Söldner R, Hirsch K, Keller M, Förster R, Critchley DR, Fässler R, et al. Rapid leukocyte migration by integrin-independent flowing and squeezing. Nature. 2008 May 1;453(7191):51–55.

51. Wolf K, Mazo I, Leung H, Engelke K, Andrian von UH, Deryugina EI, Strongin AY, Bröcker E-B, Friedl P. Compensation mechanism in tumor cell migration: mesenchymal-amoeboid transition after blocking of pericellular proteolysis. The Journal of cell biology. 2003 January 20;160(2):267–277.

52. Oswald J, Boxberger S, Jørgensen B, Feldmann S, Ehninger G, Bornhäuser M, Werner C. Mesenchymal Stem Cells Can Be Differentiated Into Endothelial Cells In Vitro. Stem cells (Dayton, Ohio) [Internet]. 2004 May;22(3):377–384.

53. Ha H, Kim I, Lee SK, Yoon JI, Kim DE, Kim M. Fibrin glue improves the therapeutic effect of MSCs by sustaining survival and paracrine function. Tissue Engineering Part A. 2013 May 24.

54. Schlosser S, Dennler C, Schweizer R, Eberli D, Stein JV, Enzmann V, Giovanoli P, Erni D, Plock JA. Paracrine effects of mesenchymal stem cells enhance vascular regeneration in ischemic murine skin. Microvascular research. 2012 May;83(3):267–275.

55. Kinnaird T, Stabile E, Burnett MS, Lee CW, Barr S, Fuchs S, Epstein SE. Marrow-derived stromal cells express genes encoding a broad spectrum of arteriogenic cytokines and promote in vitro and in vivo arteriogenesis through paracrine mechanisms. Circulation research. 2004 March 19;94(5):678–685.

56. Janeczek Portalska K, Leferink A, Groen N, Fernandes H, Moroni L, van Blitterswijk C, de Boer J. Endothelial Differentiation of Mesenchymal Stromal Cells Kerkis I, editor. PloS one. 2012 October 4;7(10):e46842.

57. Stratman AN, Saunders WB, Sacharidou A, Koh W, Fisher KE, Zawieja DC, Davis MJ, Davis GE. Endothelial cell lumen and vascular guidance tunnel formation requires MT1-MMP-dependent proteolysis in 3-dimensional collagen matrices. Blood. 2009 July 9;114(2):237–247.

58. Haas TL, Madri JA. Extracellular matrix-driven matrix metalloproteinase production in endothelial cells: implications for angiogenesis. Trends in Cardiovascular Medicine. 1999 April;9(3-4):70–77.

59. Davis GE, Koh W, Stratman AN. Mechanisms controlling human endothelial lumen formation and tube assembly in three-dimensional extracellular matrices. Birth defects research. Part C, Embryo today : reviews. 2007 December;81(4):270–285.

60. Greene AK, Puder M, Roy R, Arsenault D, Kwei S, Moses MA, Orgill DP. Microdeformational wound therapy: effects on angiogenesis and matrix metalloproteinases in chronic wounds of 3 debilitated patients. Annals of plastic surgery. 2006 April 1;56(4):418–422.

61. Kachgal S, Carrion B, Janson IA, Putnam AJ. Bone marrow stromal cells stimulate an angiogenic program that requires endothelial MT1-MMP. Journal of Cellular Physiology. 2012 January 19.

62. Ahmed TAE, Griffith M, Hincke M. Characterization and inhibition of fibrin hydrogel-degrading enzymes during development of tissue engineering scaffolds. Tissue engineering. 2007 July;13(7):1469–1477.

63. Ratel D, Mihoubi S, Beaulieu E, Durocher Y, Rivard G-E, Gingras D, Béliveau R. VEGF increases the fibrinolytic activity of endothelial cells within fibrin matrices: involvement of VEGFR-2, tissue type plasminogen activator and matrix metalloproteinases. Thrombosis research. 2007;121(2):203–212.

64. Chetty C, Lakka SS, Bhoopathi P, Rao JS. MMP-2 alters VEGF expression via alphaVbeta3 integrin-mediated PI3K/AKT signaling in A549 lung cancer cells. International journal of cancer Journal international du cancer. 2010 September 1;127(5):1081–1095.

65. Valentijn KM, Sadler JE, Valentijn JA, Voorberg J, Eikenboom J. Functional architecture of Weibel-Palade bodies. Blood. 2011 May 12;117(19):5033–5043.

66. Starke RD, Ferraro F, Paschalaki KE, Dryden NH, McKinnon TAJ, Sutton RE, Payne EM, Haskard DO, Hughes AD, Cutler DF, et al. Endothelial von Willebrand factor regulates angiogenesis. Blood. 2011 January 20;117(3):1071–1080.

67. Wang Y, Kaiser MS, Larson JD, Nasevicius A, Clark KJ, Wadman SA, Roberg-Perez SE, Ekker SC, Hackett PB, McGrail M, et al. Moesin1 and Ve-cadherin are required in endothelial cells during in vivo tubulogenesis. Development (Cambridge, England). 2010 September;137(18):3119–3128.

68. Grainger SJ, Putnam AJ. Assessing the permeability of engineered capillary networks in a 3D culture. PloS one. 2011;6(7):e22086.

69. Kiran MS, Viji RI, Kumar SV, Prabhakaran AA, Sudhakaran PR. Changes in expression of VE-cadherin and MMPs in endothelial cells: Implications for angiogenesis. Vascular cell. 2011;3(1):6.

70. Griffith CK, Miller C, Sainson RCA, Calvert JW, Jeon NL, Hughes CCW, George SC. Diffusion limits of an in vitro thick prevascularized tissue. Tissue engineering. 2005 January 1;11(1-2):257–266.

71. Malda J, Klein TJ, Upton Z. The roles of hypoxia in the in vitro engineering of tissues. Tissue engineering. 2007 September;13(9):2153–2162.

72. Basciano L, Nemos C, Foliguet B, de Isla N, de Carvalho M, Tran N, Dalloul A. Long term culture of mesenchymal stem cells in hypoxia promotes a genetic program maintaining their undifferentiated and multipotent status. BMC cell biology. 2011;12:12.

73. Lönne M, Lavrentieva A, Walter J-G, Kasper C. Analysis of oxygen-dependent cytokine expression in human mesenchymal stem cells derived from umbilical cord. Cell and tissue research. 2013 July;353(1):117–122.

74. Némos C, Basciano L, Dalloul A. [Biological effects and potential applications of mesenchymal stem cell culture under low oxygen pressure]. Pathologie-biologie. 2012 June;60(3):193–198.

75. Tsai C-C, Yew T-L, Yang D-C, Huang W-H, Hung S-C. Benefits of hypoxic culture on bone marrow multipotent stromal cells. American journal of blood research. 2012;2(3):148–159.

76. Das R, Jahr H, van Osch GJVM, Farrell E. The role of hypoxia in bone marrow-derived mesenchymal stem cells: considerations for regenerative medicine approaches. Tissue engineering. Part B, Reviews. 2010 April;16(2):159–168.

77. Grayson WL, Zhao F, Izadpanah R, Bunnell B, Ma T. Effects of hypoxia on human mesenchymal stem cell expansion and plasticity in 3D constructs. Journal of Cellular Physiology. 2006 May;207(2):331–339.

78. Jiang BH, Semenza GL, Bauer C, Marti HH. Hypoxia-inducible factor 1 levels vary exponentially over a physiologically relevant range of O2 tension. The American journal of physiology. 1996 October;271(4 Pt 1):C1172–80.

79. Liu K, Chi L, Guo L, Liu X, Luo C, Zhang S, He G. The interactions between brain microvascular endothelial cells and mesenchymal stem cells under hypoxic conditions. Microvascular research. 2008 January;75(1):59–67.

80. Lee EY, Xia Y, Kim W-S, Kim MH, Kim TH, Kim KJ, Park B-S, Sung J-H. Hypoxia-enhanced wound-healing function of adipose-derived stem cells: increase in stem cell proliferation and up-regulation of VEGF and bFGF. Wound repair and regeneration : official publication of the Wound Healing Society [and] the European Tissue Repair Society. 2009 July;17(4):540–547.

81. Vartanian AA. Signaling pathways in tumor vasculogenic mimicry. Biochemistry. Biokhimiiâ. 2012 September;77(9):1044–1055.

82. Paulis YWJ, Soetekouw PMMB, Verheul HMW, Tjan-Heijnen VCG, Griffioen AW. Signalling pathways in vasculogenic mimicry. Biochimica et biophysica acta. 2010 August;1806(1):18–28.

83. Galas RJ, Liu JC. Vascular endothelial growth factor does not accelerate endothelial differentiation of human mesenchymal stem cells. Journal of Cellular Physiology. 2013 June 21.

84. Piret J-P, Mottet D, Raes M, Michiels C. CoCl2, a chemical inducer of hypoxia-inducible factor-1, and hypoxia reduce apoptotic cell death in hepatoma cell line HepG2. Annals of the New York Academy of Sciences. 2002 November;973:443–447.

85. Zan T, Du Z, Li H, Li Q, Gu B. Cobalt chloride improves angiogenic potential of CD133+ cells. Frontiers in bioscience : a journal and virtual library. 2012;17:2247–2258.

86. Vengellur A, LaPres JJ. The role of hypoxia inducible factor 1alpha in cobalt chloride induced cell death in mouse embryonic fibroblasts. Toxicological sciences : an official journal of the Society of Toxicology. 2004 December;82(2):638–646.

87. Ren H, Cao Y, Zhao Q, Li J, Zhou C, Liao L, Jia M, Zhao Q, Cai H, Han ZC, et al. Proliferation and differentiation of bone marrow stromal cells under hypoxic conditions. Biochemical and biophysical research communications. 2006 August 18;347(1):12–21.

88. Peters K, Schmidt H, Unger RE, Kamp G, Pröls F, Berger BJ, Kirkpatrick CJ. Paradoxical effects of hypoxia-mimicking divalent cobalt ions in human endothelial cells in vitro. Molecular and Cellular Biochemistry. 2005 February;270(1-2):157–166.

89. Borcar A, Menze MA, Toner M, Hand SC. Metabolic preconditioning of mammalian cells: mimetic agents for hypoxia lack fidelity in promoting phosphorylation of pyruvate dehydrogenase. Cell and tissue research. 2013 January;351(1):99–106.

90. Rappolee DA, Xie Y, Slater JA, Zhou S, Puscheck EE. Toxic stress prioritizes and imbalances stem cell differentiation: implications for new biomarkers and in vitro toxicology tests. Systems biology in reproductive medicine. 2012 February;58(1):33–40.

Chapter 4: Vasculogenic mimicry as a new model for understanding endothelial-like behavior of MSCs

Overview and Aims

Chapter 4 relies on findings from Chapter 3 to pursue directed investigation of mechanisms responsible for MSC behavior in PEGylated fibrin. Though Chapters 3 and 4 have been independently presented in this document, they will be merged into a single manuscript for future publication. The goals of Chapter 4 are outlined by Aim 3.

Aim 3: Investigate the mechanisms responsible for endothelial-like MSC behavior in PEGylated fibrin gels.

Rationale: MSCs in PEGylated fibrin exhibit a partial endothelial phenotype. The utility of endothelial-like cell behavior and why PEGylated fibrin elicits this cell response remains unknown. Understanding both questions is central to directing future applications of our cell-based ischemic therapy.

A. Compare phenotypic and morphologic outcomes of MSCs to endothelial cells.

B. From results of 2E, explore how implicated mechanisms modulate endothelial-like behavior of MSCs.

C. Validate findings of 3B with an *in vivo* model.

INTRODUCTION

Stem cell-based therapies are a developing avenue for treating ischemia and chronic wounds.[1-4] One strategy aims to locally deliver autologous cells within a biomaterial carrier, encouraging neovascularization and tissue recovery.[5-7] Our group is working towards once such cell therapy: the delivery of bone marrow-derived mesenchymal stem cells (MSCs) within an *in situ* gelling PEGylated fibrin matrix.[8] We have previously shown that PEGylated fibrin promotes spontaneous formation of MSC tubular networks without soluble factors.[9] However, the vascular morphology is accompanied by an incomplete endothelial immunophenotype. As shown in Figure 4.1, MSCs in PEGylated fibrin consistently express von Willebrand factor (vWF) and vascular endothelial cadherin (VE-cadherin) but not platelet endothelial cell adhesion molecule (PECAM-1), which is highly specific to mature endothelial populations.[10] The lack of complete differentiation towards an endothelial lineage has raised questions regarding the clinical utility of these MSC networks. Alternative cell-based approaches to neovascularization are developing endothelial-MSC co-culture systems, which instead use MSCs as a pericytic vascular support.[11-13] The present lack of fully mature MSC-derived endothelium motivated us to seek alternative explanations for this endothelial-*like* behavior, aside from terminal transdifferentiation mechanisms.

The majority of vascular tissue engineering strategies are inspired by normative developmental and postnatal biological processes. Diseased states, though, may offer new insights for achieving similar outcomes. A cancer-derived process for tissue perfusion, termed "vasculogenic mimicry" (VM), was first described in melanoma tumors in 1999.[14] As tumors reach critical levels of hypoxic stress, some develop an aggressive survival mechanism whereby dedifferentiated cancer cells adopt endothelial-*like* qualities and

become VM cells (see Figure 4.2 diagram).[15,16] These VM cells form functional channels that anastomose with normal vasculature to divert blood flow into the tumor.[17] Thus, VM-capable tumors are able to alleviate hypoxic stress independent of classical endothelial cell (EC) mechanisms. In vascular biology, VM was the first evidence that perfusion of non-endothelialized networks is possible without clotting.[18]

In regards to our research, VM cells notably share the same immunophenotype as MSCs in PEGylated fibrin, which first piqued our interest in this model. Specifically, both populations are vWF+/VE-cadherin+/PECAM1- and share mesenchymal-lineage characteristics.[14,19] The functional abilities of VM cells in cancer, coupled with a semi-endothelial immunophenotype, suggest that *mature endothelialization may not be a requirement for therapeutically beneficial transient perfusion*. This paradigm provides our field with a new perspective towards understanding how and why mesenchymal cell types may self-organize and perfuse tissues.

Elucidating the driving mechanisms of MSC network development is necessary for understanding PEGylated fibrin's therapeutic significance. Given the shared phenotypic characteristics of our MSCs and VM cells, we hypothesized that a mechanistic resemblance may also exist. Hypoxia is a catalyzing stressor that drives tumors towards VM; [20-22] thus, hypoxia should be investigated as similarly crucial for MSC tubulogenesis, specifically the hypoxia inducible factor (HIF) pathway. Furthermore, pilot studies from Chapter 3 established early indications that hypoxia modulates MSC behavior in our system as well. Under hypoxic conditions, MSC networks exhibited increased their production of VEGF and MMP-2.

Additionally, three-dimensional (3D) substrates (by design) raise hypoxic stress compared to their two-dimensional (2D) analogues. As a recent study showed, cells in 3D substrates under normoxic conditions will still experience hypoxia while cells on 2D

substrates will not.[23] Not all 3D substrates drive spontaneous MSC tubulogenesis, though. In a related study,[24] we have observed that fibrin uniquely increases angiogenic signaling over other extracellular substrates, such as collagen or Matrigel. Cryo-SEM imaging has also demonstrated that fibrin PEGylation introduces amorphous packing regions within the typically fibrous gel, which slowed dye penetration and liquid filtration in diffusional studies (Chapter 3). These physical attributes suggest that PEGylated fibrin is more likely to cause a greater degree of hypoxia than unmodified fibrin gels alone. In light of VM, we now hypothesize that *spontaneous MSC tubulogenesis is achieved through the synergy of two mechanisms: (1) biochemical signaling of angiogenic cues from fibrin and (2) increased hypoxia from PEGylation*.

With VM as a model, we aim to investigate (1) whether endothelial mimicry is unique to MSCs or also present in other mesenchymal populations and (2) if MSC network development is similar to VM in its dependence on HIF-mediated mechanisms. To our knowledge, this is the first time VM has been applied as an explanation for matrix-driven MSC network development.

MATERIALS AND METHODS

Materials

Low-glucose Dulbecco's modified Eagle's medium (DMEM), phosphate buffered saline (PBS), fetal bovine serum (FBS), and Gluta-MAX™ -I (100x) were purchased from Invitrogen (Carlsbad, CA). Penicillin-streptomycin and trypsin/ethylenediaminetetraa-acetic acid were purchased from ATCC (Manassas, VA). Sigma-Solohill microcarrier beads (MCBs) coated in porcine collagen were obtained from Sigma-Aldrich (St. Louis, MO) as well as fibrinogen and thrombin from human plasma. Linear homo-difunctional

succinimidylglutarate polyethylene glycol (PEG-$(SG)_2$, 3400 Da) was purchased from NOF America (White Plains, NY).

Cell culture of mesenchymal stem cells and normal dermal fibroblasts

Human bone marrow-derived mesenchymal stem cells (MSCs) from Lonza (Basel, Switzerland) were cultured according to manufacturer specifications with growth medium in tissue culture-treated plastic flasks (Corning, Corning, NY) at 5000 cells/cm^2. Normal human dermal fibroblasts (NHDFs; Promocell; Heidelberg, Germany) from adult skin were cultured with the same protocol. Growth medium consisted of DMEM supplemented with 10% FBS, 1% penicillin-streptomycin, and 2mM GlutaMAX™-I. MSCs were tested by the manufacturer for trilineage differentiation potential and for positive expression of CD105, CD166, CD29, and CD44; cells were negative for CD14, CD34, and CD45. Population purity was greater than 95%. NHDFs were tested for positive expression of the fibroblast specific antigen, CD90. Cultures were maintained at 37°C and 5% CO_2.

Cell culture of microvascular endothelial cells

Human dermal microvascular endothelial cells (HDMECs; Promocell; Heidelberg, Germany) from capillary vessels were cultured with endothelial growth medium in tissue culture-treated plastic flasks at 10000 cells/cm^2. Endothelial growth medium consisted of DMEM supplemented with the Endothelial Growth Medium MV 2 SupplementPack (Promocell), additional FBS up to 10%, and 1% penicillin-streptomycin. HDMECs were tested for positive expression of vWF, CD31, and Podoplanin. Cultures were maintained at 37°C and 5% CO_2.

Cell seeding of microcarrier-beads

Cells were seeded on MCBs according to our previously described protocol, based on the modified bead-outgrowth assay developed by Nakatsu and Hughes.[25,26] Briefly, MCBs were suspended at 2 mg/mL in PBS, autoclaved, and stored at 4°C before use. Prior to seeding, MCBs were distributed as 4mg aliquots into FACS tubes and briefly centrifuged into a pellet to remove the PBS. Growth media was added for 1h to prime MCBs for cell seeding, which was then removed immediately before adding cells. Cells at passages 4-6 were trypsinized, centrifuged into a pellet, and re-suspended at a minimum concentration of 1.4×10^5 cells/mL growth media. MSCs and NHDFs were added to FACS tubes of MCBs for a final concentration of 7.0×10^4 cells/mg MCB and a total of 2mL growth media per FACS tube. HDMECs were seeded at a density 4× higher. Cells and MCBs were gently resuspended every 30min for the first 4h to evenly coat MCBs with cells. The cells and MCBs were then transferred to ultra-low adhesion 6-well plates for further coating overnight; the plate was gently agitated on an orbital shaker to minimize MCB aggregation. Seeded MCBs were strained through a 70μm mesh and rinsed with PBS to remove any unattached cells. Finally, MBCs were resuspended in 300μL growth media/mg MCB.

Three-dimensional gel culture *in vitro*

Gel fabrication followed our previously described protocol for enzymatically crosslinked PEGylated fibrin and fibrin gels.[8,9] Human fibrinogen was solubilized in PBS (without calcium or magnesium, pH 7.8) at 80 mg/mL. PEG-SG_2 was similarly dissolved in PBS at 8 mg/mL. The PEG-SG_2 concentrations correspond with a 10:1 molar ratio of reactive groups to each fibrinogen solution. Human thrombin was reconstituted in nanopure ddH_2O to 100U/mL, which was further diluted to 25U/mL with 40mM $CaCl_2$.

Gel components were passed through 0.22μm filters for sterility before use. Gels with 1mL total volumes were fabricated in 12-well plates and those with 0.5mL total volumes in 24-well plates. Gel components were mixed in the following order using the same volumetric ratio: 1 fibrinogen: 1 PEG-SG_2: 2 seeded MCBs: 4 thrombin. Gelation was finalized at 37°C for 15min before rinsing with PBS (with calcium and magnesium), followed by growth media rinses at 5min, 10min, 30min, and 1h to remove cytotoxic unreacted PEG-SG_2. Gel culture was carried out to Day 7 with cell-specific growth media unless otherwise specified.

Hypoxia cell culture

For some experimental groups, MSCs in PEGylated fibrin were also cultured under 1% O_2 using a hypoxia chamber (Stemcell Technologies; Tukwila, WA), generously loaned to us from Dr. Aaron Baker. The hypoxic gas mix was composed of 5% CO_2, 1% O_2, and 94% N_2 (Praxair; Danbury, CT). Cell cultures were environmentally isolated inside the hypoxia chamber with an open petri dish of water for humidity and placed in a 37°C oven. The chamber was purged with the hypoxic gas mixture for 5min and then purged again 90min later to evacuate any residual oxygen content from the culture media. Thereafter, the chamber was purged every 48h to maintain hypoxic cultures unless opened for assay endpoints.

Fluorescent cell staining

On day 7 of gel culture, samples were rinsed six times with PBS (with calcium and magnesium) for 15min each. Calcein AM (Invitrogen; Carlsbad, CA), a live-cell cytoplasm stain, was added at 10μM for 1h. Samples were rinsed four times with PBS

every 5min and then fixed with 4% neutral-buffered formalin for 30min. Finally, gels were briefly rinsed with 3 volumes of PBS to remove residual fixative and stored at 4°C overnight for imaging the next day.

Two-photon microscopy

Fluorescent z-stacks were collected of cell outgrowth from individual microcarrier beads with an Ultima Multiphoton Microscopy System (Prairie Technologies; Middleton, WI). Two-photon excitation was achieved with a tunable Ti:sapphire laser (Spectra-Physics Mai Tai HP; Newport; Irvine, CA) set to 720nm under a 10x water-immersion objective. Z-slice thicknesses were adjusted to maintain isometric voxel dimensions. A thickness of 500-700μm was imaged along the z-axis for each image stack.

Three-dimensional morphological quantification

Image processing and three-dimensional morphological quantification followed our recently described method.[9] As before, z-stacks were preprocessed in ImageJ (Release 1.2.4; ImageJ Plugin Project) and exported as Visualization Toolkit (.vtk) files and loaded into 3D Slicer (Release 3.6, 64-bit Linux), an open-source program for MRI/CT analysis. The Vascular Modeling Toolkit in 3D Slicer was used for image segmentation and 3D model generation. Centerline tracings of 3D models were exported as large data clouds of x,y,z coordinates with corresponding radii; the measured radius represented the model's maximum cross-sectional diameter at each coordinate point. The data cloud was processed in MATLAB (Release 2008a for Macintosh) to calculate the average 3D network length per MCB.

Cellular protein detection with western blot

Cells in gel matrices were lysed with RIPA buffer (Santa Cruz Biotechnology; Dallas, TX) and homogenized for 30s with a soft tissue grinder (OMNI International; Kennesaw, GA). Cell-gel lysates were passed through a 21-gauge needle 20× for further homogenization and solid gel remnants were removed through sample centrifugation at 14000×*g* for 10min at 4°C. The supernatants were denatured in a reducing buffer of Laemmli sample buffer with 5% β-mercaptoethanol at 95°C for 5min. Denatured samples were separated with 10% mini-Protean® TGX™ precast gels (Biorad; Hercules, CA) at 20μg protein per gel lane and blotted onto PVDF membranes. Membranes were blocked for 1h at room temperature with 5% (w/v) nonfat milk in TBST and then incubated overnight with a primary antibody at 4°C. Membranes were then rinsed with TBST 3× for 5min each and incubated with an HRP-conjugated secondary antibody for 1h at room temperature. After a second set of TBST rinses, 3mL of SuperSignal West Dura Chemiluminescent Substrate (Pierce Thermo Fisher Scientific; Rockford, IL) was added per membrane for 5min prior to image capture with a FluorChem CCD system (ProteinSimple; Santa Clara, CA). Chemiluminescent signal was quantified with AlphaView software for statistical analysis. For a list of antibodies and their dilutions, refer to Table 4.1.

HIF-1α protein detection with ELISA

Due to the small quantity of HIF produced in cells (compared to total sample protein of cells + degraded matrix) western blot analysis was insufficient for detecting this protein. Interference of the gel's protein matrix also prevented fractionation of the sample to enrich for nuclear content, where stabilized HIF-1a is located. A DuoSet ELISA (R&D Systems; Minneapolis, MN) was procured instead for detecting HIF-1a

using a larger sample volume. Since HIF-1α degrades rapidly upon exposure to normal oxygen levels, the method of obtaining protein supernatants was modified to minimize this risk. Briefly, all reagents were prepared and chilled before removing hypoxic cultures from the chamber environment. Once the chamber was opened, samples were immediately placed on ice and culture media quickly aspirated. As each sample was aspirated, RIPA buffer was added in succession. Samples (on ice) were placed on a side-to-side rocker for 15min and then transferred to centrifuge tubes for centrifugation at 14000×*g* for 10min at 4°C. Supernatants were directly used for ELISA according to the manufacturer's instruction. Optical density was measured at 490nm. These OD values were normalized to DNA content, measured by nanodrop at 230nm.

Chorioallantoic membrane assay

Common quail embryos (*Coturnix coturnix*) were cultivated *ex ovo* in a modified version of the chorioallantoic membrane (CAM) assay.[27-29] A cell culture incubator was modified to accommodate embryo growth. Briefly, the temperature was raised to 37.8°C and CO_2 lowered to 0%. Instead of adding Fungizone to the humidity pan, autoclaved water with 1mM cupric sulfate (antibacterial) was used to minimize harmful vapors. A small fan was attached to the side port of the incubator to increase air circulation, improving embryo survival. One hundred quail eggs (Northwest Gamebirds; Kennewick, WA) were incubated until E2.5 before shell removal. Specialized egg-topping scissors were used to carefully remove eggshells and embryos were transferred to 60mm Petri dishes. Four open 60mm Petri dishes (each containing one embryo) were placed within 150mm Petri dishes. Autoclaved water (with 1mM cupric sulfate) was added to the bottom of the 150mm Petri dishes to provide secondary humidification. During this time,

MSCs were pre-stained with DiI and encapsulated in 10mg/mL PEGylated fibrin gels at a concentration of 5×10^5 cells per mL *ex vivo*; microcarrier beads were not used for this study. On E8 (also, MSC culture Day 4), gels were sliced into six pieces. Two small pieces of gel were carefully laid on the peripheral CAM vasculature, avoiding direct coverage of major vessels. Onplants were covered with 100μL of media to maintain cell viability. On E11, quail embryos were sedated with isofluorene and intracardially injected with 2MDa FITC-dextran dye.[30] The dye was allowed to circulate for 2min before terminating embryos by decapitation and removing the embryos from the CAM. CAMs were immediately fixed with 4% neutral buffered formalin overnight at 4°C. Fixed CAMs were rinsed with PBS, dissected further to remove any opaque yolk fragments, and oriented for imaging. Images were collected under wide-field fluorescence and phase-contrast. While the University of Texas at Austin IACUC does not require a protocol for avian embryos, American Veterinary Medicine Association guidelines for embryos beyond 50% gestational development were followed.[31]

Statistical analysis

A one- or two-way analysis of variance was used to determine significance between experimental groups. Where significance was found, post-hoc tests were performed to further determine specific relationships of statistical significance. Tukey's correction for multiple comparisons was applied where appropriate. P-values less than 0.05 were considered statistically significant. All statistical tests were completed in Prism (Version 6.0 for Mac OS X; GraphPad, La Jolla, CA).

RESULTS AND DISCUSSION

MSC networks have more fibroblastic than endothelial character

Our initial assumption was that MSC vascular morphogenesis behaviorally resembled normal endothelial cells during capillary development.[32] Hence, we designed an experiment to validate this assumption of endothelial-type MSC behavior. In this experiment, MSC network morphology and phenotype were compared to mature microvascular endothelial cells and dermal fibroblasts. Human dermal microvascular endothelial cells (HDMECs) served as a positive control for capillary morphogenesis and represented the target MSC lineage. Similarly, undifferentiated MSCs and fibroblasts are well known to express overlapping surface markers and posses a characteristic spindle-like morphology.[33] Thus, normal human dermal fibroblasts (NHDFs) served as an appropriate negative control and represented the initial behavior of undifferentiated MSCs.

Differences in matrix tunneling were immediately evident between HDMECs versus MSCs and NHDFs. In pilot studies, HDMECs were unable to sprout in PEGylated fibrin (without added VEGF stimulus) and were therefore cultured in pure fibrin gels at the same concentration as the PEGylated fibrin gels for MSCs and NHDFs. Even so, HDMEC networks were limited and unstable (Figure 4.3A), requiring morphological analysis after Day 4 (for all samples). Difficulty in achieving network formation from endothelial cells is well-known; mature endothelial cells have limited proteolytic abilities, requiring co-culture with fibroblasts or MSCs to rescue and sustain tubule assembly.[34-37] MSCs and NHDFs both formed typical networks without regard for matrix density or PEGylation, as shown in Figure 4.3B and 4.3C, respectively. Quantification of these network morphologies reflected general observations. HDMEC networks were significantly shorter and more discontinuous than MSC and NHDF networks (Figure

4.3D). Furthermore, MSCs and NHDFs had networks of statistically similar lengths, indicating that MSC network coalescence more closely resembled fibroblastic than endothelial assembly. Morphological differences between MSCs and endothelial cells also carried through to their phenotypic character. While all three-cell populations expressed vWF (Figure 4.3E,G) and VE-cadherin (Figure 4.3F,G), HDEMCs expressed significantly higher levels than MSCs and NHDFs. MSCs and NHDFs were again statistically similar to each other.

The results of this experiment were a pivotal turning point in our research path. MSC network morphology and phenotype strongly resembled fibroblastic more than endothelial behavior. The ability of MSCs to robustly migrate through dense PEGylated fibrin matrices indicated a clear departure from endothelial cell mechanisms, which allow for limited independent migration. Additionally, the *inability* of MSCs match endothelial cell expression of phenotypic markers highlighted their lack of complete differentiation towards an endothelial cell type. Endothelial-like behavior of NHDFs was also a remarkable result. Only one previous study clearly showed that NHDFs are capable of endothelial marker expression when cultured in monolayer with angiogenic growth factor-supplemented medium.[38] In retrospect, the shared mesenchymal lineage of MSCs and NHDFs types suggests a behavioral overlap should (and does) exist, and fibroblasts are similarly known for having a mutable phenotype.[39] Together, these findings suggest that endothelial-based literature is unlikely to shed light on mechanisms of MSC network development since this cell population departs from described endothelial behaviors.

We sought an alternative (non-endothelial) literature base that would provide a more appropriate context and accurate explanation as to why (1) MSCs form tubular networks and (2) express endothelial markers suggestive of functional microvasculature but (3) lack a complete, mature endothelial phenotype. Functionally, vWF is secreted by

endothelial cells (and megakaryocytes) to carry clotting factor VIII in the circulation and is membrane-bound on activated endothelium to facilitate platelet adhesion;[40,41] VE-cadherin enables the formation of homotypic cell-cell junctions, which are necessary for regulating vascular permeability and promoting non-leaky transport.[42] Non-endothelial presentation of VE-cadherin has been noted in literature but reports were limited to cells of the central nervous system, specifically astrocytoma cells and glioma.[43] Generally, cell junctions mediated by cadherins (and combinations of cadherin accessory proteins) are regarded as cell-specific, and "cadherin switching" is associated with malignant phenotype cells transitions. Therefore, the presence of both vWF and VE-cadherin supports the conclusion that MSCs are pursuing vascular-type architecture with perfusional functionality.

Vasculogenic mimicry (VM), a mechanism of tumor survival, offers a unique example of functional non-endothelialized networks.[14] Tumor cells develop an endothelial-*like* phenotype, characterized by strong VE-cadherin expression along with a complement of other endothelial or stem markers, including vWF, Nodal, and CD133.[44-46] Importantly, these networks also have little-to-no PECAM-1 expression.[14] Despite their immature endothelial phenotype, VM networks are capable of perfusing blood through microvascular channels without clotting.[15] Thus, VM suggests that a mature endothelial phenotype may not be required to achieve functional microvasculature and endothelial-like cell types are still therapeutically valuable.

Mechanistically, vasculogenic mimicry is driven by a combination of integrin-mediated matrix cues and the hypoxic stress of an increasingly dense tumor environment.[46] Hypoxia leads to HIF-1α stabilization and nuclear translocation, where it promotes gene expression of VEGF, EphA2, Twist1, COX-2, and OPN.[17,45] Twist1 in turn promotes expression of VE-cadherin, which is a hallmark protein of VM. Melanoma

cells that express negligible levels of VE-cadherin are unable to undergo vasculogenic mimicry.[19,20] VE-cadherin is central in regulating phosphorylation of EphA2 and subsequent downstream activation of MMP-2 via MT1-MMP via phosphatidylinositol-3 kinase (PI3K).[47] Conversely, blocking EphA2 will lead to a decrease in VE-cadherin expression, VEGF production, and MMP-2 activity. Activation of MMP-2 leads to an increase in laminin γ2' and γ2x deposition, and both laminin chains reciprocally encourage further cell migration and more laminin deposition.[17] VM can be further potentiated by VEGF stimulation through autocrine VEGF production as well as "outside-in" integrin activation of focal adhesion kinase (FAK).[48,49] Additionally, EphA2 phosphorylation is associated with FAK-mediated Rac/Cdc42 activation of survival and proliferation cascades and "inside-out" signaling of integrin binding.[49] The cumulative result of these self-perpetuating cascades is the significant upregulation of cell motility machinery and hypoxia responsive elements responsible for neovascularization, facilitating the invasive endothelial-like behavior of these tumor cells.

With vasculogenic mimicry as a potential model for understanding endothelial-like MSC behavior, we moved forward to investigate further similarities between VM and vascular morphogenesis in PEGylated fibrin. Here, fibrin provides the integrin-adhesive matrix environment and the diffusion limitations of PEGylated fibrin, hypothetically, provide the necessary hypoxic stress. In particular, the following experiments were designed to differentiate between matrix-induced and hypoxia-induced endothelial-like behavior of MSCs and to what extent (if any) each contributes to vascular morphogenesis.

Fibrin bioactivity induces endothelial marker expression

Our first experiment inspired by the VM model sought to uncover the impact of substrate cues on endothelial marker expression. To eliminate diffusion-associated hypoxia, MSCs were instead seeded as a 2D monolayer on top of three different thin gel substrates: fibrin, PEGylated fibrin, and collagen, all at 4mg/mL protein. Collagen served as a non-fibrin control to highlight any fibrin-specific outcomes. After seven days of culture, MSCs on PEGylated fibrin expressed significantly higher quantities of vWF (Figure 4.4A,C) and VE-cadherin (Figure 4.4B,C) proteins than MSCs on collagen. However, MSCs on fibrin expressed comparable levels of both proteins to MSCs on PEGylated fibrin.

The results of this experiment indicate that fibrin is the bioactive component responsible for basal levels of endothelial marker expression. Furthermore, PEGylation does not alter the bioactivity of fibrin-mediated cuing. Some reports have suggested that PEG-fibrin conjugates have reduced fibrin bioactivity,[50,51] but the fibrin in our gels appears unaffected. The results here also agree with another related study conducted by our group. We have previously observed that collagen increases adipose-derived MSC expression of smooth muscle actin, a marker of smooth muscle cell development.[24] On fibrin-based substrates, MSC expression of smooth muscle actin was significantly lower. Prior and present results suggest a substrate-induced differentiation tradeoff may exist between endothelial-like and smooth muscle cell development.

Hypoxic stress is key difference between fibrin and PEGylated fibrin outcomes in MSC vascular morphogenesis

Our second experiment inspired by the VM model sought to elucidate the role of hypoxia in driving the endothelial-like behavior of MSCs in PEGylated fibrin. Here we

cultured MSCs in fibrin and PEGylated fibrin (in 3D) under normoxic conditions (Figure 4.5A-C,G,H) to establish a normative trend. We then compared these results to a parallel set of gels cultured under hypoxia (1% O_2) as a "gain of function" study (Figure 4.5D-F,I, J). Hypoxic stress under 1% O_2 was confirmed by measuring HIF-1α protein levels of both normoxic and hypoxic samples after 24h of culture; HIF-1α protein was significantly higher in the hypoxic cultures of both fibrin and PEGylated fibrin MSCs relative to their respective normoxic controls (Figure 4.5K).

Under normoxia, MSCs in PEGylated fibrin expressed significantly higher levels of vWF (Figure 4.5A,C) and VE-cadherin (Figure 4.5B,C) proteins. Given similar levels in 2D culture, this enhanced endothelial phenotype of MSCs in 3D PEGylated fibrin can be directly attributed to slowed diffusion profile caused by PEGylation, which is the only changed variable between the two groups. When fibrin and PEGylated fibrin gels are cultured under hypoxia, we find that the two gels once again induce similar levels of endothelial marker expression (Figure 4.5D-F). This equilibration between MSCs in fibrin and PEGylated fibrin suggests that fibrin-encapsulated MSCs may be "gaining function" through hypoxia-mediated upregulation of their endothelial program.

As previously discussed in Chapter 3, the inability of hypoxia to further potentiate an endothelial phenotype in PEGylated fibrin-encapsulated MSCs may alternatively indicate that we have reached a stress plateau.[52] Based on prior observations of slowed diffusion in PEGylated fibrin matrices, the oxygen available to MSCs in PEGylated fibrin will always be lower than that of MSCs in fibrin, all other factors being equal. Additional hypoxic stress, beyond that generated by the gel environment, may simply have diminishing benefits despite elevations in HIF-1α levels.[53] So, at 1% O_2, MSCs in fibrin may experience a desirable level of hypoxic stress that increases endothelial marker expression while MSCs in PEGylated fibrin experience slightly harsher hypoxic stress

that fails to elicit any further biological benefit. Thus, the equilibrated levels of endothelial markers may be a combinatorial effect of fibrin-encapsulated MSCs "gaining function" under hypoxia and PEGylated fibrin-encapsulated MSCs simply plateauing. In any case, hypoxic stress is clearly modulating the expression of an endothelial-like phenotype, which is sufficient evidence to implicate its importance within MSC vascular morphogenesis.

In contrast to the phenotypic results, MSCs cultured under hypoxic environments were morphologically no different than their normoxic counterparts (Figure 4.5L). Networks formed in PEGylated fibrin were significantly longer than those in fibrin, regardless of oxygen levels. However, the general data trend suggests that MSC networks were slightly shorter under hypoxia, likely due to slower cell proliferation. Our previous characterization of MSC proliferation under hypoxic conditions indicated a dramatic decline under 1% O_2 compared to normoxic controls (Chapter 3). Other studies have also demonstrated that MSCs are metabolically limited at early time points of hypoxic culture.[54,55] Typically, hypoxia-stressed MSCs do not accelerate their growth (relative to normoxic controls) until after three weeks of culture so our results here are still reflective of normal behavior. Since vascular networks are multicellular structures, we can reasonably assume that hypoxia-limited cell proliferation would adversely impact network size. Statistically, the extent of impact here was minimal.

Significance of VM-features in MSC vascular morphogenesis

Despite improvements in vascular morphology and phenotype, MSCs in PEGylated fibrin are still not fully endothelial in nature. Endothelial and stem cell literature provided insufficient context for this hybrid cell state. Without context, we had

no foundation for validating its usefulness. In order to move forward with our work on stem cell-based ischemic therapies, we needed to understand the mechanisms underlying endothelial-like MSC behavior and uncover its functional meaning.

The outcomes of this second study demonstrate that hypoxia is capable of catalyzing a stronger endothelial profile in MSCs, as it does for tumor cells in vasculogenic mimicry.[20,21] Where the first study implicates fibrin-activated signaling as responsible for baseline endothelial expression, the second implicates a hypoxia-mediated response as the distinguishing cue between vascular morphogenesis in PEGylated fibrin versus fibrin. These findings draw stronger parallels between cancer cell and stem cell behavior. In many tumors, including VM-capable tumors, cells have previously de-differentiated through an epithelial-to-mesenchymal transition.[44,56] In VM, a portion of these cells gain new specificity towards an endothelial-like lineage while retaining some malignant and stem markers.[44] With MSCs, we observe a similar phenomenon: MSCs develop characteristics of an endothelial-like lineage while retaining some mesenchymal features. In both cases, the presence of dual phenotypes raises interesting questions regarding hybrid cell states and cell functionality. Phenotypic overlap between VM cells and endothelial-like MSCs suggests the possibility of a shared function (i.e., development of perfusable networks). The additional ability of fibroblasts to match endothelial-like MSC behavior further suggests that VM-type behavior may be a more broadly shared trait of mesenchymal lineages. Disease models from cancer and non-normative biology, therefore, may be able to enlighten our understanding of less common cell states. Vasculogenic mimicry opens up new possibilities for achieving and validating tissue perfusion. Though VM-inspired approaches will likely produce imperfect networks, we can avoid the complexities of co-culture methods and soluble factor delivery. Transiently stable or leaky vasculature may be *functional enough* to sustain transplanted tissues in the

critical stages of host integration and rescue these tissues from necrosis. Until we can demonstrate functional perfusion of MSC networks, the evidence here should be regarded as circumstantial and more representative of a new perspective for vascular tissue engineering than a proven paradigm.

FUTURE WORK

Validating VM-type MSC vascular morphogenesis with an *in vivo* model

Vasculogenic mimicry posits the utility of non-endothelial channels as perfusable networks for nutrient and oxygen transport. We have piloted the chorioallantoic membrane (CAM) assay as an *in vivo* model for demonstrating the utility of MSC-derived vascular networks. The CAM assay is typically used for evaluating the angiogenic or anti-angiogenic characteristics of proteins, materials, and small molecules.[27,57,58] More recently it has been adapted for more complex analytical methods, including vascular permeability studies, tumor metastases, and even cell-laden onplants.[30,59,60] Here, we combine the *ex ovo* cultivation of *Coturnix coturnix* (i.e., the common quail) embryos with techniques for vascular permeability and cell-laden onplant studies to show perfusion of MSC networks. Although our application of the CAM assay is unconventional, we reasoned the lack of a host-mounted immune response to the onplants would enable clear observation of MSC-vascular interactions without the inundation of macrophages and other infiltrates. Inflammatory responses can obfuscate the contributions of transplanted cells to the local environment, complicating endpoint analysis.

For our CAM protocol, MSCs were pre-stained with DiI and encapsulated in PEGylated fibrin gels *ex vivo* and cultivated for four days before being transplanted onto

the CAM of E8 quail embryos (Figure 4.6A). Three days later, E11 quail embryos (Figure 4.6B) were perfused with 2MDa FITC-dextran and terminated. The FITC-dextran size of 2MDa was chosen to mimic the size of low-density lipoprotein (LDL), a lipoprotein normally carried and taken up by healthy endothelium.[30] CAM onplants were imaged with the intent of detecting FITC-dextran localization within DiI-stained MSC tubules. Figure 4.6C illustrates the fluorescent labeling schema of our *in vivo* model.

We observed successful perfusion of FITC-dextran within the CAM vasculature, but no co-localization of FITC-dextran within DiI-MSCs was found. Instead, MSCs were clearly localized within the gel and CAM vasculature was clearly localized to the gel periphery (Figure 4.6D-I), suggesting a boundary layer issue between the inner and outer gel environments. The experimental variables that could have contributed to this outcome were too many to isolate individually. The boundary could have been caused by an unfavorable biomechanical gradient from the CAM to the onplant, discouraging vascular ingrowth; mature endothelial cells notably favor a softer matrix.[61-63] MSCs, however, are typically more flexible in their migratory response to matrix densities. Their unwillingness to migrate from the gel suggests, instead, that the boundary layer is bi-directional in inhibiting cell motility. This type of boundary issue is more likely to arise from the *ex vivo* formation of the gel onplants. A study on subcutaneous UV-crosslinking of PEG-dimethacrylate showed that *ex vivo* gelation incurred a significant gap between the gel and the surrounding tissue where as *in situ* gelation provided uniform gel-tissue integration.[64] Hence, we recommend that future iterations of this *in vivo* model use *in situ* gelation to minimize the potential for boundary-layer issues.

In situ gelation, though, introduces a new difficulty to overcome. MSC networks take approximately 7 days to form clear network structures and the CAM window for onplant integration is limited to 3-5 days due to the rapid fetal development of quails.[65]

This window is too short to allow for an ideal of study of MSC network behavior. A better model would 1) enable us to create *in situ* gels, 2) have 1-2 weeks of gel incubation, and 3) exert a minimal inflammatory response so we can isolate MSC-vascular interactions. We propose an immunodeficient mouse model as a better candidate for *in vivo* examination of MSC vascular morphogenesis and its subsequent utility. Specifically, NOD/LtSzJ JAX mice (jaxmice.jax.org), which have a severely compromised innate immunity, advantageously support engraftment of human cells.

CONCLUSIONS

Our previous work focused on characterizing differences in biomaterial properties and MSC behaviors between fibrin and PEGylated fibrin matrices. Importantly, we found that PEGylated fibrin strongly drives vascular morphogenesis of encapsulated MSC populations, promoting the production of paracrine factors, matrix remodeling enzymes, tubular networks, and endothelial markers. However, the MSCs do not fully transdifferentiate towards an endothelial lineage and appear to depart from normative endothelial vascular assembly. A key experiment described here clearly demonstrated that MSC behavior is more characteristic of their originating fibroblastic character than the targeted endothelial lineage. The hybrid endothelial-mesenchymal features of MSCs (and fibroblasts) warranted the exploration of an alternative avenue for explaining the presence of such a cell type.

The core work here encompasses a series of experiments predicated on vasculogenic mimicry as a new model for validating endothelial-like outcomes of MSCs. Vasculogenic mimicry provides a foundation for validating the development of hybrid, endothelial-like cell behavior. These experiments aim to clarify cellular mechanisms that

underlie our prior observations of MSC tubulogenesis in PEGylated fibrin and open up a new paradigm for understanding the therapeutic value of stem cell behavior.

Despite hypoxic stress being a well-known cellular motivator in ischemic revascularization—and hypoxic preconditioning being a well-documented form of increasing transplanted cell survival—hypoxic stress as a biomaterial cue appears to be vastly overlooked and underestimated. Based on the results of this 3D study, hypoxia is clearly relevant in catalyzing endothelial-like MSC behavior. While fibrin matrices are capable of inducing basal levels of endothelial markers, the added hypoxic stress from PEGylated fibrin synergistically improves these cellular outcomes. Not only can vascular tissue engineering strategies target VM-type mechanisms of neovascularization, they can also incorporate hypoxia as an auxiliary biomaterial cue.

Antibody target	*1°/2°*	*Species*	*Dilution*	*Manufacturer*
CD31 (clone P2B1)	primary	mouse	1:100	Abcam (ab24590)
von Willebrand factor	primary	rabbit	1:1000	Abcam (ab6994)
VE-cadherin	primary	rabbit	1:700	Abcam (ab33168)
β-actin	primary	rabbit	1:1000	Abcam (ab75186)
Mouse IgG	secondary	rabbit	1:5000	Abcam (ab6728)
Rabbit IgG	secondary	goat	1:5000	Santa Cruz Bio (sc-2004)

Table 4.1: List of polyclonal primary and secondary antibodies used for western blot detection of cellular proteins. Antibodies were diluted in blocking buffer (5% nonfat milk in TBST).

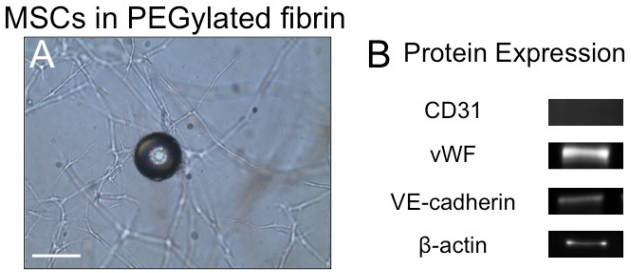

Figure 4.1: Summary of previously described endothelial-like behavior of MSCs in PEGylated fibrin with the addition of CD31- data. (A) Spontaneous MSC outgrowth from a microcarrier bead, Day 7; scale bar = 150μm. (B) Chemiluminescent bands detected via western blot analysis of cellular proteins; protocol used antibodies listed in Table 1.

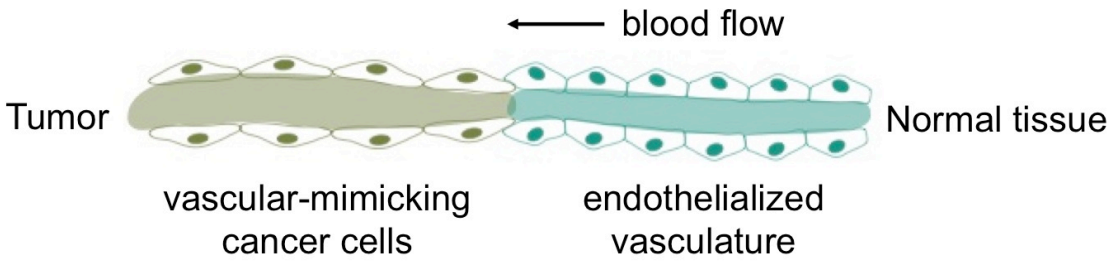

Figure 4.2: Diagram of tubular vasculogenic mimicry, as first described by Maniotis *et al* in 1999. As the cell density of a tumor rapidly increases, the intratumoral environment becomes increasingly hypoxic. In response to the hypoxia, a subpopulation of de-differentiated tumor cells adopts an endothelial-like phenotype and begins forming tumor-lined tubular spaces. These non-endothelialized tubes inosculate with normal endothelialized vasculature to divert blood flow into the tumor's microenvironment. Tumors capable of this aggressive survival mechanism are associated with significantly poorer patient prognoses.

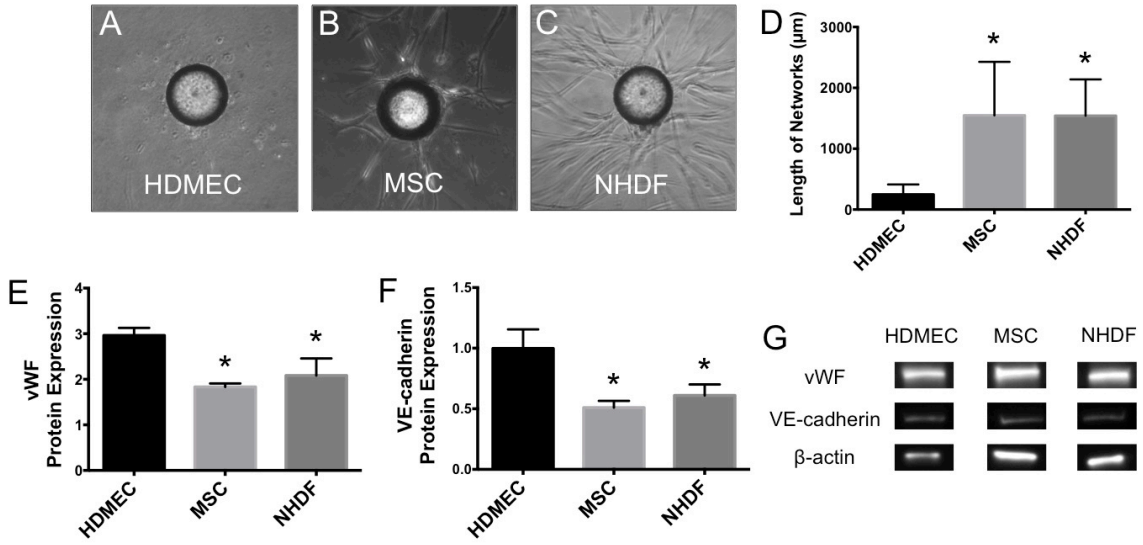

Figure 4.3: Mapping the degree of endothelial-like MSC behavior. (A-C) Phase contrast images of cell outgrowth from the microcarrier bead (center; approximately 150μm diameter). Specifically, (A) Human dermal microvascular endothelial cells (HDMECs) in a pure fibrin gel; (B) Bone marrow-derived human MSCs in PEGylated fibrin; (C) normal human dermal fibroblasts (NHDFs) in PEGylated fibrin. (D) Three-dimensional quantification of network outgrowth represented by (A-C). (E and F) Chemiluminescent signal of vWF and VE-cadherin protein, respectively, normalized to sample-appropriate B-actin signal. (G) Chemiluminescent bands detected via western blot, as quantified in (E and F). *$p < 0.05$, versus HDMEC.

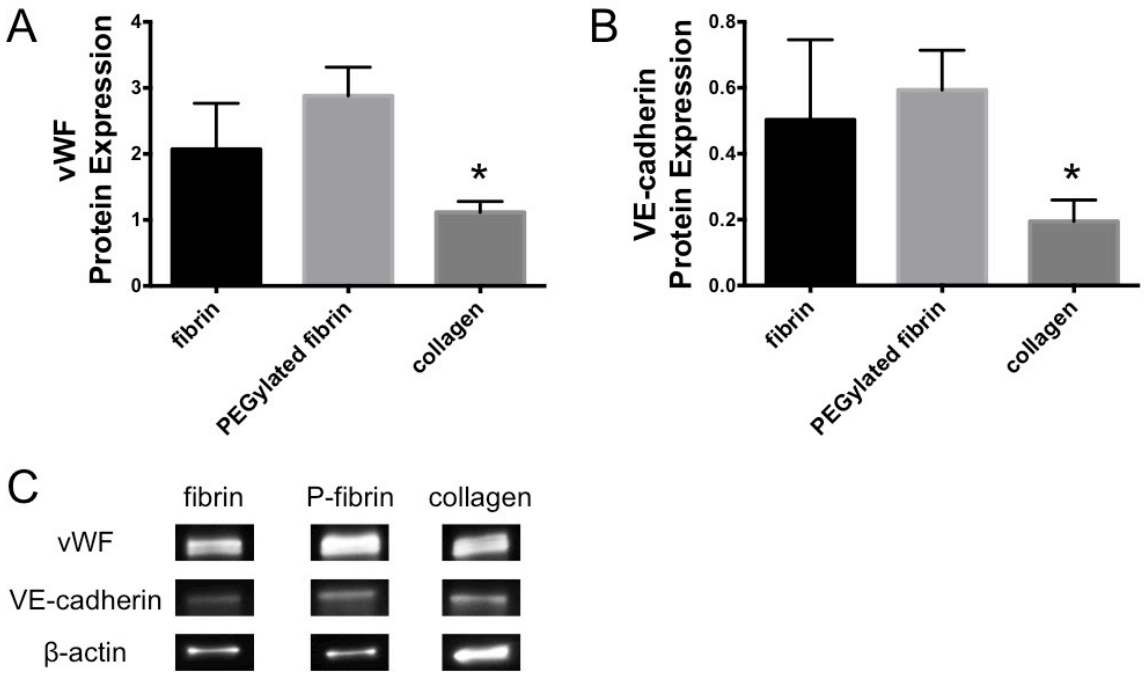

Figure 4.4: Comparison of substrate-induced endothelial marker expression in 2D gel culture of MSCs. MSCs were seeded on top of thin gel substrates and cultured for 7 days under normoxic conditions. (A and B) Chemiluminescent signal of vWF and VE-cadherin protein, respectively, normalized to sample-appropriate B-actin signal. (C) Chemiluminescent bands detected via western blot, as quantified in (A and B). *$p < 0.5$, versus PEGylated fibrin.

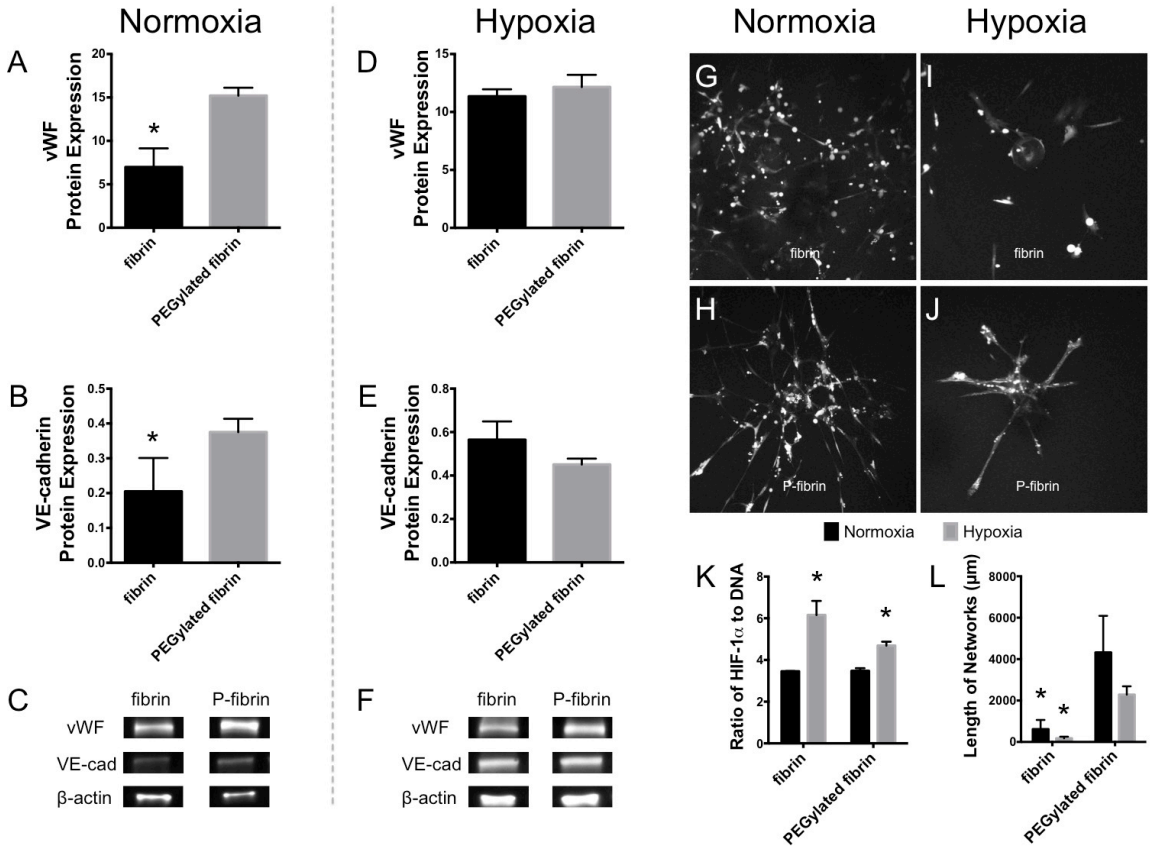

Figure 4.5: Comparison of normoxia- and hypoxia-induced endothelial marker expression in 3D gel culture of MSCs. MSCs were seeded on microcarrier beads and encapsulated within gels, as previously described. Under normoxic conditions, (A and B) Chemiluminescent signal of vWF and VE-cadherin protein, respectively, normalized to sample-appropriate B-actin signal. (C) Chemiluminescent bands detected via western blot, as quantified in (A and B). Under 1% O_2 hypoxic conditions, (D and E) Chemiluminescent signal of vWF and VE-cadherin protein, respectively, normalized to sample-appropriate B-actin signal. (F) Chemiluminescent bands detected via western blot, as quantified in (D and E). Fluorescent z-projections of MSC outgrowth in (G) fibrin and (H) PEGylated fibrin under normoxia; (I) fibrin and (J) PEGylated fibrin under 1% O_2 hypoxia. (K) HIF-1α protein normalized to sample DNA content. (L) Three-dimensional quantification of network outgrowth represented by (G-J). *$p < 0.05$, versus PEGylated fibrin in (A-E, L), versus normoxic control in (K).

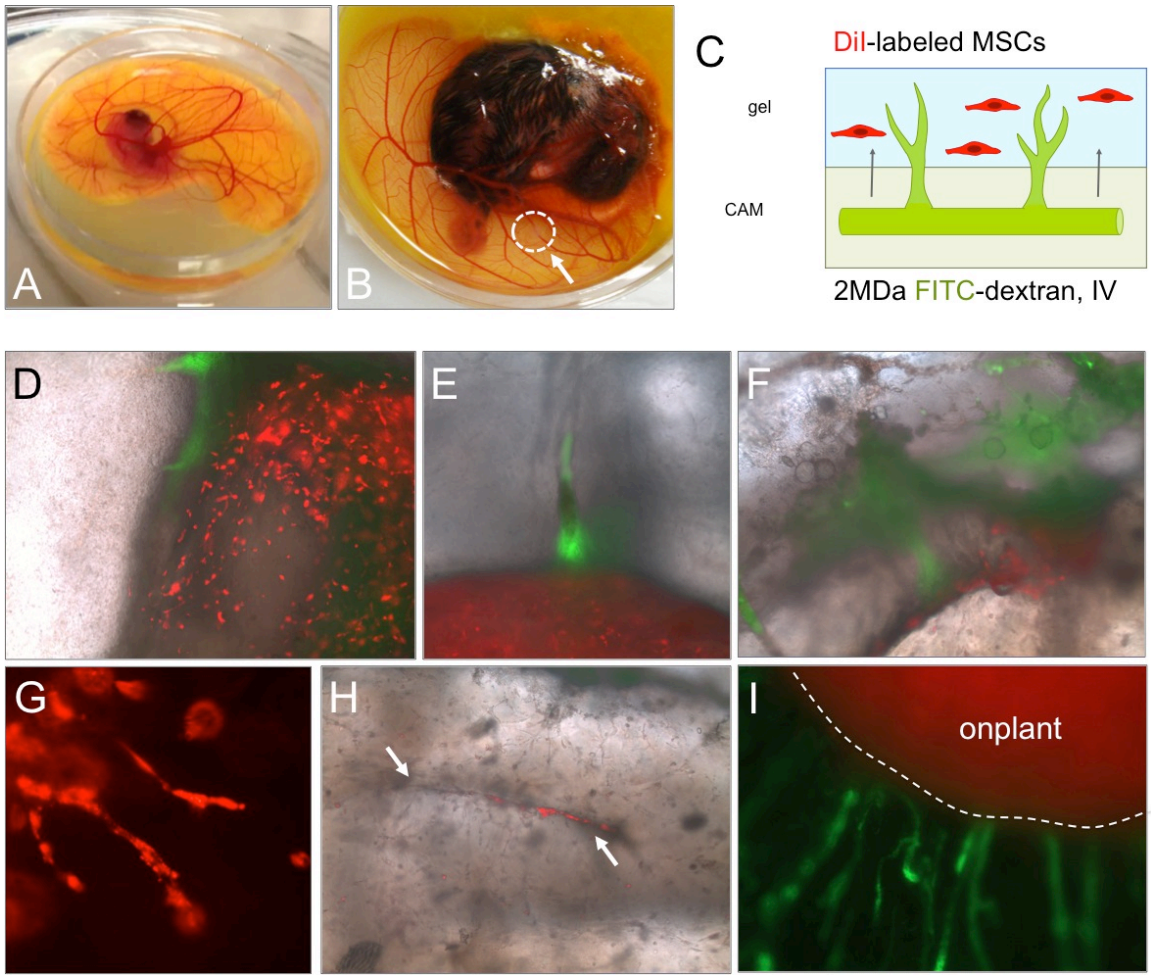

Figure 4.6: Chorioallantoic membrane assay with quail embryos. Photographs of (A) E8 embryo just prior to onplant addition and (B) E11 just prior to assay termination. PEGylated fibrin CAM onplant in (B) is indicated by circled area. (C) Diagram of fluorescent dyes utilized in the CAM assay. MSCs were labeled with DiI prior to gel encapsulation (red); the CAM vessels were visualized with a FITC-dextran injection on E11 (green). (D-I) Phase-contrast images with fluorescent overlays of the CAM assay endpoint. (D and F) Peripheral growth of CAM vessels along onplant. (E) Termination of a CAM vessel directly into the boundary of an onplant. (G) Visualization of MSCs forming tubular structures; fluorescence only. (H) MSCs formed a large linear structure within the onplant, indicated by white arrows. (I) Radial growth of CAM vessels towards onplant; fluorescence only.

REFERENCES

1. Lasala GP, Silva JA, Minguell JJ. Therapeutic angiogenesis in patients with severe limb ischemia by transplantation of a combination stem cell product. The Journal of thoracic and cardiovascular surgery. 2012 August;144(2):377–382.

2. Yan J, Tie G, Xu TY, Cecchini K, Messina LM. Mesenchymal stem cells as a treatment for peripheral arterial disease: current status and potential impact of type II diabetes on their therapeutic efficacy. Stem Cell Reviews and Reports. 2013 June;9(3):360–372.

3. Wu Y, Chen L, Scott PG, Tredget EE. Mesenchymal stem cells enhance wound healing through differentiation and angiogenesis. Stem cells (Dayton, Ohio). 2007 October;25(10):2648–2659.

4. Hocking AM, Gibran NS. Mesenchymal stem cells: paracrine signaling and differentiation during cutaneous wound repair. Experimental Cell Research. 2010 August 15;316(14):2213–2219.

5. Barsotti MC, Magera A, Armani C, Chiellini F, Felice F, Dinucci D, Piras AM, Minnocci A, Solaro R, Soldani G, et al. Fibrin acts as biomimetic niche inducing both differentiation and stem cell marker expression of early human endothelial progenitor cells. Cell proliferation. 2011 February 1;44(1):33–48.

6. Falanga V, Iwamoto S, Chartier M, Yufit T, Butmarc J, Kouttab N, Shrayer D, Carson P. Autologous bone marrow-derived cultured mesenchymal stem cells delivered in a fibrin spray accelerate healing in murine and human cutaneous wounds. Tissue engineering. 2007 June 1;13(6):1299–1312.

7. Sorrell JM, Caplan AI. Topical delivery of mesenchymal stem cells and their function in wounds. Stem cell research & therapy. 2010 September 24;1(4):30.

8. Zhang G, Drinnan CT, Geuss LR, (null). Vascular differentiation of bone marrow stem cells is directed by a tunable three-dimensional matrix. Acta Biomaterialia. 2010 September;6(9):3395–3403.

9. Rytlewski JA, Geuss LR, Anyaeji CI, Merchant AG, (null). Three-dimensional image quantification as a new morphometry method for tissue engineering. Tissue Engineering Part C: Methods. 2012 July;18(7):507–516.

10. Pusztaszeri MP, Seelentag W, Bosman FT. Immunohistochemical expression of endothelial markers CD31, CD34, von Willebrand factor, and Fli-1 in normal human tissues. Journal of Histochemistry and Cytochemistry. 2006 April;54(4):385–395.

11. Athanassopoulos A, Tsaknakis G, Newey SE, Harris AL, Kean J, Tyler MP, Watt SM. Microvessel networks in pre-formed in artificial clinical grade dermal substitutes in vitro using cells from haematopoietic tissues. Burns : journal of the International Society for Burn Injuries. 2012 August;38(5):691–701.

12. Chan JM, Zervantonakis IK, Rimchala T, Polacheck WJ, Whisler J, Kamm RD. Engineering of in vitro 3D capillary beds by self-directed angiogenic sprouting. PloS one. 2012;7(12):e50582.

13. Pedroso DCS, Tellechea A, Moura L, Fidalgo-Carvalho I, Duarte J, Carvalho E, Ferreira L. Improved survival, vascular differentiation and wound healing potential of stem cells co-cultured with endothelial cells. PloS one. 2011;6(1):e16114–.

14. Maniotis AJ, Folberg R, Hess A, Seftor EA, Gardner LM, Pe'er J, Trent JM, Meltzer PS, Hendrix MJ. Vascular channel formation by human melanoma cells in vivo and in vitro: vasculogenic mimicry. The American journal of pathology. 1999 September;155(3):739–752.

15. Seftor REB, Hess AR, Seftor EA, Kirschmann DA, Hardy KM, Margaryan NV, Hendrix MJC. Tumor cell vasculogenic mimicry: from controversy to therapeutic promise. The American journal of pathology. 2012 October;181(4):1115–1125.

16. Folberg R, Maniotis AJ. Vasculogenic mimicry. APMIS : acta pathologica, microbiologica, et immunologica Scandinavica. 2004 July;112(7-8):508–525.

17. Kirschmann DA, Seftor EA, Hardy KM, Seftor REB, Hendrix MJC. Molecular pathways: vasculogenic mimicry in tumor cells: diagnostic and therapeutic implications. Clinical cancer research : an official journal of the American Association for Cancer Research. 2012 May 15;18(10):2726–2732.

18. Hillen F, Griffioen AW. Tumour vascularization: sprouting angiogenesis and beyond. Cancer metastasis reviews. 2007 December;26(3-4):489–502.

19. Hendrix MJ, Seftor EA, Meltzer PS, Gardner LM, Hess AR, Kirschmann DA, Schatteman GC, Seftor RE. Expression and functional significance of VE-cadherin in aggressive human melanoma cells: role in vasculogenic mimicry. Proceedings of the National Academy of Sciences of the United States of America. 2001 July 3;98(14):8018–8023.

20. Zhao N, Sun B-C, Sun T, Ma Y-M, Zhao X-L, Liu Z-Y, Dong X-Y, Che N, Mo J, Gu Q. Hypoxia-induced vasculogenic mimicry formation via VE-cadherin regulation by Bcl-2. Medical Oncology. 2012 December;29(5):3599–3607.

21. Misra RM, Bajaj MS, Kale VP. Vasculogenic mimicry of HT1080 tumour cells in vivo: critical role of HIF-1α-neuropilin-1 axis. PloS one. 2012;7(11):e50153.

22. Zhu P, Ning Y, Yao L, Chen M, Xu C. The proliferation, apoptosis, invasion of endothelial-like epithelial ovarian cancer cells induced by hypoxia. Journal of experimental & clinical cancer research : CR. 2010;29:124.

23. Sahai S, McFarland R, Skiles ML, Sullivan D, Williams A, Blanchette JO. Tracking hypoxic signaling in encapsulated stem cells. Tissue Engineering Part C: Methods. 2012 July;18(7):557–565.

24. Chung E, Rytlewski JA, Merchant AG, Lewis EW, Suggs LJ. Fibrin-based 3D matrices induce angiogenic behavior of adipose-derived stem cells for tissue engineering. Biomaterials. 2013 August 19:1–42.

25. Nakatsu MN, Hughes CCW. An optimized three-dimensional in vitro model for the analysis of angiogenesis. Methods in enzymology. 2008;443:65–82.

26. Nehls V, Drenckhahn D. A novel, microcarrier-based in vitro assay for rapid and reliable quantification of three-dimensional cell migration and angiogenesis. Microvascular research. 1995 November;50(3):311–322.

27. González-Iriarte M, Carmona R, Pérez-Pomares JM, Macías D, Angel Medina M, Quesada AR, Muñoz-Chápuli R. A modified chorioallantoic membrane assay allows for specific detection of endothelial apoptosis induced by antiangiogenic substances. Angiogenesis. 2003;6(3):251–254.

28. Kunzi-Rapp K, Rück A, Kaufmann R. Characterization of the chick chorioallantoic membrane model as a short-term in vivo system for human skin. Archives of dermatological research. 1999 May;291(5):290–295.

29. Dohle DS, Pasa SD, Gustmann S, Laub M, Wissler JH, Jennissen HP, Dünker N. Chick ex ovo culture and ex ovo CAM assay: how it really works. Journal of visualized experiments : JoVE. 2009;(33).

30. Pink DBS, Schulte W, Parseghian MH, Zijlstra A, Lewis JD. Real-time visualization and quantitation of vascular permeability in vivo: implications for drug delivery. PloS one. 2012;7(3):e33760.

31. Euthanasia APO. AVMA Guidelines for the Euthanasia of Animals (2013 Edition). 2013.

32. Davis GE, Stratman AN, Sacharidou A, Koh W. Molecular basis for endothelial lumen formation and tubulogenesis during vasculogenesis and angiogenic sprouting. International review of cell and molecular biology. 2011;288:101–165.

33. Alt E, Yan Y, Gehmert S, Song Y-H, Altman A, Gehmert S, Vykoukal D, Bai X. Fibroblasts share mesenchymal phenotypes with stem cells, but lack their differentiation and colony-forming potential. Biology of the Cell. 2011;103(4):197–208.

34. Ghajar CM, Kachgal S, Kniazeva E, Mori H, Costes SV, George SC, Putnam AJ. Mesenchymal cells stimulate capillary morphogenesis via distinct proteolytic mechanisms. Experimental Cell Research. 2010 March 10;316(5):813–825.

35. Laranjeira MS, Fernandes MH, Monteiro FJ. Reciprocal induction of human dermal microvascular endothelial cells and human mesenchymal stem cells: time-dependent profile in a co-culture system. Cell proliferation. 2012 May 18.

36. Lesman A, Koffler J, Atlas R, Blinder YJ, Kam Z, Levenberg S. Engineering vessel-like networks within multicellular fibrin-based constructs. Biomaterials. 2011 November;32(31):7856–7869.

37. Sukmana I, Vermette P. The effects of co-culture with fibroblasts and angiogenic growth factors on microvascular maturation and multi-cellular lumen formation in HUVEC-oriented polymer fibre constructs. Biomaterials. 2010 July;31(19):5091–5099.

38. Karlsson LK, Junker JPE, Grenegard M, Kratz G. Human Dermal Fibroblasts: A Potential Cell Source for Endothelialization of Vascular Grafts. Annals of Vascular Surgery. 2009;23(5):663–674.

39. Lorenz K, Sicker M, Schmelzer E, Rupf T, Salvetter J, Schulz-Siegmund M, Bader A. Multilineage differentiation potential of human dermal skin-derived fibroblasts. Experimental Dermatology. 2008;17(11):925–932.

40. van Mourik JA, Romani de Wit T, Voorberg J. Biogenesis and exocytosis of Weibel-Palade bodies. Histochemistry and cell biology. 2002 February;117(2):113–122.

41. Starke RD, Ferraro F, Paschalaki KE, Dryden NH, McKinnon TAJ, Sutton RE, Payne EM, Haskard DO, Hughes AD, Cutler DF, et al. Endothelial von Willebrand factor regulates angiogenesis. Blood. 2011 January 20;117(3):1071–1080.

42. Grainger SJ, Putnam AJ. Assessing the permeability of engineered capillary networks in a 3D culture. PloS one. 2011;6(7):e22086.

43. Boda-Heggemann J, Régnier-Vigouroux A, Franke WW. Beyond vessels: occurrence and regional clustering of vascular endothelial (VE-)cadherin-containing junctions in non-endothelial cells. Cell and tissue research. 2009 January;335(1):49–65.

44. Lirdprapamongkol K, Chiablaem K, Sila-Asna M, Surarit R, Bunyaratvej A, Svasti J. Exploring stemness gene expression and vasculogenic mimicry capacity in well- and poorly-differentiated hepatocellular carcinoma cell lines. Biochemical and biophysical research communications. 2012 June 8;422(3):429–435.

45. Vartanian AA. Signaling pathways in tumor vasculogenic mimicry. Biochemistry. Biokhimiiâ. 2012 September;77(9):1044–1055.

46. Paulis YWJ, Soetekouw PMMB, Verheul HMW, Tjan-Heijnen VCG, Griffioen AW. Signalling pathways in vasculogenic mimicry. Biochimica et biophysica acta. 2010 August;1806(1):18–28.

47. Hess AR, Seftor EA, Gruman LM, Kinch MS, Seftor REB, Hendrix MJC. VE-cadherin regulates EphA2 in aggressive melanoma cells through a novel signaling pathway: implications for vasculogenic mimicry. Cancer biology & therapy. 2006 February;5(2):228–233.

48. Hendrix MJC, Seftor EA, Hess AR, Seftor REB. Molecular plasticity of human melanoma cells. Oncogene. 2003 May 19;22(20):3070–3075.

49. Vartanian A, Stepanova E, Grigorieva I, Solomko E, BELKIN V, Baryshnikov A, LICHINITSER M. Melanoma vasculogenic mimicry capillary-like structure formation depends on integrin and calcium signaling. Microcirculation (New York, N.Y. : 1994). 2011 July;18(5):390–399.

50. Dikovsky D, Bianco-Peled H, Seliktar D. The effect of structural alterations of PEG-fibrinogen hydrogel scaffolds on 3-D cellular morphology and cellular migration. Biomaterials. 2006 March 1;27(8):1496–1506.

51. Almany L, Seliktar D. Biosynthetic hydrogel scaffolds made from fibrinogen and polyethylene glycol for 3D cell cultures. Biomaterials [Internet]. 2005 May 1;26(15):2467–2477.

52. Mansouri L, Xie Y, Rappolee DA. Adaptive and Pathogenic Responses to Stress by Stem Cells during Development. Cells. 2012.

53. Jiang BH, Semenza GL, Bauer C, Marti HH. Hypoxia-inducible factor 1 levels vary exponentially over a physiologically relevant range of O2 tension. The American journal of physiology. 1996 October;271(4 Pt 1):C1172–80.

54. Grayson WL, Zhao F, Izadpanah R, Bunnell B, Ma T. Effects of hypoxia on human mesenchymal stem cell expansion and plasticity in 3D constructs. Journal of Cellular Physiology. 2006 May;207(2):331–339.

55. Das R, Jahr H, van Osch GJVM, Farrell E. The role of hypoxia in bone marrow-derived mesenchymal stem cells: considerations for regenerative medicine approaches. Tissue engineering. Part B, Reviews. 2010 April;16(2):159–168.

56. Tong M, Han BB, Holpuch AS, Pei P, He L, Mallery SR. Inherent phenotypic plasticity facilitates progression of head and neck cancer: Endotheliod characteristics enable angiogenesis and invasion. Experimental Cell Research. 2013 April 15;319(7):1028–1042.

57. Ribatti D, Nico B, Vacca A, Presta M. The gelatin sponge-chorioallantoic membrane assay. Nature Protocols. 2006;1(1):85–91.

58. West DC, Thompson WD, Sells PG, Burbridge MF. Angiogenesis assays using chick chorioallantoic membrane. Methods in molecular medicine. 2001;46:107–129.

59. Deryugina EI, Quigley JP. Chick embryo chorioallantoic membrane model systems to study and visualize human tumor cell metastasis. Histochemistry and cell biology. 2008 December;130(6):1119–1130.

60. Lokman NA, Elder ASF, Ricciardelli C, Oehler MK. Chick Chorioallantoic Membrane (CAM) Assay as an In Vivo Model to Study the Effect of Newly Identified Molecules on Ovarian Cancer Invasion and Metastasis. International journal of molecular sciences. 2012;13(8):9959–9970.

61. Shamloo A, Heilshorn SC. Matrix density mediates polarization and lumen formation of endothelial sprouts in VEGF gradients. Lab on a chip. 2010 November 21;10(22):3061–3068.

62. Rao RR, Peterson AW, Ceccarelli J, Putnam AJ, Stegemann JP. Matrix composition regulates three-dimensional network formation by endothelial cells and mesenchymal stem cells in collagen/fibrin materials. Angiogenesis. 2012 June;15(2):253–264.

63. Kniazeva E, Kachgal S, Putnam AJ. Effects of extracellular matrix density and mesenchymal stem cells on neovascularization in vivo. Tissue Engineering Part A. 2011 April;17(7-8):905–914.

64. Lin R-Z, Chen Y-C, Moreno-Luna R, Khademhosseini A, Melero-Martin JM. Transdermal regulation of vascular network bioengineering using a photopolymerizable methacrylated gelatin hydrogel. Biomaterials. 2013 September;34(28):6785–6796.

65. Ainsworth SJ, Stanley RL, Evans DJR. Developmental stages of the Japanese quail. Journal of anatomy. 2010 January;216(1):3–15.

Chapter 5: Conclusions and Recommendations for Future Work

PROJECT HISTORY

The overall goal of this project was to deconstruct the mechanisms responsible for MSC tubulogenesis in PEGylated fibrin. This novel material was originally developed by Dr. Laura Suggs and colleagues at the University of Minnesota. Our group at the University of Texas at Austin has continued developing PEGylated fibrin as a therapeutic matrix for stem cell delivery in ischemic and wound-healing applications. The original design aimed to promote neovascularization via *de novo* assembly of perfusable MSC networks within PEGylated fibrin. The multipotency of MSCs held the promise of achieving simultaneous differentiation towards endothelial, smooth muscle cells, and pericytes—three cell types that comprise normal endothelial vasculature. Successful development of such a therapy where we can achieve neovascularization (1) with a single transplanted cell population and (2) without the need for additional soluble factors is of tremendous clinical interest. The simplicity would avoid many barriers to clinical translation. However, we have experienced issues when translating *in vitro* results to *in vivo* models. MSCs do not from robust networks *in vivo*, which have been the hallmark success of our *in vitro* studies. The project here sought to understand mechanisms of *in vitro* network formation so we may revisionally improve PEGylated fibrin for future *in vivo* trials.

SUMMARY OF PRESENT FINDINGS AND CONCLUSIONS

The development of a morphological quantification method based on three-dimensional data has been a valuable technique in statistical analyses of MSC network outcomes (Chapter 2). Morphological analysis, combined with biological assays (surface

markers, protein production, and proliferation) allowed us to fully characterize MSC behaviors in PEGylated fibrin (Chapter 3). We found that MSC network development was inconsistent with that of normal endothelial cells (Chapter 4). Instead, these networks are more representative of a hybrid MSC cell state, with fibroblastic motility and endothelial-like marker expression. A similar event occurs in aggressive tumors though vasculogenic mimicry, whereby a subpopulation of tumor cells express a partial endothelial phenotype and self-assemble into perfusable networks. Vasculogenic mimicry in tumors is catalyzed by a combination of matrix cues (e.g., laminin deposition) and hypoxic stress from high cell densities. MSC tubulogenesis appears to be motivated by similar cues in PEGylated fibrin.

Fibrin initiates a basic endothelial-like program in MSCs, resulting in baseline expression of vWF and VE-cadherin and production of VEGF. PEGylating fibrin slows the rate of diffusion in these matrices, increasing the hypoxic stress experienced by encapsulated cells. The added hypoxic stress appears key in differentiating PEGylated fibrin from naked fibrin matrices: MSCs in PEGylated fibrin exhibit significantly higher levels of endothelial markers and more robustly form continuous networks than in fibrin. These networks also form lumenal spaces, indicative of developing vasculature, through cell-hollowing mechanisms. These studies collectively provide new context for the presence of endothelial-*like* MSCs and suggests that complete transdifferentiation towards an endothelial lineage may not be necessary for therapeutic tissue perfusion.

We recognize that immature vascular networks may have limitations. In vasculogenic mimicry, the tumor channels are functional but leaky and potentially less stable. Endothelial-*like* MSC networks may suffer from similar issues. With these limitations, MSC networks could still be *functional enough* to realize therapeutic benefits. Ischemic tissues, chronic wounds, and grafts simply need an early source of

perfusion to maintain viability until the host is able to fully integrate and remodel the tissue. MSC networks, which assemble much more quickly than normal endothelium, may transiently provide the necessary sustenance while the host vasculature invades. Essentially, the PEGylated fibrin patch could provide a vascular "band aid" in the treatment of ischemic tissue.

AVENUES OF FURTHER INVESTIGATION

PEGylation and integrin masking

PEGylated fibrin-mediated MSC tubulogenesis may also be morphology-driven. Studies have shown that changes in cell morphology correlate with lineage-specific differentiation. In optimizing PEGylation of fibrinogen, we observed a terminal level of PEGylation where thrombin could no longer enzymatically crosslink fibrinogen. We hypothesized that PEGylation masked thrombin cleavage sites along fibrinogen and inhibited crosslinking. If PEGylation is capable of masking cleavage sites, it may also be masking integrin-binding moieties. Masking (some) integrin-binding sites on fibrin would force cells to extent further before establishing the next cell-matrix adhesion. Matrix-forced cell extension may enhance the vascular differentiation mechanisms of MSCs given the extended tubular nature of vascular-related cells. A study that was conceptualized (but not yet executed) would elucidate if and to what degree PEGylation masks integrin-binding sites in fibrin. By titrating doses of cyclic GRGDSP in fibrin-based matrices, we can determine the saturation point where the peptide outcompetes matrix moieties. If our hypothesis holds true, we would expect that lower doses of cyclic GRGDSP to inhibit MSC migration in PEGylated fibrin than fibrin matrices. This finding

would provide another variable in our engineering arsenal that we can fine-tune for optimizing MSC tubulogenesis.

Increasing matrix density to improve network maturity

As described in Chapter 4, MSC networks are more fibroblastic than endothelial. A part of this character includes narrower lumens and overall cell diameter, which was more qualitatively observed than quantitatively measured. Endothelial networks described in literature have a more substantial lumenal width. Additionally, MSCs are highly migratory and produce significantly higher quantities of matrix-degrading MMPs than activated endothelial cells. While MMPs are necessary to facilitate cell tunneling, too much matrix degradation can lead to network overextension. Robust network development requires a balance of network-promoting and network-limiting (or stabilizing) kinetics. Increased production of MMPs may overdrive network-promoting kinetics and lead to rapid network extension without allowing time for cells to establish supportive adhesions and undergo necessary apical-basal polarization. Therefore, the advantageous motility of MSCs may also a detriment to network maturity and stability. A possible method of addressing this issue would be to increase the density of the PEGylated fibrin matrix, slowing MSC tunneling. However, a dramatic difference between the stiffness of PEGylated fibrin and the surrounding tissue may shift wound-healing dynamics. Endothelial cells preferentially migrate on softer substrates. If our implanted matrix is too dense and too stiff, we risk inhibiting ingrowth of host vasculature. Studies would need to optimize the density of PEGylated fibrin that slows MSC growth but still yields to invading vessels.

In vivo models of MSC-endothelial inosculation

As discussed in Chapter 4, the CAM assay may not be an ideal candidate for evaluating the possibility of MSC-endothelial inosculation. *Ex vivo*-formed gels create a significant boundary layer to vascular invasion by the CAM and MSC exodus from the gel. *In situ*-formed gels, due to the short gestational period of quail embryos, cannot be incubated on the CAM long enough for MSCs to establish networks. A subcutaneous model in a severely immunocompromised rat would allow longer 1-2 week incubation periods to better evaluate MSC-endothelial inosculation. The lack of an innate immune system would minimize obfuscation of MSC-specific events; analyzing the role of MSCs in the wound environment is easily complicated by a tremendous influx of macrophages and other inflammatory cells. This approach would mimic the naïve immune system of the CAM assay in a more durable model.

Despite the appeal of evaluating isolated MSC-endothelial interactions, recent studies in our lab have implicated MSC modulation of macrophages as an important contribution to wound healing. An animal model lacking innate immunity would fail to recapitulate this aspect of normative healing. Additionally, prior experiences with subcutaneous models have periodically suffered from implant encapsulation and generally poor vascular invasion. More direct contact with vascularized tissue, such as subfascial implants, may be desirable for encouraging MSC-host interaction.

Other *in vivo* models of clinical significance

Alternatively, a free fat flap rat model could provide clinically relevant validation of PEGylated fibrin-encapsulated MSCs. Free fat flaps are a common reconstructive surgery technique to restore volume and vasculature to damaged tissue. However, surgeons must isolate subdermal vessels with the flap to facilitate graft survival. If MSCs

can indeed be a vascular “band aid,” this model would allow us to demonstrate transient sustenance of grafted tissue (by MSCs) and demonstrate relevance in another clinical application.

Bibliography

Abdul-Karim M-A, Al-Kofahi K, Brown EB, Jain RK, Roysam B. Automated tracing and change analysis of angiogenic vasculature from in vivo multiphoton confocal image time series. Microvascular research. 2003 September;66(2):113–125.

Ahmed TAE, Griffith M, Hincke M. Characterization and inhibition of fibrin hydrogel-degrading enzymes during development of tissue engineering scaffolds. Tissue engineering. 2007 July;13(7):1469–1477.

Ainsworth SJ, Stanley RL, Evans DJR. Developmental stages of the Japanese quail. Journal of anatomy. 2010 January;216(1):3–15.

Akavia UD, Veinblat O, Benayahu D. Comparing the transcriptional profile of mesenchymal cells to cardiac and skeletal muscle cells. Journal of Cellular Physiology. 2008 September 1;216(3):663–672.

Almany L, Seliktar D. Biosynthetic hydrogel scaffolds made from fibrinogen and polyethylene glycol for 3D cell cultures. Biomaterials [Internet]. 2005 May 1;26(15):2467–2477.

Al-Kofahi KA, Lasek S, Szarowski DH, Pace CJ, Nagy G, Turner JN, Roysam B. Rapid automated three-dimensional tracing of neurons from confocal image stacks. IEEE transactions on information technology in biomedicine : a publication of the IEEE Engineering in Medicine and Biology Society. 2002 June 1;6(2):171–187.

Allen P, Melero-Martin J, Bischoff J. Type I collagen, fibrin and PuraMatrix matrices provide permissive environments for human endothelial and mesenchymal progenitor cells to form neovascular networks. Journal of tissue engineering and regenerative medicine. 2011 April;5(4):e74–86.

Al-Nbaheen M, Vishnubalaji R, Ali D, Bouslimi A, Al-Jassir F, Megges M, Prigione A, Adjaye J, Kassem M, Aldahmash A. Human Stromal (Mesenchymal) Stem Cells from Bone Marrow, Adipose Tissue and Skin Exhibit Differences in Molecular Phenotype and Differentiation Potential. Stem Cell Reviews and Reports. 2012 April 14.

Alt E, Yan Y, Gehmert S, Song Y-H, Altman A, Gehmert S, Vykoukal D, Bai X. Fibroblasts share mesenchymal phenotypes with stem cells, but lack their differentiation and colony-forming potential. Biology of the Cell. 2011;103(4):197–208.

Antiga L, Ene-Iordache B, Remuzzi A. Computational geometry for patient-specific reconstruction and meshing of blood vessels from MR and CT angiography. IEEE Transactions on Medical Imaging. 2003 May;22(5):674–684.

Antiga L, Piccinelli M, Botti L, Ene-Iordache B, Remuzzi A, Steinman DA. An image-based modeling framework for patient-specific computational hemodynamics.

Medical & biological engineering & computing. 2008 November;46(11):1097–1112.

Athanassopoulos A, Tsaknakis G, Newey SE, Harris AL, Kean J, Tyler MP, Watt SM. Microvessel networks in pre-formed in artificial clinical grade dermal substitutes in vitro using cells from haematopoietic tissues. Burns : journal of the International Society for Burn Injuries. 2012 August;38(5):691–701.

Barsotti MC, Magera A, Armani C, Chiellini F, Felice F, Dinucci D, Piras AM, Minnocci A, Solaro R, Soldani G, et al. Fibrin acts as biomimetic niche inducing both differentiation and stem cell marker expression of early human endothelial progenitor cells. Cell proliferation. 2011 February 1;44(1):33–48.

Basciano L, Nemos C, Foliguet B, de Isla N, de Carvalho M, Tran N, Dalloul A. Long term culture of mesenchymal stem cells in hypoxia promotes a genetic program maintaining their undifferentiated and multipotent status. BMC cell biology. 2011;12:12.

Bayless K, Davis G. The Cdc42 and Rac1 GTPases are required for capillary lumen formation in three-dimensional extracellular matrices. Journal of cell science. 2002;115(6):1123–1136.

Bayless KJ, Salazar R, Davis GE. RGD-dependent vacuolation and lumen formation observed during endothelial cell morphogenesis in three-dimensional fibrin matrices involves the alpha(v)beta(3) and alpha(5)beta(1) integrins. The American journal of pathology. 2000 May;156(5):1673–1683.

Becquart P, Cambon-Binder A, Monfoulet L-E, Bourguignon M, Vandamme K, Bensidhoum M, Petite H, Logeart-Avramoglou D. Ischemia is the prime but not the only cause of human multipotent stromal cell death in tissue-engineered constructs in vivo. Tissue Engineering Part A. 2012 October;18(19-20):2084–2094.

Benavides OM, Petsche JJ, Moise KJ, Johnson A, Jacot JG. Evaluation of endothelial cells differentiated from amniotic fluid-derived stem cells. Tissue Engineering Part A. 2012 June;18(11-12):1123–1131.

Black AF, Berthod F, L'heureux N, Germain L, Auger FA. In vitro reconstruction of a human capillary-like network in a tissue-engineered skin equivalent. The FASEB journal : official publication of the Federation of American Societies for Experimental Biology. 1998 October;12(13):1331–1340.

Bock F, Onderka J, Hos D, Horn F, Martus P, Cursiefen C. Improved semiautomatic method for morphometry of angiogenesis and lymphangiogenesis in corneal flatmounts. Experimental eye research. 2008 November;87(5):462–470.

Boda-Heggemann J, Régnier-Vigouroux A, Franke WW. Beyond vessels: occurrence and regional clustering of vascular endothelial (VE-)cadherin-containing junctions in non-endothelial cells. Cell and tissue research. 2009 January;335(1):49–65.

Borcar A, Menze MA, Toner M, Hand SC. Metabolic preconditioning of mammalian cells: mimetic agents for hypoxia lack fidelity in promoting phosphorylation of pyruvate dehydrogenase. Cell and tissue research. 2013 January;351(1):99–106.

Bruggeman LA, Doan RP, Loftis J, Darr A, Calabro A. A cell culture system for the structure and hydrogel properties of basement membranes; Application to capillary walls. Cellular and molecular bioengineering. 2012 June 1;5(2):194–204.

Cassell OCS, Hofer SOP, Morrison WA, Knight KR. Vascularisation of tissue-engineered grafts: the regulation of angiogenesis in reconstructive surgery and in disease states. British journal of plastic surgery. 2002 December;55(8):603–610.

Chan JM, Zervantonakis IK, Rimchala T, Polacheck WJ, Whisler J, Kamm RD. Engineering of in vitro 3D capillary beds by self-directed angiogenic sprouting. PloS one. 2012;7(12):e50582.

Chang EI, Bonillas RG, El-Ftesi S, Chang EI, Ceradini DJ, Vial IN, Chan DA, Michaels J, Gurtner GC. Tissue engineering using autologous microcirculatory beds as vascularized bioscaffolds. The FASEB journal : official publication of the Federation of American Societies for Experimental Biology. 2009 March 1;23(3):906–915.

Chen X, Aledia AS, Ghajar CM, Griffith CK, Putnam AJ, Hughes CCW, George SC. Prevascularization of a fibrin-based tissue construct accelerates the formation of functional anastomosis with host vasculature. Tissue Engineering Part A. 2009 June;15(6):1363–1371.

Chen S-L, Fang W-W, Ye F, Liu Y-H, Qian J, Shan S-J, Zhang J-J, Chunhua RZ, Liao L-M, Lin S, et al. Effect on left ventricular function of intracoronary transplantation of autologous bone marrow mesenchymal stem cell in patients with acute myocardial infarction. The American journal of cardiology. 2004 July 1;94(1):92–95.

Chetty C, Lakka SS, Bhoopathi P, Rao JS. MMP-2 alters VEGF expression via alphaVbeta3 integrin-mediated PI3K/AKT signaling in A549 lung cancer cells. International journal of cancer Journal international du cancer. 2010 September 1;127(5):1081–1095.

Chung E, Rytlewski JA, Merchant AG, Lewis EW, Suggs LJ. Fibrin-based 3D matrices induce angiogenic behavior of adipose-derived stem cells for tissue engineering. Biomaterials. 2013 August 19:1–42.

Cipriani P, Guiducci S, Miniati I, Cinelli M, Urbani S, Marrelli A, Dolo V, Pavan A, Saccardi R, Tyndall A, et al. Impairment of endothelial cell differentiation from bone marrow-derived mesenchymal stem cells: new insight into the pathogenesis of systemic sclerosis. Arthritis and Rheumatism. 2007 June;56(6):1994–2004.

Cohen LD, Deschamps T. Segmentation of 3D tubular objects with adaptive front propagation and minimal tree extraction for 3D medical imaging. Computer methods in biomechanics and biomedical engineering. 2007 August;10(4):289–305.

Coolen NA, Vlig M, van den Bogaerdt AJ, Middelkoop E, Ulrich MMW. Development of an in vitro burn wound model. Wound repair and regeneration : official publication of the Wound Healing Society [and] the European Tissue Repair Society. 2008 July;16(4):559–567.

Copland IB. Mesenchymal stromal cells for cardiovascular disease. Journal of cardiovascular disease research. 2011 January;2(1):3–13.

Corotchi MC, Popa MA, Remes A, Sima LE, Gussi I, Lupu Plesu M. Isolation method and xeno-free culture conditions influence multipotent differentiation capacity of human Wharton's jelly-derived mesenchymal stem cells. Stem cell research & therapy. 2013 July 11;4(4):81.

Crabtree B, Subramanian V. Behavior of endothelial cells on Matrigel and development of a method for a rapid and reproducible in vitro angiogenesis assay. In vitro cellular & developmental biology Animal. 2007 February 1;43(2):87–94.

Cregg JM, Wiseman SL, Pietrzak-Goetze NM, Smith MR, Jaroch DB, Clupper DC, Gilbert RJ. A rapid, quantitative method for assessing axonal extension on biomaterial platforms. Tissue Engineering Part C: Methods. 2010 April;16(2):167–172.

Crisan M. Transition of mesenchymal stem/stromal cells to endothelial cells. Stem cell research & therapy. 2013 August 14;4(4):95.

Das R, Jahr H, van Osch GJVM, Farrell E. The role of hypoxia in bone marrow-derived mesenchymal stem cells: considerations for regenerative medicine approaches. Tissue engineering. Part B, Reviews. 2010 April;16(2):159–168.

Davis GE, Bayless KJ. An integrin and Rho GTPase-dependent pinocytic vacuole mechanism controls capillary lumen formation in collagen and fibrin matrices. Microcirculation (New York, N.Y. : 1994). 2003 January;10(1):27–44.

Davis GE, Bayless KJ, Mavila A. Molecular basis of endothelial cell morphogenesis in three-dimensional extracellular matrices. The Anatomical record. 2002 November 1;268(3):252–275.

Davis GE, Camarillo CW. An alpha 2 beta 1 integrin-dependent pinocytic mechanism involving intracellular vacuole formation and coalescence regulates capillary lumen and tube formation in three-dimensional collagen matrix. Experimental Cell Research. 1996 April 10;224(1):39–51.

Davis GE, Koh W, Stratman AN. Mechanisms controlling human endothelial lumen formation and tube assembly in three-dimensional extracellular matrices. Birth defects research. Part C, Embryo today : reviews. 2007 December;81(4):270–285.

Davis GE, Stratman AN, Sacharidou A, Koh W. Molecular basis for endothelial lumen formation and tubulogenesis during vasculogenesis and angiogenic sprouting. International review of cell and molecular biology. 2011;288:101–165.

Demol J, Lambrechts D, Geris L, Schrooten J, Van Oosterwyck H. Towards a quantitative understanding of oxygen tension and cell density evolution in fibrin hydrogels. Biomaterials. 2011 January;32(1):107–118.

Deryugina EI, Quigley JP. Chick embryo chorioallantoic membrane model systems to study and visualize human tumor cell metastasis. Histochemistry and cell biology. 2008 December;130(6):1119–1130.

Dikovsky D, Bianco-Peled H, Seliktar D. The effect of structural alterations of PEG-fibrinogen hydrogel scaffolds on 3-D cellular morphology and cellular migration. Biomaterials. 2006 March 1;27(8):1496–1506.

Dohle DS, Pasa SD, Gustmann S, Laub M, Wissler JH, Jennissen HP, Dünker N. Chick ex ovo culture and ex ovo CAM assay: how it really works. Journal of visualized experiments : JoVE. 2009;(33).

Doukas CN, Maglogiannis I, Chatziioannou A, Papapetropoulos A. Automated angiogenesis quantification through advanced image processing techniques. Conference proceedings: Annual International Conference of the IEEE Engineering in Medicine and Biology Society. IEEE Engineering in Medicine and Biology Society. Conference. 2006;1:2345–2348.

Engler AJ, Sen S, Sweeney HL, Discher DE. Matrix elasticity directs stem cell lineage specification. Cell. 2006 August 25;126(4):677–689.

Enquobahrie A, Ibanez L, Bullitt E. Vessel enhancing diffusion filter. The Insight Journal. 2007.

Euthanasia APO. AVMA Guidelines for the Euthanasia of Animals (2013 Edition). 2013.

Fadini GP, Agostini C, Avogaro A. Autologous stem cell therapy for peripheral arterial disease meta-analysis and systematic review of the literature. Atherosclerosis. 2010 March;209(1):10–17.

Falanga V, Iwamoto S, Chartier M, Yufit T, Butmarc J, Kouttab N, Shrayer D, Carson P. Autologous bone marrow-derived cultured mesenchymal stem cells delivered in a fibrin spray accelerate healing in murine and human cutaneous wounds. Tissue engineering. 2007 June 1;13(6):1299–1312.

Folberg R, Maniotis AJ. Vasculogenic mimicry. APMIS: acta pathologica, microbiologica, et immunologica Scandinavica. 2004 July;112(7-8):508–525.

Fox SB, Harris AL. Histological quantitation of tumour angiogenesis. APMIS : acta pathologica, microbiologica, et immunologica Scandinavica. 2004 June;112(7-8):413–430.

Fox SB, Leek RD, Weekes MP, Whitehouse RM, Gatter KC, Harris AL. Quantitation and prognostic value of breast cancer angiogenesis: comparison of microvessel density, Chalkley count, and computer image analysis. The Journal of pathology. 1995 November;177(3):275–283.

Frangi AF, Niessen WJ, Vincken KL, Viergever MA. Lecture Notes in Computer Science. (Wells WM, Colchester A, Delp S, editors.). Berlin/Heidelberg: Springer-Verlag; 1998 pp. 130–137.

Frisman I, Orbach R, Seliktar D, Bianco-Peled H. Structural investigation of PEG-fibrinogen conjugates. Journal of Materials Science: Materials in Medicine. 2010 January 1;21(1):73–80.

Fukuda S, Yoshii S, Kaga S, Matsumoto M, Kugiyama K, Maulik N. Angiogenic strategy for human ischemic heart disease: Brief overview. Molecular and Cellular Biochemistry. 2005;264(1/2):143–149.

Gaafar TM, Abdel Rahman HA, Attia W, Hamza HS, Brockmeier K, Hawary El RE. Comparative characteristics of endothelial-like cells derived from human adipose mesenchymal stem cells and umbilical cord blood-derived endothelial cells. Clinical and experimental medicine. 2013 May 7.

Galas RJ, Liu JC. Vascular endothelial growth factor does not accelerate endothelial differentiation of human mesenchymal stem cells. Journal of Cellular Physiology. 2013 June 21.

Gao F, Hu X-Y, Xie X-J, Xu Q-Y, Wang Y-P, Liu X-B, Xiang M-X, Sun Y, Wang J-A. Heat shock protein 90 protects rat mesenchymal stem cells against hypoxia and serum deprivation-induced apoptosis via the PI3K/Akt and ERK1/2 pathways. Journal of Zhejiang University. Science. B. 2010 August;11(8):608–617.

Gering D, Nabavi A, Kikinis R, Grimson W, Hata N, Everett P, Jolesz F, Wells WM. An integrated visualization system for surgical planning and guidance using image fusion and interventional imaging. … Image Computing and …. 1999.

Ghajar CM, Kachgal S, Kniazeva E, Mori H, Costes SV, George SC, Putnam AJ. Mesenchymal cells stimulate capillary morphogenesis via distinct proteolytic mechanisms. Experimental Cell Research. 2010 March 10;316(5):813–825.

Gibot L, Galbraith T, Huot J, Auger FA. A preexisting microvascular network benefits in vivo revascularization of a microvascularized tissue-engineered skin substitute. Tissue Engineering Part A. 2010 October;16(10):3199–3206.

Go RS, Owen WG. The rat aortic ring assay for in vitro study of angiogenesis. Methods in molecular medicine. 2003;85:59–64.

Gonen-Wadmany M, Goldshmid R, Seliktar D. Biological and mechanical implications of PEGylating proteins into hydrogel biomaterials. Biomaterials. 2011 September;32(26):6025–6033.

Gonen-Wadmany M, Oss-Ronen L, Seliktar D. Protein-polymer conjugates for forming photopolymerizable biomimetic hydrogels for tissue engineering. Biomaterials. 2007 September 1;28(26):3876–3886.

González-Iriarte M, Carmona R, Pérez-Pomares JM, Macías D, Angel Medina M, Quesada AR, Muñoz-Chápuli R. A modified chorioallantoic membrane assay allows for specific detection of endothelial apoptosis induced by antiangiogenic substances. Angiogenesis. 2003;6(3):251–254.

Gould DJ, Vadakkan TJ, Poché RA, Dickinson ME. Multifractal and lacunarity analysis of microvascular morphology and remodeling. Microcirculation (New York, N.Y. : 1994). 2011 February;18(2):136–151.

Grainger SJ, Putnam AJ. Assessing the permeability of engineered capillary networks in a 3D culture. PloS one. 2011;6(7):e22086.

Grayson WL, Zhao F, Izadpanah R, Bunnell B, Ma T. Effects of hypoxia on human mesenchymal stem cell expansion and plasticity in 3D constructs. Journal of Cellular Physiology. 2006 May;207(2):331–339.

Greene AK, Puder M, Roy R, Arsenault D, Kwei S, Moses MA, Orgill DP. Microdeformational wound therapy: effects on angiogenesis and matrix metalloproteinases in chronic wounds of 3 debilitated patients. Annals of plastic surgery. 2006 April 1;56(4):418–422.

Griffith CK, Miller C, Sainson RCA, Calvert JW, Jeon NL, Hughes CCW, George SC. Diffusion limits of an in vitro thick prevascularized tissue. Tissue engineering. 2005 January 1;11(1-2):257–266.

Grizzi F, Colombo P, Taverna G, Chiriva-Internati M, Cobos E, Graziotti P, Muzzio PC, Dioguardi N. Geometry of human vascular system: is it an obstacle for quantifying antiangiogenic therapies? Applied immunohistochemistry & molecular morphology : AIMM / official publication of the Society for Applied Immunohistochemistry. 2007 June;15(2):134–139.

Ha H, Kim I, Lee SK, Yoon JI, Kim DE, Kim M. Fibrin glue improves the therapeutic effect of MSCs by sustaining survival and paracrine function. Tissue Engineering Part A. 2013 May 24.

Haas TL, Madri JA. Extracellular matrix-driven matrix metalloproteinase production in endothelial cells: implications for angiogenesis. Trends in Cardiovascular Medicine. 1999 April;9(3-4):70–77.

Hamou C, Callaghan MJ, Thangarajah H, Chang E, Chang EI, Grogan RH, Paterno J, Vial IN, Jazayeri L, Gurtner GC. Mesenchymal stem cells can participate in

ischemic neovascularization. Plastic and reconstructive surgery. 2009 February;123(2 Suppl):45S–55S.

Hendrix MJC, Seftor EA, Hess AR, Seftor REB. Molecular plasticity of human melanoma cells. Oncogene. 2003 May 19;22(20):3070–3075.

Hendrix MJ, Seftor EA, Meltzer PS, Gardner LM, Hess AR, Kirschmann DA, Schatteman GC, Seftor RE. Expression and functional significance of VE-cadherin in aggressive human melanoma cells: role in vasculogenic mimicry. Proceedings of the National Academy of Sciences of the United States of America. 2001 July 3;98(14):8018–8023.

Hess AR, Seftor EA, Gruman LM, Kinch MS, Seftor REB, Hendrix MJC. VE-cadherin regulates EphA2 in aggressive melanoma cells through a novel signaling pathway: implications for vasculogenic mimicry. Cancer biology & therapy. 2006 February;5(2):228–233.

Hillen F, Griffioen AW. Tumour vascularization: sprouting angiogenesis and beyond. Cancer metastasis reviews. 2007 December;26(3-4):489–502.

Hocking AM, Gibran NS. Mesenchymal stem cells: paracrine signaling and differentiation during cutaneous wound repair. Experimental Cell Research. 2010 August 15;316(14):2213–2219.

Hong H, Stegemann JP. 2D and 3D collagen and fibrin biopolymers promote specific ECM and integrin gene expression by vascular smooth muscle cells. Journal of biomaterials science. Polymer edition. 2008;19(10):1279–1293.

Huang NF, Chu J, Lee RJ, Li S. Biophysical and chemical effects of fibrin on mesenchymal stromal cell gene expression. Acta Biomaterialia. 2010 October;6(10):3947–3956.

Huang F, Fang Z-F, Hu X-Q, Tang L, Zhou S-H, Huang J-P. Overexpression of mir-126 promotes the differentiation of mesenchymal stem cells toward endothelial cells via activation of pi3k/akt and mapk/erk pathways and release of paracrine factors. Biological chemistry. 2013 May 28.

Hutton DL, Logsdon EA, Moore EM, Mac Gabhann F, Gimble JM, Grayson WL. Vascular morphogenesis of adipose-derived stem cells is mediated by heterotypic cell-cell interactions. Tissue Engineering Part A. 2012 August;18(15-16):1729–1740.

Iruela-Arispe ML, Davis GE. Cellular and molecular mechanisms of vascular lumen formation. Developmental Cell. 2009 February;16(2):222–231.

Janeczek Portalska K, Leferink A, Groen N, Fernandes H, Moroni L, van Blitterswijk C, de Boer J. Endothelial Differentiation of Mesenchymal Stromal Cells Kerkis I, editor. PloS one. 2012 October 4;7(10):e46842.

Janmey PA, Winer JP, Weisel JW. Fibrin gels and their clinical and bioengineering applications. Journal of the Royal Society, Interface / the Royal Society. 2009 January 6;6(30):1–10.

Jazayeri M, Allameh A, Soleimani M, Jazayeri SH, Piryaei A, Kazemnejad S. Molecular and ultrastructural characterization of endothelial cells differentiated from human bone marrow mesenchymal stem cells. Cell biology international. 2008 October;32(10):1183–1192.

Jiang BH, Semenza GL, Bauer C, Marti HH. Hypoxia-inducible factor 1 levels vary exponentially over a physiologically relevant range of O2 tension. The American journal of physiology. 1996 October;271(4 Pt 1):C1172–80.

Jockenhoevel S, Zund G, Hoerstrup SP, Chalabi K, Sachweh JS, Demircan L, Messmer BJ, Turina M. Fibrin gel -- advantages of a new scaffold in cardiovascular tissue engineering. European journal of cardio-thoracic surgery : official journal of the European Association for Cardio-thoracic Surgery. 2001 April;19(4):424–430.

Kachgal S, Carrion B, Janson IA, Putnam AJ. Bone marrow stromal cells stimulate an angiogenic program that requires endothelial MT1-MMP. Journal of Cellular Physiology. 2012 January 19.

Karlsson LK, Junker JPE, Grenegard M, Kratz G. Human Dermal Fibroblasts: A Potential Cell Source for Endothelialization of Vascular Grafts. Annals of Vascular Surgery. 2009;23(5):663–674.

Kim CH, Lee JH, Won JH, Cho MK. Mesenchymal stem cells improve wound healing in vivo via early activation of matrix metalloproteinase-9 and vascular endothelial growth factor. Journal of Korean medical science. 2011 June;26(6):726–733.

Kinnaird T, Stabile E, Burnett MS, Lee CW, Barr S, Fuchs S, Epstein SE. Marrow-derived stromal cells express genes encoding a broad spectrum of arteriogenic cytokines and promote in vitro and in vivo arteriogenesis through paracrine mechanisms. Circulation research. 2004 March 19;94(5):678–685.

Kiran MS, Viji RI, Kumar SV, Prabhakaran AA, Sudhakaran PR. Changes in expression of VE-cadherin and MMPs in endothelial cells: Implications for angiogenesis. Vascular cell. 2011;3(1):6.

Kirbas C, Quek F. A review of vessel extraction techniques and algorithms. ACM Computing Surveys. 2004;36(2):81–121.

Kirschmann DA, Seftor EA, Hardy KM, Seftor REB, Hendrix MJC. Molecular pathways: vasculogenic mimicry in tumor cells: diagnostic and therapeutic implications. Clinical cancer research : an official journal of the American Association for Cancer Research. 2012 May 15;18(10):2726–2732.

Kniazeva E, Kachgal S, Putnam AJ. Effects of extracellular matrix density and mesenchymal stem cells on neovascularization in vivo. Tissue Engineering Part A. 2011 April;17(7-8):905–914.

Koh W, Mahan RD, Davis GE. Cdc42-and rac1-mediated endothelial lumen formation requires Pak2, Pak4 and Par3, and PKC-dependent signaling. Journal of cell science. 2008;121(7):989–1001.

Kunzi-Rapp K, Rück A, Kaufmann R. Characterization of the chick chorioallantoic membrane model as a short-term in vivo system for human skin. Archives of dermatological research. 1999 May;291(5):290–295.

Lämmermann T, Bader BL, Monkley SJ, Worbs T, Wedlich-Söldner R, Hirsch K, Keller M, Förster R, Critchley DR, Fässler R, et al. Rapid leukocyte migration by integrin-independent flowing and squeezing. Nature. 2008 May 1;453(7191):51–55.

Lammert E, Axnick J. Vascular lumen formation. Cold Spring Harbor perspectives in medicine. 2012 April;2(4):a006619.

Laranjeira MS, Fernandes MH, Monteiro FJ. Reciprocal induction of human dermal microvascular endothelial cells and human mesenchymal stem cells: time-dependent profile in a co-culture system. Cell proliferation. 2012 May 18.

Lasala GP, Silva JA, Minguell JJ. Therapeutic angiogenesis in patients with severe limb ischemia by transplantation of a combination stem cell product. The Journal of thoracic and cardiovascular surgery. 2012 August;144(2):377–382.

Lawall H, Bramlage P, Amann B. Treatment of peripheral arterial disease using stem and progenitor cell therapy. Journal of vascular surgery : official publication, the Society for Vascular Surgery [and] International Society for Cardiovascular Surgery, North American Chapter. 2011 February;53(2):445–453.

Lee EY, Xia Y, Kim W-S, Kim MH, Kim TH, Kim KJ, Park B-S, Sung J-H. Hypoxia-enhanced wound-healing function of adipose-derived stem cells: increase in stem cell proliferation and up-regulation of VEGF and bFGF. Wound repair and regeneration : official publication of the Wound Healing Society [and] the European Tissue Repair Society. 2009 July;17(4):540–547.

Leonardi D, Oberdoerfer D, Fernandes MC, Meurer RT, Pereira-Filho GA, Cruz P, Vargas M, Chem RC, Camassola M, Nardi NB. Mesenchymal stem cells combined with an artificial dermal substitute improve repair in full-thickness skin wounds. Burns : journal of the International Society for Burn Injuries. 2012 December;38(8):1143–1150.

Lesman A, Koffler J, Atlas R, Blinder YJ, Kam Z, Levenberg S. Engineering vessel-like networks within multicellular fibrin-based constructs. Biomaterials. 2011 November;32(31):7856–7869.

Lin R-Z, Chen Y-C, Moreno-Luna R, Khademhosseini A, Melero-Martin JM. Transdermal regulation of vascular network bioengineering using a photopolymerizable methacrylated gelatin hydrogel. Biomaterials. 2013 September;34(28):6785–6796.

Lindig TM, Kumar V, Kikinis R, Pieper S, Schrödl F, Neuhuber WL, Brehmer A. Spiny versus stubby: 3D reconstruction of human myenteric (type I) neurons. Histochemistry and cell biology. 2009 January;131(1):1–12.

Lirdprapamongkol K, Chiablaem K, Sila-Asna M, Surarit R, Bunyaratvej A, Svasti J. Exploring stemness gene expression and vasculogenic mimicry capacity in well- and poorly-differentiated hepatocellular carcinoma cell lines. Biochemical and biophysical research communications. 2012 June 8;422(3):429–435.

Liu K, Chi L, Guo L, Liu X, Luo C, Zhang S, He G. The interactions between brain microvascular endothelial cells and mesenchymal stem cells under hypoxic conditions. Microvascular research. 2008 January;75(1):59–67.

Liu H, Collins SF, Suggs LJ. Three-dimensional culture for expansion and differentiation of mouse embryonic stem cells. Biomaterials. 2006 December 1;27(36):6004–6014.

Liu J, Hu Q, Wang Z, Xu C, Wang X, Gong G, Mansoor A, Lee J, Hou M, Zeng L, et al. Autologous stem cell transplantation for myocardial repair. American Journal of Physiology- Heart and Circulatory Physiology. 2004 August 1;287(2):H501–11.

Lokman NA, Elder ASF, Ricciardelli C, Oehler MK. Chick Chorioallantoic Membrane (CAM) Assay as an In Vivo Model to Study the Effect of Newly Identified Molecules on Ovarian Cancer Invasion and Metastasis. International journal of molecular sciences. 2012;13(8):9959–9970.

Lönne M, Lavrentieva A, Walter J-G, Kasper C. Analysis of oxygen-dependent cytokine expression in human mesenchymal stem cells derived from umbilical cord. Cell and tissue research. 2013 July;353(1):117–122.

Lorenz K, Sicker M, Schmelzer E, Rupf T, Salvetter J, Schulz-Siegmund M, Bader A. Multilineage differentiation potential of human dermal skin-derived fibroblasts. Experimental Dermatology. 2008;17(11):925–932.

Lutolf MP, Gilbert PM, Blau HM. Designing materials to direct stem-cell fate. Nature. 2009 November 26;462(7272):433–441.

Malda J, Klein TJ, Upton Z. The roles of hypoxia in the in vitro engineering of tissues. Tissue engineering. 2007 September;13(9):2153–2162.

Maniotis AJ, Folberg R, Hess A, Seftor EA, Gardner LM, Pe'er J, Trent JM, Meltzer PS, Hendrix MJ. Vascular channel formation by human melanoma cells in vivo and in vitro: vasculogenic mimicry. The American journal of pathology. 1999 September;155(3):739–752.

Mansouri L, Xie Y, Rappolee DA. Adaptive and Pathogenic Responses to Stress by Stem Cells during Development. Cells. 2012.

Martineau L, Doillon CJ. Angiogenic response of endothelial cells seeded dispersed versus on beads in fibrin gels. Angiogenesis. 2007 January 1;10(4):269–277.

Medici D, Shore EM, Lounev VY, Kaplan FS, Kalluri R, Olsen BR. Conversion of vascular endothelial cells into multipotent stem-like cells. Nature medicine. 2010 December;16(12):1400–1406.

Menasché P. Stem cells for clinical use in cardiovascular medicine. Thromb Haemost. 2005.

Minar E. Critical limb ischaemia. Hämostaseologie. 2009.

Misra RM, Bajaj MS, Kale VP. Vasculogenic mimicry of HT1080 tumour cells in vivo: critical role of HIF-1α-neuropilin-1 axis. PloS one. 2012;7(11):e50153.

Moldovan NI, Goldschmidt-Clermont PJ, Parker-Thornburg J, Shapiro SD, Kolattukudy PE. Contribution of monocytes/macrophages to compensatory neovascularization: the drilling of metalloelastase-positive tunnels in ischemic myocardium. Circulation research. 2000;(87):378–384.

Moloney TC, Hoban DB, Barry FP, Howard L, Dowd E. Kinetics of thermally induced heat shock protein 27 and 70 expression by bone marrow-derived mesenchymal stem cells. Protein science : a publication of the Protein Society. 2012 June;21(6):904–909.

Mund J. The ontogeny of endothelial progenitor cells through flow cytometry. Current opinion in hematology. 2011.

Nakatsu MN, Hughes CCW. An optimized three-dimensional in vitro model for the analysis of angiogenesis. Methods in enzymology. 2008;443:65–82.

Nehls V, Drenckhahn D. A novel, microcarrier-based in vitro assay for rapid and reliable quantification of three-dimensional cell migration and angiogenesis. Microvascular research. 1995 November;50(3):311–322.

Nelson KS, Beitel GJ. More than a pipe dream: uncovering mechanisms of vascular lumen formation. Developmental Cell. 2009 October;17(4):435–437.

Némos C, Basciano L, Dalloul A. [Biological effects and potential applications of mesenchymal stem cell culture under low oxygen pressure]. Pathologie-biologie. 2012 June;60(3):193–198.

Oswald J, Boxberger S, Jørgensen B, Feldmann S, Ehninger G, Bornhäuser M, Werner C. Mesenchymal Stem Cells Can Be Differentiated Into Endothelial Cells In Vitro. Stem cells (Dayton, Ohio) [Internet]. 2004 May;22(3):377–384.

Pankajakshan D, Krishnan LK. Design of fibrin matrix composition to enhance endothelial cell growth and extracellular matrix deposition for in vitro tissue engineering. Artificial Organs. 2009 January 1;33(1):16–25.

Pankajakshan D, Kansal V, Agrawal DK. In vitro differentiation of bone marrow derived porcine mesenchymal stem cells to endothelial cells. Journal of tissue engineering and regenerative medicine. 2012 May 18.

Patan S. Vasculogenesis and angiogenesis as mechanisms of vascular network formation, growth and remodeling. Journal of neuro-oncology. 2000 January 1;50(1-2):1–15.

Paulis YWJ, Soetekouw PMMB, Verheul HMW, Tjan-Heijnen VCG, Griffioen AW. Signalling pathways in vasculogenic mimicry. Biochimica et biophysica acta. 2010 August;1806(1):18–28.

Pedroso DCS, Tellechea A, Moura L, Fidalgo-Carvalho I, Duarte J, Carvalho E, Ferreira L. Improved survival, vascular differentiation and wound healing potential of stem cells co-cultured with endothelial cells. PloS one. 2011;6(1):e16114–.

Peters K, Schmidt H, Unger RE, Kamp G, Pröls F, Berger BJ, Kirkpatrick CJ. Paradoxical effects of hypoxia-mimicking divalent cobalt ions in human endothelial cells in vitro. Molecular and Cellular Biochemistry. 2005 February;270(1-2):157–166.

Piccinelli M, Veneziani A, Steinman DA, Remuzzi A, Antiga L. A framework for geometric analysis of vascular structures: application to cerebral aneurysms. IEEE Transactions on Medical Imaging. 2009 August;28(8):1141–1155.

Pieper S, Halle M, Kikinis R. 2004 2nd IEEE International Symposium on Biomedical Imaging: Macro to Nano (IEEE Cat No. 04EX821). In: Vol. 2. IEEE; 2004. pp. 632–635.

Pieper S, Lorensen B, Schroeder W, Kikinis R. The NA-MIC Kit: ITK, VTK, pipelines, grids and 3D slicer as an open platform for the medical image computing community. 2006:698–701.

Pink DBS, Schulte W, Parseghian MH, Zijlstra A, Lewis JD. Real-time visualization and quantitation of vascular permeability in vivo: implications for drug delivery. PloS one. 2012;7(3):e33760.

Pinner SE, Sahai E. Integrin-independent movement of immune cells. F1000 biology reports. 2009;1:67.

Piret J-P, Mottet D, Raes M, Michiels C. CoCl2, a chemical inducer of hypoxia-inducible factor-1, and hypoxia reduce apoptotic cell death in hepatoma cell line HepG2. Annals of the New York Academy of Sciences. 2002 November;973:443–447.

Pons J, Huang Y, Takagawa J, Arakawa-Hoyt J, Ye J, Grossman W, Kan YW, Su H. Combining angiogenic gene and stem cell therapies for myocardial infarction. The Journal of Gene Medicine. 2009 September 1;11(9):743–753.

Pusztaszeri MP, Seelentag W, Bosman FT. Immunohistochemical expression of endothelial markers CD31, CD34, von Willebrand factor, and Fli-1 in normal human tissues. Journal of Histochemistry and Cytochemistry. 2006 April;54(4):385–395.

Rao RR, Peterson AW, Ceccarelli J, Putnam AJ, Stegemann JP. Matrix composition regulates three-dimensional network formation by endothelial cells and mesenchymal stem cells in collagen/fibrin materials. Angiogenesis. 2012 June;15(2):253–264.

Rappolee DA, Xie Y, Slater JA, Zhou S, Puscheck EE. Toxic stress prioritizes and imbalances stem cell differentiation: implications for new biomarkers and in vitro toxicology tests. Systems biology in reproductive medicine. 2012 February;58(1):33–40.

Ratel D, Mihoubi S, Beaulieu E, Durocher Y, Rivard G-E, Gingras D, Béliveau R. VEGF increases the fibrinolytic activity of endothelial cells within fibrin matrices: involvement of VEGFR-2, tissue type plasminogen activator and matrix metalloproteinases. Thrombosis research. 2007;121(2):203–212.

Razban V, Lotfi AS, Soleimani M, Ahmadi H, Massumi M, Khajeh S, Ghaedi M, Arjmand S, Najavand S, Khoshdel A. HIF-1α Overexpression Induces Angiogenesis in Mesenchymal Stem Cells. BioResearch open access. 2012 August;1(4):174–183.

Reilly GC, Engler AJ. Intrinsic extracellular matrix properties regulate stem cell differentiation. Journal of biomechanics. 2010 January 5;43(1):55–62.

Ren H, Cao Y, Zhao Q, Li J, Zhou C, Liao L, Jia M, Zhao Q, Cai H, Han ZC, et al. Proliferation and differentiation of bone marrow stromal cells under hypoxic conditions. Biochemical and biophysical research communications. 2006 August 18;347(1):12–21.

Ribatti D, Nico B, Vacca A, Presta M. The gelatin sponge-chorioallantoic membrane assay. Nature Protocols. 2006;1(1):85–91.

Rissanen TT, Ylä-Herttuala S. Current status of cardiovascular gene therapy. Molecular therapy : the journal of the American Society of Gene Therapy. 2007 July;15(7):1233–1247.

Rüger BM, Breuss J, Hollemann D, Yanagida G, Fischer MB, Mosberger I, Chott A, Lang I, Davis PF, Höcker P, et al. Vascular morphogenesis by adult bone marrow progenitor cells in three-dimensional fibrin matrices. Differentiation; research in biological diversity. 2008 September;76(7):772–783.

Rytlewski JA, Geuss LR, Anyaeji CI, Lewis EW, Suggs LJ. Three-dimensional image quantification as a new morphometry method for tissue engineering. Tissue Engineering Part C: Methods. 2012 July;18(7):507–516.

Sacharidou A, Stratman AN, Davis GE. Molecular mechanisms controlling vascular lumen formation in three-dimensional extracellular matrices. Cells, tissues, organs. 2012;195(1-2):122–143.

Sahai S, McFarland R, Skiles ML, Sullivan D, Williams A, Blanchette JO. Tracking hypoxic signaling in encapsulated stem cells. Tissue Engineering Part C: Methods. 2012 July;18(7):557–565.

Schlosser S, Dennler C, Schweizer R, Eberli D, Stein JV, Enzmann V, Giovanoli P, Erni D, Plock JA. Paracrine effects of mesenchymal stem cells enhance vascular regeneration in ischemic murine skin. Microvascular research. 2012 May;83(3):267–275.

Seftor REB, Hess AR, Seftor EA, Kirschmann DA, Hardy KM, Margaryan NV, Hendrix MJC. Tumor cell vasculogenic mimicry: from controversy to therapeutic promise. The American journal of pathology. 2012 October;181(4):1115–1125.

Shamloo A, Heilshorn SC. Matrix density mediates polarization and lumen formation of endothelial sprouts in VEGF gradients. Lab on a chip. 2010 November 21;10(22):3061–3068.

Shipp C, Derhovanessian E, Pawelec G. Effect of culture at low oxygen tension on the expression of heat shock proteins in a panel of melanoma cell lines. PloS one. 2012;7(6):e37475.

Smith TG, Marks WB, Lange GD, Sheriff WH, Neale EA. A fractal analysis of cell images. Journal of neuroscience methods. 1989 March;27(2):173–180.

Soker S, Machado M, Atala A. Systems for therapeutic angiogenesis in tissue engineering. World journal of urology. 2000 February 1;18(1):10–18.

Sorrell JM, Caplan AI. Topical delivery of mesenchymal stem cells and their function in wounds. Stem cell research & therapy. 2010 September 24;1(4):30.

Starke RD, Ferraro F, Paschalaki KE, Dryden NH, McKinnon TAJ, Sutton RE, Payne EM, Haskard DO, Hughes AD, Cutler DF, et al. Endothelial von Willebrand factor regulates angiogenesis. Blood. 2011 January 20;117(3):1071–1080.

Staton CA, Reed MWR, Brown NJ. A critical analysis of current in vitro and in vivo angiogenesis assays. International Journal of Experimental Pathology. 2009 June 1;90(3):195–221.

Stratman AN, Saunders WB, Sacharidou A, Koh W, Fisher KE, Zawieja DC, Davis MJ, Davis GE. Endothelial cell lumen and vascular guidance tunnel formation requires MT1-MMP-dependent proteolysis in 3-dimensional collagen matrices. Blood. 2009 July 9;114(2):237–247.

Sukmana I, Vermette P. The effects of co-culture with fibroblasts and angiogenic growth factors on microvascular maturation and multi-cellular lumen formation in

HUVEC-oriented polymer fibre constructs. Biomaterials. 2010 July;31(19):5091–5099.

Tips, stalks, tubes: notch-mediated cell fate determination and mechanisms of tubulogenesis during angiogenesis. 2012 February;2(2):a006601–a006601.

Tong M, Han BB, Holpuch AS, Pei P, He L, Mallery SR. Inherent phenotypic plasticity facilitates progression of head and neck cancer: Endotheliod characteristics enable angiogenesis and invasion. Experimental Cell Research. 2013 April 15;319(7):1028–1042.

Tsai C-C, Yew T-L, Yang D-C, Huang W-H, Hung S-C. Benefits of hypoxic culture on bone marrow multipotent stromal cells. American journal of blood research. 2012;2(3):148–159.

Tschoeke B, Flanagan TC, Koch S, Harwoko MS, Deichmann T, Ellå V, Sachweh JS, Kellomåki M, Gries T, Schmitz-Rode T, et al. Tissue-engineered small-caliber vascular graft based on a novel biodegradable composite fibrin-polylactide scaffold. Tissue Engineering Part A. 2009 August 1;15(8):1909–1918.

Ueda EK, Walker AM. Rat aorta ring ex-vivo angiogenesis assay. 2010 June 29:1–9.

Urbich C, Dimmeler S. Endothelial progenitor cells: characterization and role in vascular biology. Circulation research. 2004 August 20;95(4):343–353.

Urech L, Bittermann AG, Hubbell JA, Hall H. Mechanical properties, proteolytic degradability and biological modifications affect angiogenic process extension into native and modified fibrin matrices in vitro. Biomaterials. 2005.

Valentijn KM, Sadler JE, Valentijn JA, Voorberg J, Eikenboom J. Functional architecture of Weibel-Palade bodies. Blood. 2011 May 12;117(19):5033–5043.

van Hinsbergh VWM, Collen A, Koolwijk P. Role of fibrin matrix in angiogenesis. Annals of the New York Academy of Sciences. 2001 January 1;936:426–437.

van Mourik JA, Romani de Wit T, Voorberg J. Biogenesis and exocytosis of Weibel-Palade bodies. Histochemistry and cell biology. 2002 February;117(2):113–122.

van Winterswijk P, Nout E, Matrix E. Tissue engineering and wound healing: an overview of the past, present, and future. Wounds. 2007.

Vartanian AA. Signaling pathways in tumor vasculogenic mimicry. Biochemistry. Biokhimiiâ. 2012 September;77(9):1044–1055.

Vartanian A, Stepanova E, Grigorieva I, Solomko E, Belkin V, Baryshnikov A, Lichinitser M. Melanoma vasculogenic mimicry capillary-like structure formation depends on integrin and calcium signaling. Microcirculation (New York, N.Y. : 1994). 2011 July;18(5):390–399.

Varu VN, Hogg ME, Kibbe MR. Critical limb ischemia. Journal of vascular surgery : official publication, the Society for Vascular Surgery [and] International Society

for Cardiovascular Surgery, North American Chapter. 2010 January;51(1):230–241.

Vengellur A, LaPres JJ. The role of hypoxia inducible factor 1alpha in cobalt chloride induced cell death in mouse embryonic fibroblasts. Toxicological sciences : an official journal of the Society of Toxicology. 2004 December;82(2):638–646.

Veronese FM. Peptide and protein PEGylation: a review of problems and solutions. Biomaterials. 2001 March;22(5):405–417.

Vilanova A, Gröller E. Cylindrical approximation of tubular organs for virtual endoscopy. Proc of Comput Graphics and Imaging. 2000;283.

Walter T, Shattuck D, Baldock R, Bastin M. Visualization of image data from cells to organisms. Nat Methods. 2010.

Wang Y, Kaiser MS, Larson JD, Nasevicius A, Clark KJ, Wadman SA, Roberg-Perez SE, Ekker SC, Hackett PB, McGrail M, et al. Moesin1 and Ve-cadherin are required in endothelial cells during in vivo tubulogenesis. Development (Cambridge, England). 2010 September;137(18):3119–3128.

Wang C-H, Wang T-M, Young T-H, Lai Y-K, Yen M-L. The critical role of ECM proteins within the human MSC niche in endothelial differentiation. Biomaterials. 2013 June;34(17):4223–4234.

Wang N, Zhang R, Wang S-J, Zhang C-L, Mao L-B, Zhuang C-Y, Tang Y-Y, Luo X-G, Zhou H, Zhang T-C. Vascular endothelial growth factor stimulates endothelial differentiation from mesenchymal stem cells via Rho/myocardin-related transcription factor-A signaling pathway. International Journal of Biochemistry and Cell Biology. 2013 July 1;45(7):1447–1456.

Wang X, Zhao T, Huang W, Wang T, Qian J, Xu M, Kranias EG, Wang Y, Fan G-C. Hsp20-engineered mesenchymal stem cells are resistant to oxidative stress via enhanced activation of Akt and increased secretion of growth factors. Stem cells (Dayton, Ohio). 2009 December;27(12):3021–3031.

Weir C, Morel-Kopp M-C, Gill A, Tinworth K, Ladd L, Hunyor SN, Ward C. Mesenchymal stem cells: isolation, characterisation and in vivo fluorescent dye tracking. Heart, lung & circulation. 2008 October;17(5):395–403.

West DC, Thompson WD, Sells PG, Burbridge MF. Angiogenesis assays using chick chorioallantoic membrane. Methods in molecular medicine. 2001;46:107–129.

Whittington CF, Yoder MC, Voytik-Harbin SL. Collagen-Polymer Guidance of Vessel Network Formation and Stabilization by Endothelial Colony Forming Cells In Vitro. Macromolecular bioscience. 2013 July 5.

Wild R, Ramakrishnan S, Sedgewick J, Griffioen AW. Quantitative assessment of angiogenesis and tumor vessel architecture by computer-assisted digital image

analysis: effects of VEGF-toxin conjugate on tumor microvessel density. Microvascular research. 2000 May;59(3):368–376.

Wingate K, Bonani W, Tan Y, Bryant SJ, Tan W. Compressive elasticity of three-dimensional nanofiber matrix directs mesenchymal stem cell differentiation to vascular cells with endothelial or smooth muscle cell markers. Acta Biomaterialia. 2012 April;8(4):1440–1449.

Wolf K, Mazo I, Leung H, Engelke K, Andrian von UH, Deryugina EI, Strongin AY, Bröcker E-B, Friedl P. Compensation mechanism in tumor cell migration: mesenchymal-amoeboid transition after blocking of pericellular proteolysis. The Journal of cell biology. 2003 January 20;160(2):267–277.

Wolfe M, Pochampally R, Swaney W, Reger RL. Isolation and culture of bone marrow-derived human multipotent stromal cells (hMSCs). Methods in molecular biology (Clifton, N.J.). 2008;449:3–25.

Wu Y, Chen L, Scott PG, Tredget EE. Mesenchymal stem cells enhance wound healing through differentiation and angiogenesis. Stem cells (Dayton, Ohio). 2007 October;25(10):2648–2659.

Wu X, Ren J, Li J. Fibrin glue as the cell-delivery vehicle for mesenchymal stromal cells in regenerative medicine. Cytotherapy. 2011 December 16.

Xu J, Liu X, Chen J, Zacharek A, Cui X, Savant-Bhonsale S, Liu Z, Chopp M. Simvastatin enhances bone marrow stromal cell differentiation into endothelial cells via notch signaling pathway. American journal of physiology Cell physiology. 2009 March;296(3):C535–43.

Yan J, Tie G, Wang S, Messina KE, DiDato S, Guo S, Messina LM. Type 2 Diabetes Restricts Multipotency of Mesenchymal Stem Cells and Impairs Their Capacity to Augment Postischemic Neovascularization in db/db Mice. Journal of the American Heart Association. 2012 October 30;1(6):e002238–e002238.

Yan J, Tie G, Xu TY, Cecchini K, Messina LM. Mesenchymal stem cells as a treatment for peripheral arterial disease: current status and potential impact of type II diabetes on their therapeutic efficacy. Stem Cell Reviews and Reports. 2013 June;9(3):360–372.

Yang D, Guo T, Nie C, Morris SF. Tissue-engineered blood vessel graft produced by self-derived cells and allogenic acellular matrix: a functional performance and histologic study. Annals of plastic surgery. 2009 March 1;62(3):297–303.

Zan T, Du Z, Li H, Li Q, Gu B. Cobalt chloride improves angiogenic potential of CD133+ cells. Frontiers in bioscience : a journal and virtual library. 2012;17:2247–2258.

Zhang G, Drinnan CT, Geuss LR, Suggs LJ. Vascular differentiation of bone marrow stem cells is directed by a tunable three-dimensional matrix. Acta Biomaterialia. 2010 September;6(9):3395–3403.

Zhang G, Wang X, Wang Z, Zhang J, Suggs L. A PEGylated fibrin patch for mesenchymal stem cell delivery. Tissue engineering. 2006 January;12(1):9–19.

Zhao N, Sun B-C, Sun T, Ma Y-M, Zhao X-L, Liu Z-Y, Dong X-Y, Che N, Mo J, Gu Q. Hypoxia-induced vasculogenic mimicry formation via VE-cadherin regulation by Bcl-2. Medical Oncology. 2012 December;29(5):3599–3607.

Zhu P, Ning Y, Yao L, Chen M, Xu C. The proliferation, apoptosis, invasion of endothelial-like epithelial ovarian cancer cells induced by hypoxia. Journal of experimental & clinical cancer research : CR. 2010;29:124.

Vita

Julie Ann Rytlewski first joined the Biomedical Engineering Department at UT Austin in the Fall of 2004 as an undergraduate. In 2006, she joined Dr. Krishnendu Roy's Laboratory for Cellular and Macromolecular Engineering under the mentorship of Dr. Gazell Mapili-Call. Her experiences with Dr. Roy and Gazell solidified her desire to pursue a PhD and continue biomedical research. After obtaining her B.S. in Biomedical Engineering in May 2008, she returned as a graduate student in the fall. As a graduate student, she joined Dr. Laura Suggs' Laboratory for Cardiovascular Tissue Engineering, where she has enjoyed the challenge of cardiovascular tissue engineering strategies. During her graduate tenure at UT, Julie was awarded the National Defense Science and Engineering Graduate Fellowship. She also enjoyed teaching undergrads alongside Dr. Randi Voss in the Engineering Communications course.

After completing her PhD in December 2013, Julie will be joining the Fred Hutchinson Cancer Research Center in Seattle for continued postdoctoral training.

Author's email address: julie.rytlewski@utexas.edu

This dissertation was typed by Julie Rytlewski.